

UNIVERSITY OF CENTRAL OKLAHOMA

Edmond, Oklahoma

Department of Biology

**Investigating Differential Gene Expression *in vivo* of Cardiac Birth Defects in
an Avian Model of Maternal Phenylketonuria**

A THESIS

SUBMITTED TO THE GRADUATE FACULTY

In partial fulfillment of the requirements

For the degree of

MASTER OF SCIENCE IN BIOLOGY

By

Jamie N. Watson

Edmond, OK

June 5, 2018

**Investigating Differential Gene Expression *in vivo* of Cardiac Birth Defects in
an Avian Model of Maternal Phenylketonuria**

A THESIS

APPROVED FOR THE DEPARTMENT OF BIOLOGY

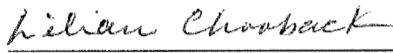
June 5, 2018

By 

Dr. Nikki Seagraves Committee Chairperson



Dr. Robert Brennan Committee Member



Dr. Lilian Chooback Committee Member

Acknowledgements

It is difficult to articulate the amount of gratitude I have for the support and encouragement I have received throughout my master's thesis. Many people have added value and support to my life during this time. I am thankful for the education, experience, and friendships I have gained at the University of Central Oklahoma. First, I would like to thank Dr. Nikki Seagraves for her mentorship and friendship. I lucked out when I met her. I have enjoyed working on this project and I am very thankful for her support. I would like to thank Thomas Crane for his support and patience throughout my master's degree. I would like to thank Dr. Shannon Conley for her continued mentorship and support. I would like to thank Liz Bullen and Dr. Eric Howard for their training and help on this project. I would like to thank Kristy Meyer for her friendship and help throughout graduate school. I would like to thank my committee members Dr. Robert Brennan and Dr. Lilian Chooback for their advisement on this project. Also, I would like to thank the biology faculty and staff. I would like to thank the Seagraves lab members: Jailene Canales, Kayley Pate, Mckayla Muse, Grace Thetford, Kody Harvey, Jordan Guffey, and Kayle Patatanian for their hard work and support. I would like to thank the University of Central Oklahoma Office of High Impact Practices (RCSA), Student Transformative Learning Record (STLR), and Sigma Xi for their grant awards. Finally, I would like to thank New England Bio Labs for their

donation of reagents and supplies. This project would not have been possible without their funding and donations.

Abstract

Cardiac malformations (CVMs) are a leading cause of infant morbidity and mortality. CVMs are particularly prevalent when the developing fetus is exposed to high levels of phenylalanine in-utero in mothers with Phenylketonuria. Yet, elucidating the underlying molecular mechanism leading to CVMs has proven difficult. In this study we used RNA-Seq to investigate an avian model of MPKU and establish differential gene expression (DEG) characteristics of the early developmental stages HH10, 12, and 14. In total, we identified 633 significantly differentially expressed genes across stages HH10, 12, and 14. As expected, functional annotation of significant DEGs identified associations seen in clinical phenotypes of MPKU including CVMs, congenital heart defects, craniofacial anomalies, central nervous system defects, and growth anomalies. Additionally, there was an overrepresentation of genes involved in cardiac muscle contraction, adrenergic signaling in cardiomyocytes, migration, proliferation, metabolism, and cell survival. Strikingly, we identified significant changes in expression with multiple genes involved in Retinoic Acid (RA) metabolism and downstream targets. Using qRT-PCR, we validated these findings and identified a total of 42 genes within the RA pathway that are differentially expressed. Here, we report the first elucidation of the molecular mechanisms of cardiovascular malformations in MPKU conducted at *early* developmental timepoints. We provide evidence

suggesting a link between PHE exposure and the alteration of RA pathway. These results are promising for potential targeted therapeutic interventions in individuals with MPKU. Additionally, we introduce genes of interest that were cloned for *in vivo* analysis of mRNA through *in situ* hybridization.

Table of Contents

Acknowledgements	iii
Abstract	v
List of Figures and Tables	ix
Chapter 1: Introduction	1
Phenylketonuria	1
Maternal Phenylketonuria and Cardiac Malformations	1
Chick Model in Heart Development	3
Retinoic Acid Signaling in Heart Development	4
Chapter 2: RNA-Seq Analysis in an Avian Model of Maternal Phenylketonuria	10
Introduction	10
Phenylketonuria	10
Maternal Phenylketonuria and Congenital Malformations.....	11
Materials and Methods.....	12
Ethics Statement	12
Injections and Incubation Conditions	13
RNA Isolation, Library Preparation, & Illumina Sequencing.....	14
Data Processing	15
Gene Ontology & Statistical Analysis	16
Validation of Results.....	16
Results.....	17
Differentially Expressed Genes & Functional Annotation.....	17
Role of Retinoic Acid (RA) in MPKU	24
Discussion	24
Conclusion	28
Acknowledgements.....	28
Funding	28
Introduction	30

Materials and Methods.....	34
RNA Extraction and Cloning	34
Plasmid Linearization and <i>in vitro</i> Transcription.....	35
Injections and Incubation Conditions of Embryos.....	36
In-situ Hybridization.....	37
Results and Discussion.....	38
<i>CRABP1</i> mRNA Expression in HH14	38
<i>FGF8</i> Expression Signaling in the Presence of PHE in HH14.....	39
Chapter 4: Summary and Conclusions	42
Retinoic Acid Signaling Plays a Role in Heart Development.....	43
Supplemental Figures.....	52
References	96

List of Figures and Tables

Figure 1. Chick Heart Development.....	4
Figure 2. Retinoic Acid metabolism from Stefanovic etal.	9
Table 1. Filtered Differentially Expressed Genes and Genetic Association Database Analysis.	21
Table 2. Functional Annotation HH10, 12, and 14.	23
Figure 3. Retinoic Acid Metabolism at HH14.	27
Table 3. Genes Cloned for In Situ Hybridization.....	33
Figure 4. CRABP1 mRNA Expression in a Microenvironment of 2.5 mM PHE.....	39
Figure 5. FGF8 mRNA Expression in a Microenvironment of 2.5 mM of PHE.....	41
Figure 6. Retinoic Acid Pathway Differential Gene Expression.....	46
Supplemental Figure 1. Per Base Sequence Quality of HH Stages 10 and 12.....	52
Supplemental Figure 2. Per Base Sequence Quality of HH14.	53
Supplemental Figure 3. Per Sequence Quality Scores for HH10 and 12.....	54
Supplemental Figure 4. Per Sequence Quality Scores for HH14.....	55
Supplemental Figure 5. Per Base Sequence Content HH10 and 12.....	56
Supplemental Figure 6. Per Base Sequence Content for HH14.	57
Supplemental Figure 7. Per Sequence GC Content for HH10 and 12.....	58
Supplemental Figure 8. Per Sequence GC Content for HH14.....	59
Supplemental Figure 9. Map for p-GEM-T plasmid.....	60
Supplemental Figure 10. Map for p-Mini-T 2.0 plasmid.	61
Supplemental Figure 11. Workflow of sample processing and bioinformatics analysis.	62
Supplemental Figure 12. QRTPCR Figure-Gene List-fold change.	63
Supplemental Table 1. DEG HH10, 12, and 14.....	90
Supplemental Table 2. Full Gene Ontology HH10, 12, and 14.	95

Chapter 1: Introduction

Phenylketonuria

Phenylketonuria (PKU) is an autosomal recessive disorder that affects 1 in 15,000 Caucasian newborns and there is lesser or greater incidence in other populations of newborns [1]. Patients with PKU are deficient in the liver enzyme, Phenylalanine Hydroxylase (PAH), causing a reduced or absent metabolism of Phenylalanine (PHE) to Tyrosine leading to a toxic serum level of PHE [2]. PHE is an essential amino acid obtained from diet and the deficiency in PAH leads to an inability to control levels of PHE, therefore it builds up to toxic levels. High levels of PHE and its metabolites cause severe intellectual disability and neurological conditions. Currently, newborn babies are routinely screened and identified at birth. However, the implementation of newborn PKU screening was not uniformly introduced across all states or worldwide and in these cases women are unaware of having PKU until later in life [3]. Currently newborns are consistently tested at birth in the US and in cases of known PKU, strict monitoring of the levels of PHE and adherence to diet has allowed individuals to live relatively normal lives with no cognitive impairment. This early identification of PKU has led to the most successful treatment [4]. Currently, the only effective treatment for PKU is the dietary restriction of PHE. Although compliance with a PHE

restricted diet is possible it is not easy and long-term adherence is less successful. Many women are going off diet leading to increased levels of PHE and an increased risk of Maternal Phenylketonuria (MPKU) in offspring/children.

Maternal Phenylketonuria and Cardiac Malformations

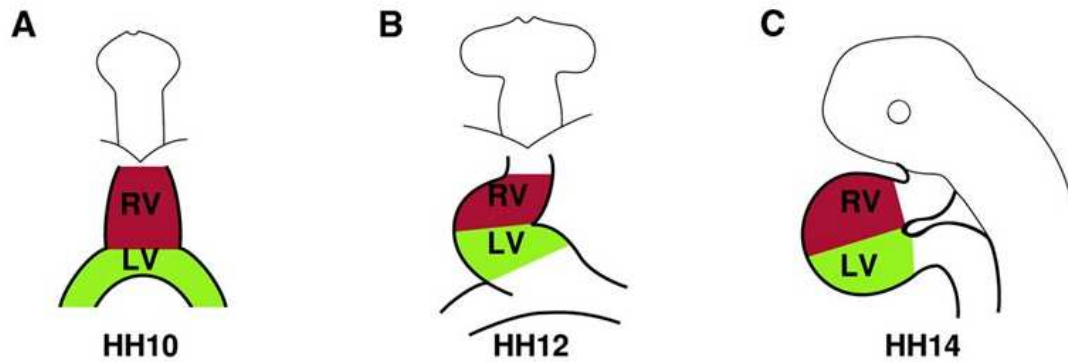
When a female with PKU is pregnant, her fetus will be negatively affected by intrauterine exposure of increased levels of PHE, this disease is known as MPKU. In cases of MPKU, offspring have exhibited cardiovascular malformations (CVMs) [5]. Additionally, offspring exhibit microcephaly, facial abnormalities, growth restriction, and mental retardation [6]. Currently among all births, CVMs are a leading cause of infant mortality, occurring at a rate of 5-8/1000 live births [7, 8]. CVMs are caused by genetic and environmental exposure such as MPKU, ethanol exposure, and maternal diabetes [9, 10]. Early identification and diet restriction has led to increased numbers of women diagnosed with PKU reaching childbearing age and the need for further investigation of MPKU is of increasing importance. Currently, treatment of MPKU is limited and not ideal. The extremely restricted diet low in PHE is difficult to maintain and it is reported that observance reduces with time [11]. More importantly in cases of MPKU, adherence to a strict diet gives the highest probability of healthy offspring. Often, women

with PKU have unintended pregnancies and may not be in compliance with PHE levels at the time of conception or even within early development of the embryo [3]. Additionally, women with PKU who discontinue diet at an early age 5-6 years, do not remember why they were on the diet or what disease they have [3]. Initial reports noted CVMs were observed in 7-15% of pregnancies of PKU mothers on uncontrolled diet [3]. The more extensive MPKU study of 412 PKU pregnancies demonstrated 14% of the offspring were born with a CVM. The most commonly occurring CVMs observed are Coarctation of the Aorta (CoA), Tetralogy of Fallot (TOF), Ventricular Septal Defect (VSD), Patent Ductus Arteriosus (PDA), Atrial Septal Defect (ASD), Persistent Truncus Arteriosus (PTA) and Hypoplastic Left Heart Syndrome (HLHS) [2, 12].

Interestingly, the molecular mechanisms of teratogenicity in the presence of PHE are not known. To date, the effects of PHE exposure on gene expression in the developing heart has not been investigated. RNA-Sequencing (RNA-Seq), a molecular technique used to identify gene expression, was used to compare vehicle control injected embryos to PHE injected animals to elucidate novel changes in gene expression that may be associated with the development of CVMs.

Chick Model in Heart Development

Historically chick embryos have been used to study patterning of early development such as axes, germ layers, and organogenesis [13]. The chicken is used in embryology and developmental studies because of *ex utero* development with availability and affordability. The chick embryo is easily manipulated and observed in many types of experiments notably, grafting, microinjection, and lineage tracing [14-16]. Most importantly, chick is the only other non-mammalian organism whose heart anatomy most resembles humans with four chambers and in- and out-flow tracts [17]. The chicken embryo developmental stages were extensively studied and documented by Hamburger and Hamilton (HH) and allow for easier staging and experimentation at specific stages in heart development [18, 19]. At HH10-14, the heart is still developing and remodeling (Figure 1) [20]. Primary and secondary heart field cells populate the heart first. Then, the cardiac neural crest cells (cNCC) begin to ingress from the neural tube through the pharyngeal arteries continuing into the heart. The cell population of cNCCs is necessary for remodeling of the aortic arch and the septation of the outflow tract into the pulmonary artery [21]. Additionally at HH14, the chambers of the heart are undergoing remodeling and atria/ventricle septation to ensure proper function and blood flow [22].



Edited from M. Sameer Rana et al. *Circ Res.* 2007;100:1000-1007

Figure 1. Chick Heart Development.

Chicken heart development from HH stages 10, 12, and 14.

Retinoic Acid Signaling in Heart Development

Vitamin A/retinol metabolized inside the cell through a series of enzymatic reactions and transport with serum proteins, cellular receptors, and nuclear receptors. Vitamin A and Carotenoids, that later become retinoic acid (RA), are sourced only through the diet. Vitamin A is acquired in the diet from milk, eggs, and liver. Carotenoids are found in plants such as carrots and sweet potato. In humans, retinoids are received from the mother across the placenta in the form of retinol or β -carotene. In chicken, the retinoids are maternally deposited in the yolk [23].

For cell signaling, hydrophobic Vitamin A is transported as retinol by Retinol Binding Protein 4 (*RBP4*) [24] and Transthyretin (*TTR*) complex to cell

surface receptors such as Stimulated by Retinoic Acid 6 (*STRA6*) or predominately through diffusion across the cell membrane (Figure 2) [25]. *STRA6* takes the metabolite into the cell and it is delivered to Cellular Retinol Binding Protein 1 (*CRBP1*, *RBP1*) [26, 27]. The metabolite is then further modified to retinaldehyde by Retinol Dehydrogenase 10 (*RDH10*) and to its active signaling molecule RA by Retinaldehyde Dehydrogenase 2 (*RALDH2*). *RALDH2* is also known as Aldehyde Dehydrogenase 1 family member A2 (*ALDH1A2*). RA is then able to act as a transcription factor by entering the nucleus through nuclear receptor Cellular Retinoic Acid Binding Protein 2 (*CRABP2*), inducing developmental gene expression or repression [25]. Cellular Retinoic Acid Binding Protein 1 (*CRABP1*) may sequester or shuttle RA to the Cytochrome P450 Family 26 (*CYP26*), family of enzymes where it can undergo catabolism and be eliminated to maintain the suitable levels of RA [28]. Mutations in the *CYP26* enzymes create a microenvironment resembling surplus RA in mouse models [29].

The ADH family of cytosolic alcohol dehydrogenases are able to oxidize retinol to retinal and produce RA *in vivo* during embryogenesis [23]. Retinaldehyde Dehydrogenase 2 (*RALDH2*) is responsible for the majority of retinaldehyde to RA during embryo development and has been shown in *RALDH2*^{-/-} mice to be necessary for survival [30]. In addition to gene expression

RA can act through paracrine signaling on neighboring cells. RA may diffuse and act as a morphogen on other cells [31].

RA signaling is involved in multiple embryonic developmental processes. RA signaling is highly regulated through development as too much, too little, or abnormal distribution negatively affects development. Too little Vitamin A is known as Vitamin A Deficiency (VAD) which causes abnormalities in the development of many organs including heart [32, 33]. Improper RA signaling has previously been shown to affect cardiogenesis in avian embryos, decreasing the expression of GATA Binding Protein 4 (*GATA-4*), a heart transcription factor. This was rescued with dietary supplementation of Vitamin A [34]. Excess Vitamin A or RA causes malformations in heart and other organs [35]. VAD can be rescued with Vitamin A or RA supplementation preventing developmental defects. Conversely, in cases of too much RA, RA acts as a teratogen causing developmental defects [23]. Correct signaling is achieved through multiple proteins functioning in Vitamin A metabolism, transport, nuclear signaling, and RA catabolism[23].

It has previously been shown that phenylalanine (PHE) effects heart development [5-8], therefore the hypothesis is chick embryos exposed to high PHE will develop heart defects in the aortic arch arteries (AAA) and the outflow tract

(OFT) resultant from alterations in gene expression in cardiac and surrounding tissues. Investigating this hypothesis will improve our understanding of how exposure to teratogens affects heart development and potentially uncover novel pathways in heart development. Additionally, the objective is to determine differentially-expressed genes in the heart and thoracic region in the presence of PHE and find potential mechanisms of CVMs in MPKU. The rationale is that while it is known that PHE affects embryonic heart development, it has not been shown which genes are differentially expressed (DE) in the microenvironment of PHE. The new knowledge gained from this research will contribute to the development of new diagnostics and treatments ultimately reducing the morbidity, mortality, and cost associated with CVMs. Furthermore, elucidating a mechanism for the development of CVMs will allow for potential therapeutic interventions for individuals with MPKU.

To test our hypothesis, first differentially expressed genes (DEGs) were determined using RNA sequencing. Genes of interest identified through RNA sequencing and with significance in heart development were further investigated through Quantitative Real Time Polymerase Chain Reaction (qRT-PCR) and *in situ* hybridization. Through this work we present novel investigations into the molecular effects of PHE on heart development in chicken. Additionally, we

suggest future directions for further investigations of CVMs in PHE treated embryos.

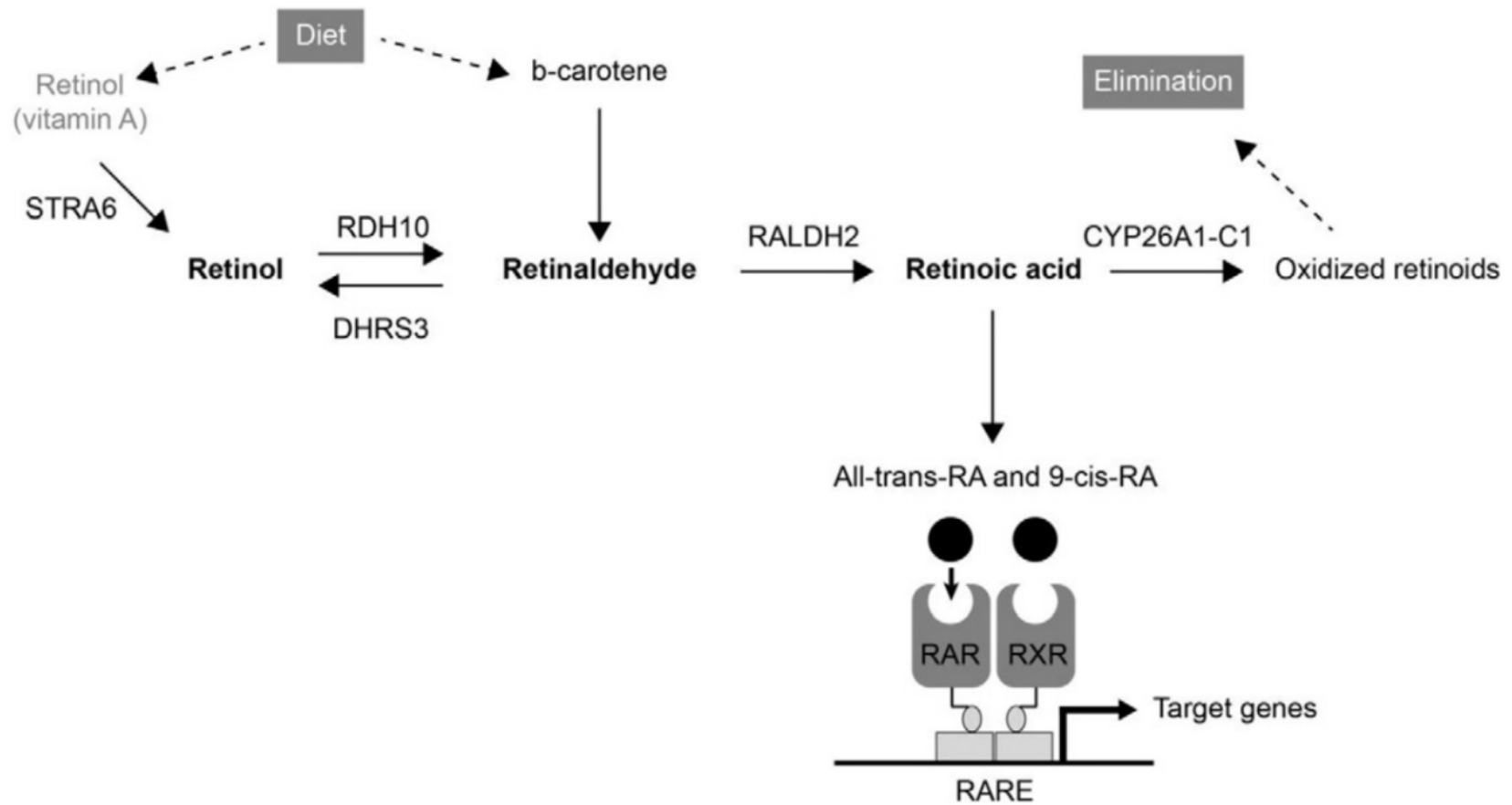


Figure 2. Retinoic Acid metabolism from Stefanovic et al.

Chapter 2: RNA-Seq Analysis in an Avian Model of Maternal Phenylketonuria

Introduction

Phenylketonuria

Phenylketonuria (PKU; OMIM #261600) is an autosomal recessive disorder of Phenylalanine (PHE) processing [36] with 1 in 10,000 newborns affected [1, 37]. The development of a rapid and inexpensive test for PKU in the 1960s resulted in early identification of affected newborns that is still done as part of routine screening at birth in the US [38, 39]. Currently, the standard treatment is a PHE-restricted diet; therefore, strict dietary adherence has allowed affected individuals to live relatively normal lives free from explicit symptoms [40].

Yet, the PKU dietary regimen is onerous and compliance is complex due to issues including convenience, cost, and availability of dietary options. As a result, adherence is inconsistent across the lifespan [41]. One unintended consequence of poor dietary adherence occurs in females of reproductive age in which their uncontrolled levels of PHE result in congenital anomalies in over 90% of children (termed “Maternal Phenylketonuria” (MPKU) [5, 42]. PHE crosses the placenta into the fetal compartment creating an adverse developmental condition in which

fetal blood levels are 1.5 to 2.0-fold higher than maternal levels[43]. This creates a direct dose-response relationship between maternal blood PHE and birth defect incidence [44, 45]. MPKU clinical phenotypes include stunted growth, facial dysmorphologies, cognitive impairment, and cardiovascular malformations (CVMs) [5, 43, 46-48].

Maternal Phenylketonuria and Congenital Malformations

One of the most severe MPKU associated congenital anomalies, CVMs, are a leading cause of infant mortality and occur in up to 15% of MPKU live-born children [5, 7, 8, 42, 49]. The most commonly occurring CVMs observed are Coarctation of the Aorta (CoA), Tetralogy of Fallot (TOF), Ventricular Septal Defect (VSD), Patent Ductus Arteriosus (PDA), Atrial Septal Defect (ASD), Persistent Truncus Arteriosus (PTA) and Hypoplastic Left Heart Syndrome (HLHS) [1-3].

To date, animal models of MPKU associated CVM development have yet to illuminate the molecular mechanisms of teratogenicity and CVM pathogenesis [46-48]. Molecular studies have been limited to late-stage mouse embryos that focus on the resultant alterations in gene expression *after* CVM occurrence [44]. Thus, in order to robustly elucidate the molecular changes that lead to the

development of CVMs, there is a clear need for an early model of gene expression changes in MPKU.

The purpose of this study is to investigate the etiology of CVMs by investigating global gene expression levels during early cardiac development. To our knowledge this is the first investigation elucidating a global picture of gene expression changes that may cause CVMs in the presence of PHE. Our significant results will allow for individually tailored preventive measures and targeted therapies.

Materials and Methods

Ethics Statement

All animal procedures were carried out in accordance with the U.S. Public Health Service Policy on Humane Care and Use of Laboratory Animals and the Animal Welfare Act. All protocols were performed with the approval of the Institutional Animal Care and Use Committee (IACUC) at University of Central Oklahoma.

Injections and Incubation Conditions

Fertilized white leghorn chicken eggs were purchased from Texas A&M Poultry Sciences. Eggs were incubated at 37.2°C and 50% humidity until Hamburger and Hamilton (HH) stage 6 [18]. Eggs were removed from the incubator and the shell of the eggs was sterilized using a 70% ethanol. Using a 16-gauge needle, a small hole was drilled through the air pocket. A 27-gauge needle was inserted into the hole and eggs were treated with 200µl of either 2.5mM PHE or vehicle control (1 x PBS) through the blunt end of the egg as described previously (yolk injection) [50]. After yolk injection the hole in the shell was sealed with tape and the embryos were further incubated until HH 10, 12 or 14. We selected HH 10, 12, and 14 due the critical changes occurring in heart at these *early* development stages (these changes include cardiac neural crest cells (cNCC) ingress from the neural tube into the pharyngeal arteries for remodeling of the aortic arch and the outflow tract [21] and atrial/ventricular septation to ensure proper function and blood flow [19, 22]. At HH 10, 12, or 14 the embryos were collected by dissection. The thoracic/cardiac region between the otic placode and the 3rd somite were dissected and used for RNA isolation. For HH stages 10 and 12, a total of 3 PHE treated embryos and 3 control embryos were used.

Experiments were repeated as described above. For HH 14, tissues from 3 control embryos were pooled. A total of 2 PHE treated samples were isolated for RNA collection.

RNA Isolation, Library Preparation, & Illumina Sequencing

Total RNA was isolated using the PicoPure™ RNA Isolation Kit (Thermo Fisher Scientific, Waltham, MA, USA, KIT0204), according to manufacturer's protocol followed by storage at -80°C. The quality and quantity were analyzed using a Nanodrop spectrophotometer (Thermo Fisher Scientific) and a total of 2.5 µg high quality RNA (RIN> 8.0) [51] was shipped to Applied Biological Materials Inc (ABM; Richmond, BC, Canada). Additional rigorous RNA quality analyses were performed by AMB (Aligent 2100 Bioanalyzer) and after the samples passed the quality verification, they were processed for library preparation and transcriptome sequencing. Subsequently, the RNA was enriched for Poly-A selection followed by fragmentation, first and second strand synthesis, adenylation of 3' ends, adaptor ligation, DNA fragment enrichment, and real-time PCR quantification. Samples were then sequenced using Next Generation Sequencing (NGS) on the Illumina NextSeq 500 at ABM.

Data Processing

The quality of the sequencing reads was determined using the Fast QC [52] program, length of fragments, and number of sequence reads (Supplemental Figures 3-8). The average size of the sequence reads were 300bp, indicating a homogenous library construction. All to the sequence reads for the samples were greater than 10 million, representing thorough coverage of the genome. Bases were trimmed for HH 10 and 12 samples (9 bases) (Supplemental Figure 1) and for HH 14 samples (6 bases) (Supplemental Figure 2). Raw FASTQ data were received and analyzed using open source software, Galaxy Suite from Penn State University (<https://usegalaxy.org/>). A workflow of sample processing is shown in Supplemental Figure 11. The RNA-Seq reads were first aligned to *Gallus gallus* genome (galGal4) using and Tophat/Hisat [53, 54]. We compared PHE treated to vehicle control (PBS) embryos to determine differential gene expression using CuffDiff [55]. Differential Gene Expression statistical analysis was conducted in Galaxy Suite. A-priori statistical significance was set (q-value ≤ 0.05 , p-value ≤ 0.05) and all significant gene name symbols were retained for further analysis.

Gene Ontology & Statistical Analysis

To identify high-level biological functions and interactions, significant gene name symbols were uploaded through The Database for Annotation, Visualization and Integrated Discovery (DAVID; vs. 6.8) and then analyzed with Kyoto Encyclopedia of Genes and Genomes (KEGG) pathway analysis, enriched Gene Ontology (GO) Terms, and Genetic Association Database (GAD) [56, 57]. All analyses were conducted with program defined defaults. The p-value was calculated using a modified Fisher Exact Test that, for a given annotation process, is calculated by considering both the number of focus genes within that process and the total number of genes that are associated with that process in the reference set [47]. It is noted that Fisher's Exact Test can be overly conservative with small sample sizes [48, 49]. For specific hypothesis testing, we used the Benjamini-Hochberg method of correction for multiple testing [46, 47].

Validation of Results

Selected genes were further validated at embryonic HH 14 through Quantitative Real Time PCR (qRTPCR). RNA was prepared for embryos as previously described (2.3). Then, the cDNA library was prepared by reverse transcribing 2 μ g of RNA using High-Capacity cDNA Reverse Transcription Kit

(Fisher Scientific, Hampton, NH, USA, 4368814) with SyberGreen Maxima Mastermix (Thermo Fisher Scientific, K0221) per the manufacturer's protocols. The reaction was carried out on iCycler™ Optical Module Thermocycler (Bio-Rad, Hercules, CA, USA). Validation genes were selected based upon significance in cardiac relevant biological pathways and statistical significance. Additionally, commercially available custom Retinoic Acid Pathway qRT-PCR plates in *Gallus gallus* were purchased (Qiagen, Hilden, Germany). Based on previous qRT-PCR work in this model, all genes were normalized to the housekeeping gene *RPL4*[58].

Results

Differentially Expressed Genes & Functional Annotation

We identified 110 (HH10) (5.37×10^{-3} to 4.92×10^{-2} q-value, -4.52 to 6.11 fold change), 412 (HH12) (2.16×10^{-3} to 4.99×10^{-2} q-value, -5.26 to 2.48 fold change), and 111 (HH14) (5.00×10^{-5} to 5.00×10^{-2} p-value, -1.95 to 5.27 fold change) differentially expressed genes (total = 633) between PHE treated and vehicle-control embryos. We identified 41 upregulated genes (37.27%) and 69 downregulated (62.73%) (HH10), 191 upregulated genes (46.36%) and 221 downregulated (53.64%) (HH12), and 44 upregulated genes (39.64%) and 67 downregulated (60.36%)

(HH14) between PHE treated and vehicle-control embryos. After filtering by $>\pm 1.5$ -fold change, we identified 31 (HH10), 43 (HH12), and 8 (HH14) differentially expressed genes (total = 82) between PHE treated and vehicle-control embryos (Table 1). Values ranged from -5.26 to +5.27 fold-change, and p-value 5.00×10^{-5} to 4.55×10^{-2} . Next, we examined the association of these genes with known disease phenotypes of MPKU using GAD. We identified associations with CVMs or congenital heart defects (genes = 13), craniofacial anomalies (genes = 8), central nervous system defects (CNSD) (genes = 13), and growth anomalies (genes = 10) for a total of 30 (42.3%) out of the 71 different significant DEGs. Additionally, 9/71 (12.7%) were associated with two or more MPKU phenotypes (Table 1).

Differential Gene Expression						GAD Analysis-MPKU Phenotype			
HH Stage	Gene ID	Gene Name	log2 fold change	p-value	q-value	Cardiac	Craniofacial	CNS	Growth
10	<i>NR2E1</i>	nuclear receptor subfamily 2 group E member 1	4.44	5.00E-05	5.37E-03			+	
10	<i>AKR1BL</i>	aldo-keto reductase family 1 member B1-like	3.97	5.00E-05	5.37E-03				
10	<i>RAX</i>	retina and anterior neural fold homeobox	3.90	5.00E-05	5.37E-03		+	+	
10	<i>NKX2-1</i>	NK2 homeobox 1	3.83	5.00E-05	5.37E-03			+	
10	<i>OLIG3</i>	oligodendrocyte transcription factor 3	3.46	5.00E-05	5.37E-03				+
10	<i>DBX1</i>	developing brain homeobox 1	3.22	5.00E-05	5.37E-03				+
10	<i>SLCO4A1</i>	solute carrier organic anion transporter family member 4A1	2.99	5.00E-05	5.37E-03				
10	<i>OTX2</i>	orthodenticle homeobox 2	2.63	5.00E-05	5.37E-03		+	+	
10	<i>OCX36</i>	BPI fold containing family B member 3	2.54	5.00E-05	5.37E-03				

10	<i>ST8SIA2</i>	ST8 alpha-N-acetylneuraminide alpha-2,8-sialyltransferase 2	1.85	5.00E-05	5.37E-03			+	
10	<i>PAX6</i>	paired box 6	1.77	5.00E-05	5.37E-03		+	+	+
10	<i>APC2</i>	adenomatosis polyposis coli 2	1.60	5.00E-05	5.37E-03				
10	<i>RBP4</i>	retinol binding protein 4	-1.66	5.00E-05	5.37E-03	+			
10	<i>ASTL</i>	astacin-like metallo-endopeptidase (M12 family)	-1.67	5.00E-05	5.37E-03				
10	<i>APOC3</i>	apolipoprotein C3	-1.67	5.00E-05	5.37E-03				
10	<i>APOA1</i>	apolipoprotein A-I	-1.75	5.00E-05	5.37E-03				
10	<i>MT4</i>	metallothionein 4	-1.75	5.00E-05	5.37E-03				
10	<i>CRABP1</i>	cellular retinoic acid binding protein 1	-1.75	5.00E-05	5.37E-03		+		
10	<i>FGA</i>	fibrinogen alpha chain	-1.88	5.00E-05	5.37E-03				
10	<i>TNNC2</i>	troponin C type 2 (fast)	-1.91	5.00E-05	5.37E-03	+			
10	<i>MYL2</i>	myosin, light chain 2, regulatory, cardiac, slow	-2.04	5.00E-05	5.37E-03	+			
10	<i>MYL3</i>	myosin, light chain 3, alkali; ventricular, skeletal, slow	-2.27	5.00E-05	5.37E-03	+			
10	<i>SEPP1</i>	selenoprotein P1	-2.32	5.00E-05	5.37E-03				
10	<i>PTGDS</i>	prostaglandin D2 synthase 21kDa (brain)	-2.53	5.00E-05	5.37E-03				
10	<i>ALDOB</i>	aldolase B, fructose-bisphosphate	-2.86	5.00E-05	5.37E-03				
10	<i>APOB</i>	apolipoprotein B	-2.97	5.00E-05	5.37E-03	+			
10	<i>RBP</i>	riboflavin binding protein	-3.12	5.00E-05	5.37E-03				
10	<i>FBP1</i>	fructose-1,6-bisphosphatase 1	-3.59	5.00E-05	5.37E-03		+		
10	<i>TGM4</i>	transglutaminase 4 (prostate)	-3.62	5.00E-05	5.37E-03				+
10	<i>HBE</i>	hemoglobin subunit epsilon	-4.33	5.00E-05	5.37E-03				
10	<i>HBG1</i>	hemoglobin beta, subunit rho	-4.52	5.00E-05	5.37E-03				
12	<i>HBG2</i>	hemoglobin, beta	2.48	5.00E-05	2.16E-03				
12	<i>HBG1</i>	hemoglobin, beta	2.33	5.00E-05	2.16E-03				
12	<i>HBE</i>	hemoglobin subunit epsilon	2.33	5.00E-05	2.16E-03				
12	<i>PLN</i>	phospholamban	1.83	5.00E-05	2.16E-03	+			
12	<i>IFI27L2</i>	interferon, alpha-inducible protein 27-like 2	1.81	5.00E-05	2.16E-03				
12	<i>MB</i>	myoglobin	1.78	5.00E-05	2.16E-03	+		+	+
12	<i>SERPINI1</i>	serpin peptidase inhibitor, clade I (neuroserpin), member 1	1.75	5.00E-05	2.16E-03				
12	<i>TNNC2</i>	troponin C type 2 (fast)	1.74	5.00E-05	2.16E-03	+			

12	<i>SLC4A1</i>	solute carrier family 4, anion exchanger, member 1	1.70	5.00E-05	2.16E-03				
12	<i>MYL2</i>	myosin, light chain 2, regulatory, cardiac, slow	1.69	5.00E-05	2.16E-03	+			
12	<i>ADCYAP1</i>	adenylate cyclase activating polypeptide 1 (pituitary)	1.60	5.00E-05	2.16E-03			+	
12	<i>ACTG2</i>	actin, gamma 2, smooth muscle, enteric	1.51	5.00E-05	2.16E-03				
12	<i>HINT1</i>	histidine triad nucleotide binding protein 1	1.51	5.00E-05	2.16E-03			+	
12	<i>KRT7</i>	keratin 7	-1.52	5.00E-05	2.16E-03				
12	<i>SCIN</i>	scinderin	-1.52	5.00E-05	2.16E-03				
12	<i>PCP4</i>	Purkinje cell protein 4	-1.53	5.00E-05	2.16E-03				+
12	<i>TGFBR3</i>	transforming growth factor, beta receptor III	-1.54	5.00E-05	2.16E-03	+	+	+	+
12	<i>HOXB4</i>	homeobox B4	-1.57	5.00E-05	2.16E-03				
12	<i>NRP2</i>	neuropilin 2	-1.61	5.00E-05	2.16E-03	+		+	
12	<i>ANXA2</i>	annexin A2	-1.65	5.00E-05	2.16E-03				
12	<i>MT4</i>	metallothionein 4-like	-1.68	5.00E-05	2.16E-03				
12	<i>TBX22</i>	T-box 22	-1.69	5.00E-05	2.16E-03		+		+
12	<i>PLCXD1</i>	phosphatidylinositol specific phospholipase C X domain containing 1	-1.72	5.00E-05	2.16E-03				
12	<i>NTN1</i>	netrin 1	-1.73	5.00E-05	2.16E-03				
12	<i>T</i>	T, brachyury homolog (mouse)	-1.82	5.00E-05	2.16E-03	+			
12	<i>KRT17</i>	keratin, type I cytoskeletal 14-like(LOC100858439)	-1.84	5.00E-05	2.16E-03				
12	<i>Pou5f3</i>	POU domain class 5 transcription factor 3	-1.92	5.00E-05	2.16E-03				
12	<i>FMOD</i>	fibromodulin	-1.98	5.00E-05	2.16E-03			+	
12	<i>PRPS2</i>	phosphoribosyl pyrophosphate synthetase 2	-2.09	5.00E-05	2.16E-03				
12	<i>CDH20</i>	cadherin 20, type 2	-2.14	5.00E-05	2.16E-03				
12	<i>EPAS1</i>	endothelial PAS domain protein 1	-2.17	5.00E-05	2.16E-03	+	+		+
12	<i>COL3A1</i>	collagen, type III, alpha 1	-2.23	5.00E-05	2.16E-03	+			
12	<i>AQP1</i>	aquaporin 1	-2.34	5.00E-05	2.16E-03				
12	<i>OTX2</i>	orthodenticle homeobox 2	-2.54	5.00E-05	2.16E-03		+	+	
12	<i>RBP</i>	riboflavin binding protein	-2.79	5.00E-05	2.16E-03				
12	<i>GUCA2B</i>	guanylate cyclase activator 2B (uroguanylin)	-2.97	5.00E-05	2.16E-03				
12	<i>CDX1</i>	caudal type homeobox 1	-3.14	5.00E-05	2.16E-03				
12	<i>CDX4</i>	caudal type homeobox 4	-3.18	5.00E-05	2.16E-03				
12	<i>CHRD</i>	chordin	-3.38	5.00E-05	2.16E-03				
12	<i>PDLIM3</i>	PDZ and LIM domain 3	-3.70	5.00E-05	2.16E-03	+			+

12	<i>RBP4</i>	retinol binding protein 4	-3.74	5.00E-05	2.16E-03				
12	<i>HOXB8</i>	homeobox B8	-3.76	5.00E-05	2.16E-03				
12	<i>APOB</i>	apolipoprotein B	-5.26	5.00E-05	2.16E-03	+			
14	<i>GUCA2B</i>	guanylate cyclase activator 2B (uroguanylin)	5.27	5.00E-05	1.23E-03				
14	<i>RBP4</i>	retinol binding protein 4	2.49	5.00E-05	1.23E-03	+			
14	<i>SLC7A9</i>	Solute Carrier Family 7 Member 9	2.39	4.50E-04	8.97E-03				
14	<i>VIPR2</i>	Vasoactive Intestinal Peptide Receptor 2	1.99	1.35E-03	2.26E-02			+	
14	<i>SULT1C3</i>	Sulfotransferase Family 1C Member 3	1.62	7.00E-03	8.66E-02				
14	<i>GBP</i>	guanylate binding protein	-1.57	4.55E-02	3.26E-01				
14	<i>AKR1B10</i>	aldo-keto reductase family 1, member B10 (aldose reductase)	-1.59	4.15E-03	5.72E-02				
14	<i>OVAL</i>	ovalbumin (SERPINB14)	-1.95	4.80E-03	6.40E-02				

Table 1. Filtered Differentially Expressed Genes and Genetic Association Database Analysis.

All DEGs were filtered for significance and a >1.5 fold or < -1.5 fold change in expression. GAD analysis was conducted to determine associated diseases.

Further, pathway enrichment analysis (KEGG) demonstrated an overrepresentation of genes involved in cardiac muscle contraction and adrenergic signaling in cardiomyocytes with a 2-fold expression increase from HH10 to HH12. With longer exposure to PHE (HH 14), pathways in cellular processes including migration, proliferation, metabolism, and survival are significantly affected. Strikingly, biological themes from the gene ontology (GO) analysis included ventricular cardiac muscle tissue morphogenesis (HH10, genes = 5, $p \leq 1.74 \times 10^{-6}$; HH12, genes = 6, $p \leq 1.92 \times 10^{-5}$), cardiac muscle contraction

(HH10, genes = 3, $p \leq 7.43 \times 10^{-3}$; HH12, genes = 6, $p \leq 1.11 \times 10^{-4}$), regulation of muscle contraction (HH10, genes = 3, $p = 7.49 \times 10^{-4}$; HH12, genes = 3, $p \leq 1.13 \times 10^{-2}$), BMP signaling pathway involved in heart development (HH10, genes = 2, $p = 1.75 \times 10^{-3}$, HH12, genes = 2, $p = 6.84 \times 10^{-2}$), heart looping (HH12, genes=6, $p = 6.00 \times 10^{-3}$, HH14, genes = 3, $p = 2.00 \times 10^{-2}$), and heart morphogenesis (HH12, genes=4, $p = 1.39 \times 10^{-2}$, HH14, genes = 2, $p = 9.30 \times 10^{-2}$). Data shown in Table 2 for all resultant cardiac specific themes.

Stage	KEGG pathway	Gene Count	p-value
HH10	Cardiac muscle contraction	6	1.14E-04
HH10	Pentose phosphate pathway	3	1.38E-02
HH10	Adrenergic signaling in cardiomyocytes	5	1.64E-02
HH10	Fructose and mannose metabolism	3	2.50E-02
HH12	Cardiac muscle contraction	13	3.59E-07
HH12	Focal adhesion	19	2.50E-05
HH12	Oxidative phosphorylation	14	8.23E-05
HH12	Tight junction	11	6.34E-03
HH12	Regulation of actin cytoskeleton	13	1.28E-02
HH12	Adrenergic signaling in cardiomyocytes	10	1.64E-02
HH12	Dorso-ventral axis formation	4	3.38E-02
HH14	Fructose and mannose metabolism	4	8.60E-04
HH14	Galactose metabolism	4	9.50E-04
HH14	Focal adhesion	6	5.70E-03
HH14	Pentose and glucuronate interconversions	3	6.40E-03
HH14	Glycerolipid metabolism	3	4.50E-02
Stage	Gene Ontology-Cardiac Specific Enriched Go Terms	Gene Count	p-value
HH10	Ventricular cardiac muscle tissue morphogenesis	5	1.74E-06
HH12		6	1.92E-05
HH12	Regulation of heart rate	6	3.20E-05
HH10	Cardiac muscle contraction	3	7.43E-03

HH12		6	1.11E-04
HH10	Regulation of muscle contraction	3	7.49E-04
HH12		3	1.13E-02
HH12	Heart development	12	5.72E-04
HH12	Regulation of cardiac muscle contraction by regulation of the release of sequestered calcium ion	3	3.54E-03
HH12	Regulation of myotube differentiation	3	3.54E-03
HH10	BMP signaling pathway involved in heart development	2	1.75E-02
HH12		2	6.84E-02
HH12	Heart looping	6	6.00E-03
HH14		3	2.00E-02
HH12	Heart morphogenesis	4	1.39E-02
HH14		2	9.30E-02
HH12	Cardiac myofibril assembly	4	1.32E-03
HH12	Artery morphogenesis	4	5.59E-03
HH12	Atrial septum morphogenesis	3	2.94E-02
HH12	Cardiac left ventricle formation	2	6.84E-02
HH12	Myoblast fusion	3	4.52E-02
HH12	Patterning of blood vessels	4	4.42E-02
HH12	Positive regulation of angiogenesis	6	2.49E-02
HH12	Positive regulation of myoblast differentiation	3	8.34E-02
HH12	Angiogenesis	9	1.46E-02
HH12	Positive regulation of myotube differentiation	3	2.26E-02
HH12	Regulation of ventricular cardiac muscle cell membrane repolarization	3	2.26E-02
HH12	Vasculogenesis	5	2.40E-02

Table 2. Functional Annotation HH10, 12, and 14.

DAVID was utilized to perform KEGG and GO analysis. Themes at each stage in development as well as gene number and significance are displayed. GO analysis is limited to cardiac specific themes.

Role of Retinoic Acid (RA) in MPKU

As the role of RA in MPKU has not been previously addressed in the literature, we further investigated gene expression in RA metabolism and target response. We analyzed 81 genes (Supplemental Figure 12) and we observed 42 genes with >1.5 or <-1.5 fold change in expression. We observed a total of 4 genes were up-regulated in response to PHE and the remaining 38 were down regulated. Combining data from RNA-Seq (Supplemental Table 1) and qRT-PCR (Supplemental Figure 12), notably, 15 unique genes with a significant role in Retinoic Acid (RA) metabolism and transport (HH10 = 4 genes, HH12 = 5 genes, HH14 = 14 genes). Interestingly, this observation was confirmed in pathway analysis (HH12, cellular response to retinoic acid, genes = 5, $p \leq 7.55 \times 10^{-3}$; HH14, RA receptor signaling pathway, genes = 2, $p = 3.80 \times 10^{-2}$) (Table 2 and Supplemental Table 2).

Discussion

In this study, we report the first elucidation of the molecular mechanisms of congenital heart defects in MPKU conducted at *early* developmental timepoints. We identified a total of 633 DEGs which provide an overabundance of possibilities for follow-up and interpretation.

Most intriguing is the unexpected significant role of RA clearly demonstrated to increase over time. RA signaling is known to be involved in multiple embryonic developmental processes and is highly regulated throughout development [58-60]. Vitamin A (retinol) is oxidized to its active metabolite RA in a developing embryo [26, 27]. RA is then able to act as a transcription factor by entering the nucleus through nuclear receptors to induce developmental gene expression or repression [25].

Not surprisingly then, perturbations in RA can lead to cardiac defects including TGA, muscular VSDs, DORV, membranous VSD, PTA and aortic arch arteries anomalies [as reviewed in [32, 33, 61]. These type of defects are very similar to those seen in MPKU associated CVMs in mouse and human [12, 45].

Strikingly, MPKU has often been compared to Fetal Alcohol Syndrome (FAS) due to their similar facial dysmorphologies (with many clinicians noting they are indistinguishable upon examination) [46]. One proposed mechanism for the development of FAS is the competitive inhibition of RA metabolism with preference for ethanol detoxification [62-65]. Thus, the clinical features of FAS are due to *decreased* presence of RA and our findings demonstrate downregulation of

gene expression directly in RA pathways are associated with CVM development in a model of MPKU.

One may predict that subsequent downstream pathways induced by RA may be affected as well. The increased effect on the RA pathway over these stages correlates with the increased demand for RA metabolism for the developing embryo [23, 31, 65]. At HH 10 the need for RA metabolism is less than in HH 12 and 14. By HH 14 the need for RA metabolism is evident in the analysis of the gene expression functioning in transport, metabolism, and catabolism of RA. A potential explanation for this is that PHE interferes with the conversion to RA and results in a deficit of nuclear RA, thus causing transcriptional increase for carrier proteins Retinol Binding Protein 4 (*RBP4*) and Transthyretin (*TTR*) to alleviate the deficit. Furthermore, Cytochrome P450 Family 26 (*CYP26*) proteins are downregulated, indicating that RA is not undergoing catabolism and elimination from the cell is not necessary. This would support the lack of RA availability for catabolism because it is not metabolized from retinol by Alcohol Dehydrogenase 1C (*ADH1C*) because of decreased levels of substrate (Figure 3). Additionally, this theory is supported by the similarity of defects observed in human and animal models of Vitamin A Deficiency (VAD) and MPKU [66-68].

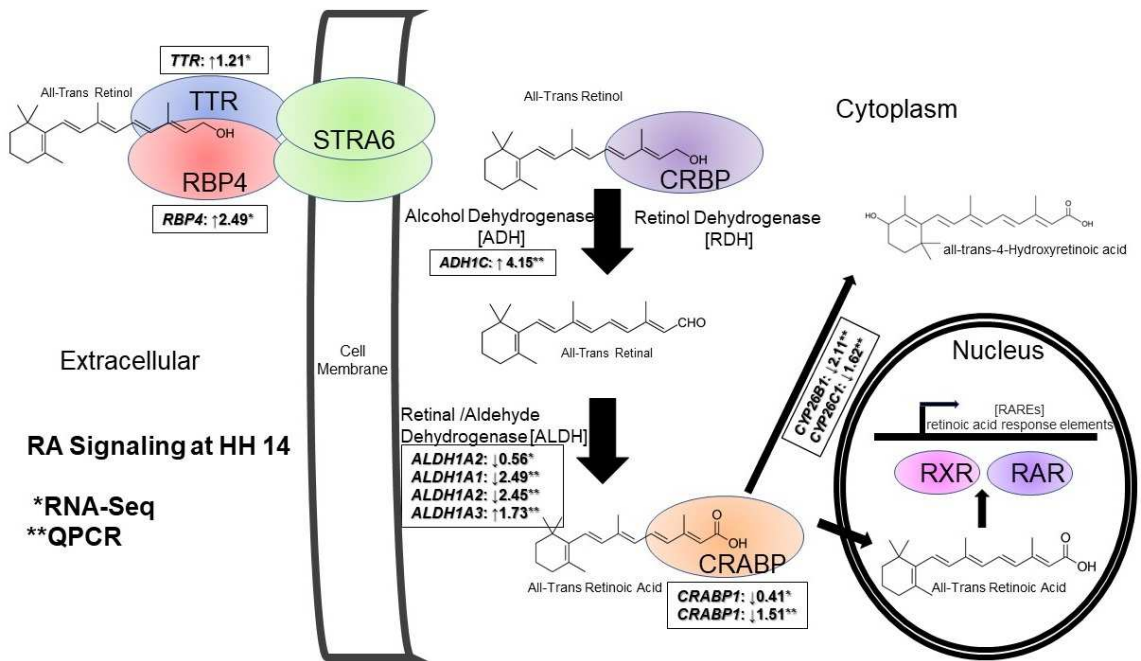


Figure 3. Retinoic Acid Metabolism at HH14.

DEGs and qRT-PCR results for HH14 of RA metabolism genes and transporters. Data from RNA-Seq denoted with 1 asterisk and qRT-PCR with 2 asterisk.

These findings lead to many additional questions. At this point, it is unclear whether perturbing the RA pathway is the only cause of MPKU associated CVMs, but there is sufficient evidence to warrant further investigation. In-vitro experiments with RA inhibitors to investigate cellular migration and proliferation are a logical next step with additional biochemical experiments to determine enzyme inhibition. One limitation in this study is the known phenotypic variability and incomplete penetrance that occur in MPKU that can

result in small gene expression difference but have a significant spectrum of developmental effects.

Conclusion

Here, we report the first elucidation of the molecular mechanisms of congenital heart defects in MPKU conducted at *early* developmental timepoints. We provide evidence suggesting a link between PHE exposure and the alteration of RA pathway.

Acknowledgements

The authors would like to thank Jennie Lynn Rowell, PhD, RN for critical manuscript editing and review. Additionally, the authors would like to thank Dr. Shannon Conley, PhD, Dr. Eric Howard, PhD and Elizabeth Bullen for technical support and advisement.

Funding

This work was supported by the National Institute of General Medical Sciences of the National Institutes of Health under award number P20GM103447. The content is solely the responsibility of the authors and does not necessarily represent the official views of the National Institutes of Health.

Additional funding was provided by University of Central Oklahoma (UCO), College of Mathematics and Science, Center for Undergraduate Research and Education in Science, Technology, Engineering, & Mathematics and UCO Office of High-Impact Practices, Student Research, Creative, and Scholarly Activities (RCSA) Grant to JNW.

CHAPTER 3. *In-vivo* Molecular Gene Expression Analysis

Introduction

In developmental biology *in-situ* hybridization (ISH) is a molecular biology technique used to investigate qualitative changes in gene expression in tissue. Most importantly, ISH is utilized to look at temporal and spatial changes in gene expression. Small changes can lead to CMVs in the developing embryo; therefore, we used this molecular technique to visualize mRNA expression in the chick embryo. Previously, ISH has been successfully established in the whole chick embryo [69-71]. Additionally, a database of ISH is published on GEISHA (Gallus Expression *In-Situ* Hybridization Analysis) and can be used as a reference for validation of probes. After analysis of RNA-Seq data from HH14, we sought to establish ISH in the lab. Therefore, we cloned genes of interest for ISH from the RA pathway and genes of known biological significance in heart development for future analysis of heart defect (Table 3). Here in we present two probes for HH14 for Fibroblast Growth Factor 8 (*FGF8*) and Cellular Retinoic Acid Binding Protein 1 (*CRABP1*). *FGF8* was used in ISH because of its known role in CVMs involving the cardiac outflow tract and *CRABP1* was DE in RNA-Seq and qRTPCR data.

CRABP1 expression results in an intracellular binding protein with a specific affinity for RA. It has similar homology to *CRBP* which binds to retinol. *CRABP1* functions among *CRABP2*, *CRBP1-3*, *STRA6*, *FABP5*, *TTR*, and *RBP4*, which all function in Vitamin A transport through retinol or RA to cells from the serum to intracellular transport regulating retinoid homeostasis. *CRABP1* functions in directing RA catabolism and delivery to nuclear receptors at which point RA can act as a transcription factor [72]. *CRABP1* is expressed in multiple tissues and functions in regulating RA concentrations. *CRABP1* may also contribute to RA toxicity when vitamin A is in excess by preventing the removal of metabolites [72].

FGF8 is part of the fibroblast growth factor (FGF) signaling pathway. The FGF pathway is a molecular pathway known to function in early cell to cell communication in embryo development. It has been previously reported that fluctuations in *FGF8* signaling can negatively affect heart development [73]. With reduced *FGF8* expression affecting heart development causing heart defects in the outflow tract and great vessels. *FGF8* signaling occurs through the pharyngeal arches (PA) epithelia to the mesenchymal cells, cNCCs, that migrate through the PA later forming the outflow tract and heart [74]. It has been previously shown

by Macatee et, al, that ablating *FGF8* signaling in the PA results in aortic arch and subclavian artery anomalies in 95% of mice with *FGF8* ablated[75]. Additionally, ablating *FGF8* in the PA ectoderm resulted in severe cardiac OFT septation, alignment, and vascular defects [75].

Gene	Marker	Function [Ref Seq]	Forward Sequence	Primer	Reverse Sequence	Primer	Ref
<i>Aldh1a2</i>	Anterior/posterior cardiac patterning. Retinol acid signaling pathway	Enzyme that catalyzes the synthesis of retinoic acid (RA) from retinaldehyde. Establish local embryonic retinoic acid levels which facilitate posterior organ development. Embryonic RA synthesis is required for heart looping, development of posterior chambers and proper differentiation of ventricular cardiomyocytes.	CACGCTATTTTCTGC TGCCT		GGGCTGGAGTTTTC AACAGG		[58]
<i>CRABP1</i>	Retinoic acid signaling	Intracellular protein that function in retinoic acid (RA) catabolism and delivery to nuclear receptors. May function in regulating RA concentrations.	AAATGCAGGAGTTT GGCCAC		GGTCACATACAACA CCGCAT		[71]
<i>FGF8</i>	Secondary heart field and outflow tract	Secreted signaling protein with mitogenic and cell survival activities, and are involved in a variety of biological processes, including embryonic development, cell growth, and morphogenesis.	GGTAACTGTTTCAGTC CCCACC		CTTGCCGATCAGTT TCCCCT		[72, 74]
<i>Isl1</i>	Heart	Transcription factor functioning in myocyte formation and function. <i>Isl1</i> is repressed by heart developmental genes such as <i>NKX 2.5</i> in normal heart development.	GCAGATGGCAGCAG AACC		TTCCAGGGTGGCT GGTAAC		[75]
<i>NKX 2.5</i>	Global patterning of the heart	Transcription factor functioning in heart formation and development. Mutations in this genes cause multiple cardiac malformations including atrial septal defect and tetralogy of Fallot.	CCTTCCCCGGCCCCT ACTAC		CTGCTGCTTGAACC TTCTCT		[76, 77]
<i>NPPA</i>	Atria	Transcription Factor, <i>Nppa</i> is initiated in the developing atrial and later in the working ventricular myocardium.	TGAACCCAAGCTAG CATCCA		GCAACAGACAGGA GAGAGGT		[78]
<i>PlexinA2</i>	Neural crest cell migration into the outflow tract	Transmembrane receptor complex for ligand semaphorins, triggering a cellular signal transduction cascade that leads to axon or neural crest cell migration guidance, either repulsion or attraction. Mutations in the <i>is</i> gene cause cardiac hypertrophy associated polymorphism.	GCTATGAGTGTGTGC TGAGC		GGGTTGGAGCATT GACGTT		[79, 80]
<i>RBP4</i>	Vitamin A/ Retinol transport	Specific carrier for retinol in the blood. Retinol is delivered by RBP4 and TTR complex from the liver to cells.	GGACAGGATGGCCT ACACAT		TCAGCACAAGTGCC ATCTTC		[23]
<i>TTR</i>	Vitamin A/ Retinol transport	Specific carrier for retinol in the blood. Retinol is delivered by RBP4 and TTR complex from the liver to cells.	AAAAGGCTGCAGAT GGAACC		GAGGAGAGCAGCG ATGGTAT		[81]

Table 3. Genes Cloned for *In Situ* Hybridization

Materials and Methods

RNA Extraction and Cloning

To prepare the cDNA library, RNA was extracted with PicoPure™ RNA Isolation Kit from 6 multistage embryos according to manufacturer's protocol (Thermo Fisher Scientific, KIT0204); a cDNA library was constructed according to manufacturer's protocol using 2 µg of cDNA (Fisher Scientific, Hampton, NH, US, Applied Biosystems, 4368814). Primers for the gene of interest were used to amplify a 200-500 bp fragment. Gene descriptions and primer sequences used are listed in Table 3. The primers were amplified using polymerase chain reaction (PCR) and cDNA. PCR products for the gene were generated using GoTaq then excised as the insert and gel purified (Promega Madison, WI, US, M7122) (Sigma St. Louis, MO, US, NA1111-1KT). Purified DNA fragments were ligated into a pGEM-T vector (Supplemental Figure 9) (Fisher Scientific, PR-A1360) or pMini T 2.0 (Supplemental Figure 10) from PCR cloning kit (NEB, Ipswich, MA, US, E1202S) and transformed into *Escherichia coli* Top10 competent cells according to manufacturer's protocol (Fisher Scientific, C404010). Competent cells were cultured on LB agar plates with ampicillin (100mg/ml) and x-gal agar then incubated at 37°C overnight. Single white colonies were selected when applicable and the insert was confirmed using colony PCR. Colonies with inserts were

cultured in 4 ml Luria–Bertani (LB) liquid medium containing ampicillin (100 mg/ml) and grown overnight 37°C.

The cultures were mini-prepped (Midsci, St. Louis, MO, US, IB47171) and sent for sequencing using primers for SP6 and T7 promoters at Oklahoma Medical Research Foundation (OK, USA). The sequences were analyzed using Snapgene (<http://www.snapgene.com>) and Blast (<https://blast.ncbi.nlm.nih.gov/Blast.cgi>) to confirm the presence of the insert and its orientation in relation to the SP6 and T7 promoters. Using the location and orientation of the insert the antisense and sense promoters were determined.

Plasmid Linearization and *in vitro* Transcription

The DNA quality and quantity was analyzed using a Nanodrop spectrophotometer (Thermo Scientific). The confirmed plasmid was then maxi-prepped (Sigma, NA0300-1KT). The plasmid was then linearized upstream of both the SP6 and T7 promoters using 10 µg of plasmid and restriction enzymes (NEB). Enzymes were incubated for 2 hrs to overnight at 37°C. The linearization was confirmed on 0.7% agarose gel. The DNA was ethanol precipitated and used for *in vitro* transcription reactions.

The linearized plasmid was purified using phenyl:chloroform:isoamyl alcohol and ETOH precipitation. The linearized plasmid DNA was then used for

in vitro transcription reaction. In separate reactions for SP6 and T7 promoters, 1 µg of the linearized plasmid DNA was incubated with either SP6 polymerase (Fisher Scientific, FEREP0131) or T7 polymerase (Sigma, 10881767001) and RNase inhibitor (Fisher Scientific, 10-777-019) to transcribe riboprobes for the antisense and sense strands with labeled digoxigenin (DIG) oligonucleotides (Sigma 11277073910) according to manufacturer's protocol. The riboprobes were then checked for synthesis using 0.7% agarose gel electrophoresis. The riboprobe was then purified and ethanol precipitated. Riboprobes were stored -80°C for *in situ* hybridization.

Injections and Incubation Conditions of Embryos

Fertilized white leghorn chicken eggs were obtained from Texas A&M Poultry Sciences. Eggs were incubated at 37.2°C and 50% humidity until HH 6. For injections eggs were removed from the incubator and the shell of the eggs was sterilized using a 70% ethanol. Using the 16 gauge needle, a small hole was drilled at the blunt end of the egg. Eggs were treated with either sterile filtered 2.5 mM PHE or vehicle control (1 x PBS) through the blunt end of the egg (yolk injection). A 27 gauge needle was inserted into the hole and 200 µl of carrier vehicle or 2.5 mM PHE was injected as described in the egg yolk Drake, et al [50]. After yolk injection the hole in the shell was sealed with tape and the embryos were further

incubated until HH14. At HH14, the whole embryo was dissected out of the yolk, rinsed with 1xPBS. Embryos were then fixed for 2 hours in 4% PFA at 4°C.

In-situ Hybridization

The samples underwent wholemount *in situ* hybridization (WISH) experiments as described in [76]. WISH was performed on at least 3 embryos each from the vehicle control and PHE treated groups using both antisense and sense riboprobes. Fixed embryos were incubated with 10 mg/ml proteinase K and re-fixed with 0.02% glutaraldehyde and 4% paraformaldehyde. Embryos were acclimated in hybridization buffer without probe for 1hr before adding riboprobes. Hybridization with digoxigenin labeled riboprobes under stringent conditions (2X SSC and 50% formamide) for 2-5 days (depending on probe properties). After incubation with riboprobes, embryos were extensively washed and blocked (Sigma 11096176001) prior to adding anti-DIG antibody. Embryos were incubated in 1:1000 anti-digoxigenin AP- conjugate (DIG) (Sigma 11093274910) overnight at 4°C. After extensive washing, embryos were then developed using 1:5 BM Purple with 10% PVA enhancement (Sigma 11093274910). Embryos were imaged with an Olympus stereomicroscope and an Olympus DP73 camera. Imaging software used was CellSens Entry from Olympus (Olympus, Tokyo, Japan). mRNA levels are assessed qualitatively by comparing vehicle only

control DIG labeling to DIG labeling in PHE treated embryos.

Results and Discussion

CRABP1 mRNA Expression in HH14

In GEISHA an online database of published *in situ* work, *CRABP1* has been previously reported at stage HH14 to be expressed in the pharyngeal arches and clefts (PA), ear and otic placode, face mesenchyme, spinal cord, and neural crest cells. In PHE treated embryos we saw reduced expression in face mesenchyme. Expression was increased in the spinal cord, ear and otic placode, and neural crest in the PHE treated when compared to vehicle control embryos. PA expression was low in both PHE and vehicle control embryos (Figure 4).

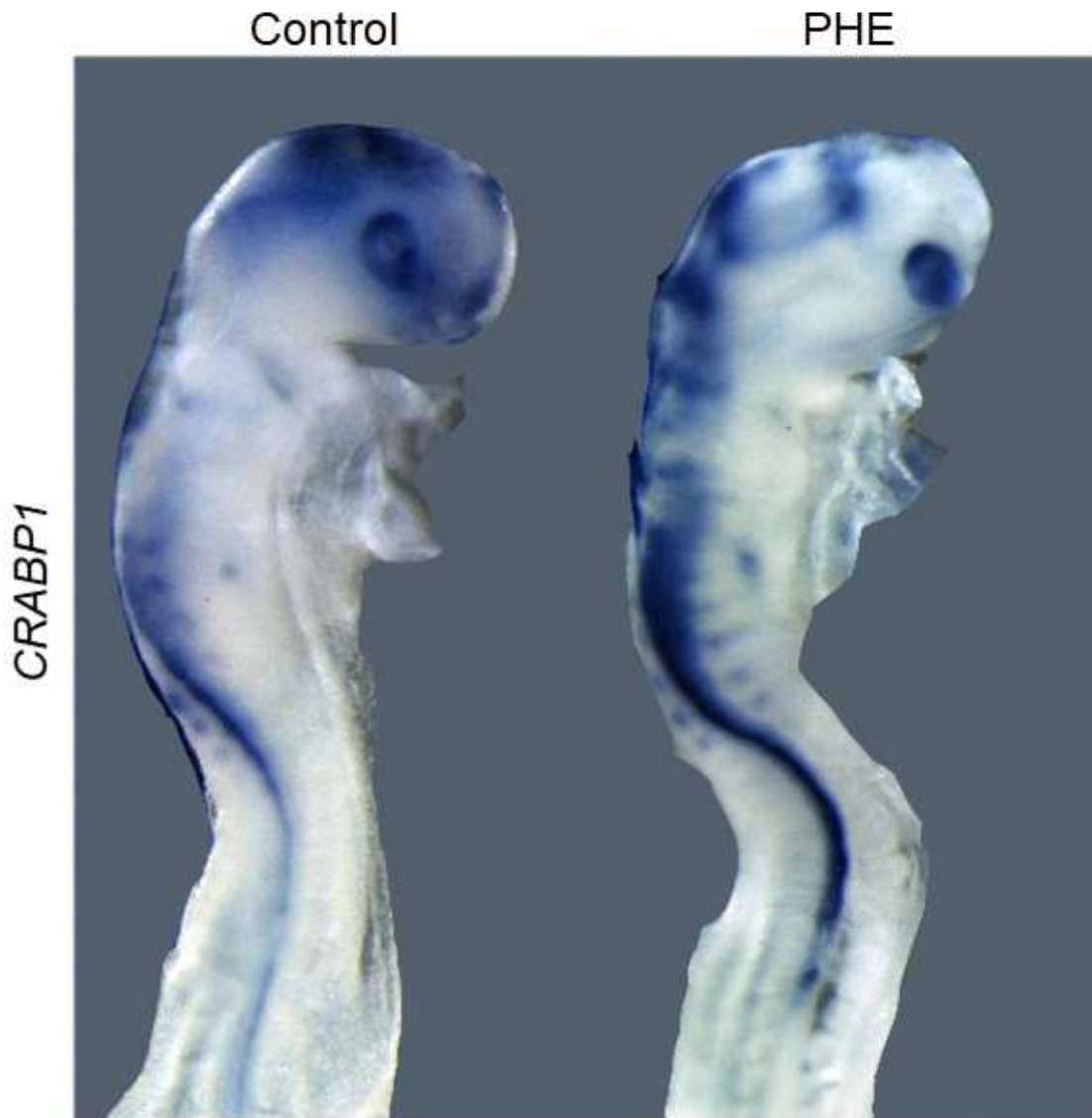


Figure 4. *CRABP1* mRNA Expression in a Microenvironment of 2.5 mM PHE.

Representative images of *CRABP1* mRNA expression in vehicle control and PHE treated embryos, 2x magnification.

***FGF8* Expression Signaling in the Presence of PHE in HH14**

At stage HH14 *FGF8* is expressed in the eye, face mesenchyme, midbrain, pharyngeal arches and clefts, somites, and tail [77]. In vehicle control embryos

expression is similar. When compared to PHE treated embryos there was reduced *FGF8* expression in the face mesenchyme, midbrain, somites, pharyngeal arches (PA), and tail (Figure 5).

Although there is no *FGF8* expression in the heart, *reduced* expression of *FGF8* signaling in the PA will negatively affect heart development of the chick embryo. This is due to *FGF8* expression inducing cNCCs to migrate in and populate the heart to later form the outflow tract and great vessels. This reduced *FGF8* expression will lead to CVMs in the developing chick heart. Data from morphological studies in the lab show gross CVMs in the developing embryos (data not shown). Considering the variable penetrance of MPKU phenotypes the effects of PHE on *FGF8* may be the cause of varying morphological changes in the heart.

In addition to CVMs, reduced expression of *FGF8* in PA also leads to craniofacial defects. As shown in PHE treated embryo expression in face mesenchyme is reduced and embryos frontonasal mass is noticeably shorter than vehicle control embryo. Craniofacial defects have been previously reported when *FGF8* signaling is ablated further lending to the effects of reduced *FGF8* signaling on NCCs [75]. Overall, these data lend to PHE interfering with *FGF8* signaling in the PA ultimately leading to CVMs and craniofacial defects.

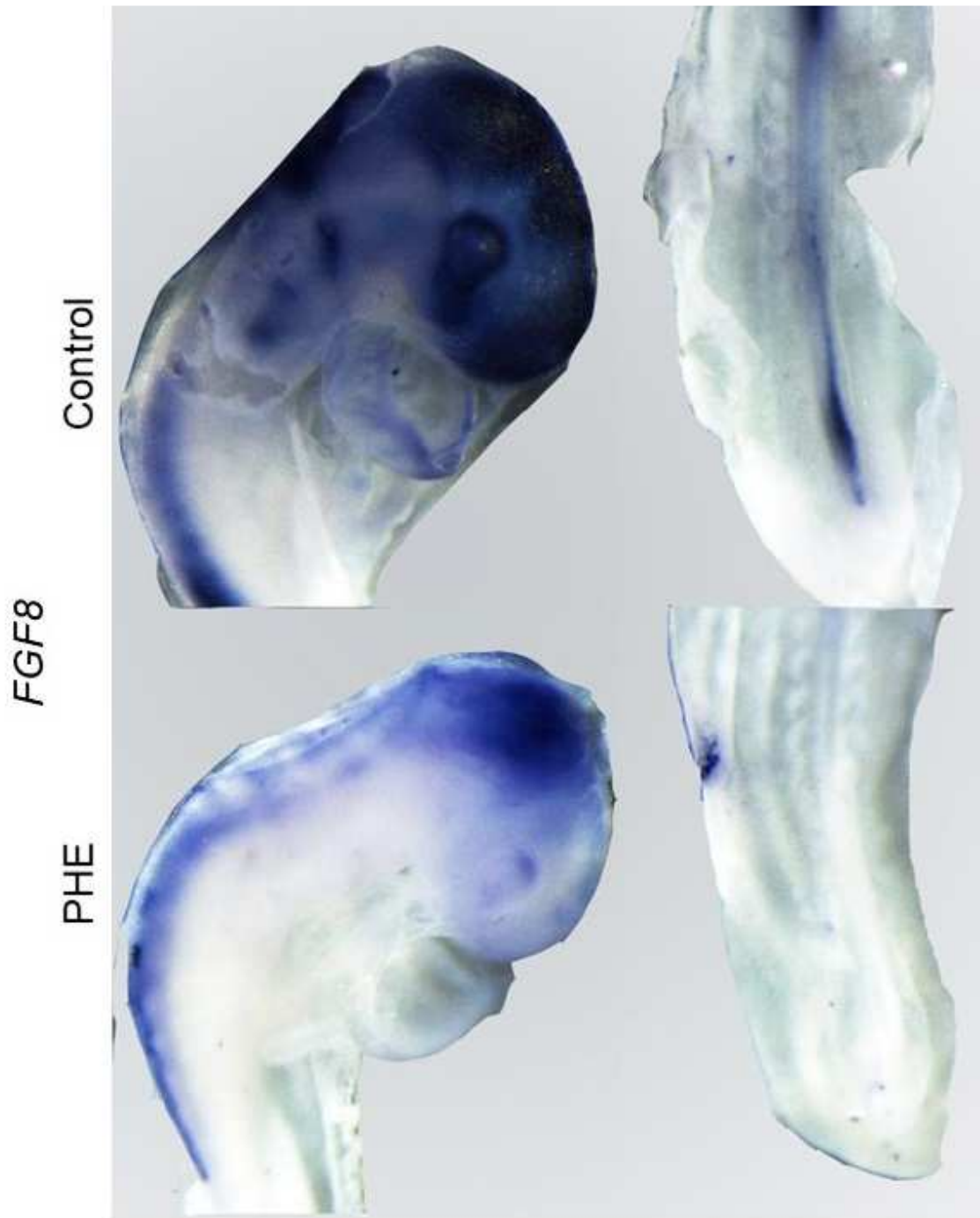


Figure 5. *FGF8* mRNA Expression in a Microenvironment of 2.5 mM of PHE.

Representative images of *FGF8* mRNA for vehicle control and PHE treated embryos, images A taken at 1.25x, B and C at 4x.

Chapter 4: Summary and Conclusions

To investigate cardiac malformations in developing chick embryos, we investigated alterations in gene expression during heart development in a microenvironment of PHE, a known teratogen. Currently, there is no known mechanism of CVMs in MPKU and this work has identified a major developmental pathway affected. We hypothesized that chick embryos exposed to high PHE will develop heart defects in the aortic arch arteries (AAA) and the outflow tract (OFT) resultant from alterations in gene and protein expression in the cardiac and surrounding tissue. To test this hypothesis, we used RNA-Seq, qRT-PCR, and *in situ* hybridizations.

We conducted whole transcriptome sequencing to analyze mRNA expression in the heart and thoracic region at HH10, 12, and 14, to generate potential targets for further investigation. We compared PHE treated embryos to vehicle control (PBS) embryos to determine DEGs in the heart. MPKU cardiac teratogenicity has no known cause; therefore, this RNA-Seq data has allowed us to better understand alterations in heart development in the presence of PHE. Genes known for their significance in heart development and genes identified through RNA sequencing were further investigated through qRT-PCR and *in situ* hybridization.

Retinoic Acid Signaling Plays a Role in Heart Development.

The metabolism of Vitamin A into RA occurs via multiple enzymes and in different locations throughout development. RA acts as a morphogen and serves as a major pathway in embryonic development. In review of the literature, RA signaling is important in heart development and alterations either increasing or decreasing levels of RA can cause significant developmental defects. Perturbations in RA have led to cardiac defects including TGA, muscular VSDs, DORV, membranous VSD, PTA and aortic arch arteries anomalies [as reviewed in [61]]. These type of defects are very similar to those seen in MPKU associated CVMs in mouse and human, thus warranting further analysis [12, 45]. Based upon the RNA-Seq data we have analyzed from HH stages 10, 12, and 14 (Supplemental Table 1) the RA pathway is consistently DE across all three stages. Beginning with HH10, 4 genes directly involved in the transport of RA are DE with additional DEGs affected by the RA pathway. Both *RBP4* and *TTR* are down-regulated indicating a decreased level of RA in the extracellular space and decreased transport of retinol to cell surface receptors. Intracellular, downstream retinal and RA carriers, *CRABP1* and *FABP2* were also DE, with a downregulation of *CRABP1*.

Gene expression testing for HH12 revealed the same genes DE as in HH10, but with the addition of *ALDH1A2*. The *ALDH1A2* gene encodes the enzyme

responsible for the metabolism of retinal to RA. In the presence of PHE at HH12, *RBP4*, *TTR*, and *ALDH1A2* are downregulated and *CRABP1* is upregulated.

Additionally, HH14 embryos were analyzed with RNA-Seq and qRT-PCR. In HH14, there are 10 DEGs found in the RA pathway including: *RBP4*, *TTR*, GATA Binding Protein 4 (*GATA4*), *CRABP1*, Alcohol Dehydrogenase 1C (*ADH1C*), Aldehyde Dehydrogenase 1 Family Member A1 (*ALDH1A1*), Aldehyde Dehydrogenase 1 Family Member A3 (*ALDH1A3*), Cytochrome P450 Family 26 Subfamily B Member 1 (*CYP26B1*), and Cytochrome P450 Family 26 Subfamily C Member 1 (*CYP26C1*). At this time point we see an increase in gene expression for *RBP4*, *TTR*, and *ADH1C*, an enzyme metabolizing retinol to retinal with the expression of all other genes in the pathway downregulated. *ALDH1A2* and *ALDH1A1*, retinal dehydrogenases are downregulated except for *ALDH1A3*, which is primarily expressed in tissues outside of the heart. *CRABP1* and the cytochromes are downregulated. These changes indicate decreased nuclear availability of RA causing a decrease in target gene expression. A potential explanation for this is that PHE interferes with *ADH1C* and prevents the conversion of retinol to retinal and a lack of nuclear RA, thus causing transcriptional increase for carrier proteins *RBP4* and *TTR* to alleviate the deficit. Furthermore, *CYP26* expression is downregulated, indicating that retinoic acid is

not undergoing catabolism and elimination from the cell is not necessary. This would support the lack of RA availability for catabolism because it is not metabolized from retinol by *ADH1C* because of decreased levels of substrate. Additionally, this theory is supported by the similarity of defects observed in human and animal models of VAD and MPKU.

Overall the effect on the RA pathway increases from HH10, 12, and 14 as demonstrated by an increasing number of genes affected over time (Figure 6). One may predict that subsequent downstream pathways induced by RA may be affected as well. The increased effect on the RA pathway over these stages correlates with the increased demand for RA metabolism for the developing embryo. At HH10 the need for RA metabolism is less than in HH12 and 14. By HH14 the need for RA metabolism is evident in the analysis of the gene expression functioning in transport, metabolism, and catabolism of RA.

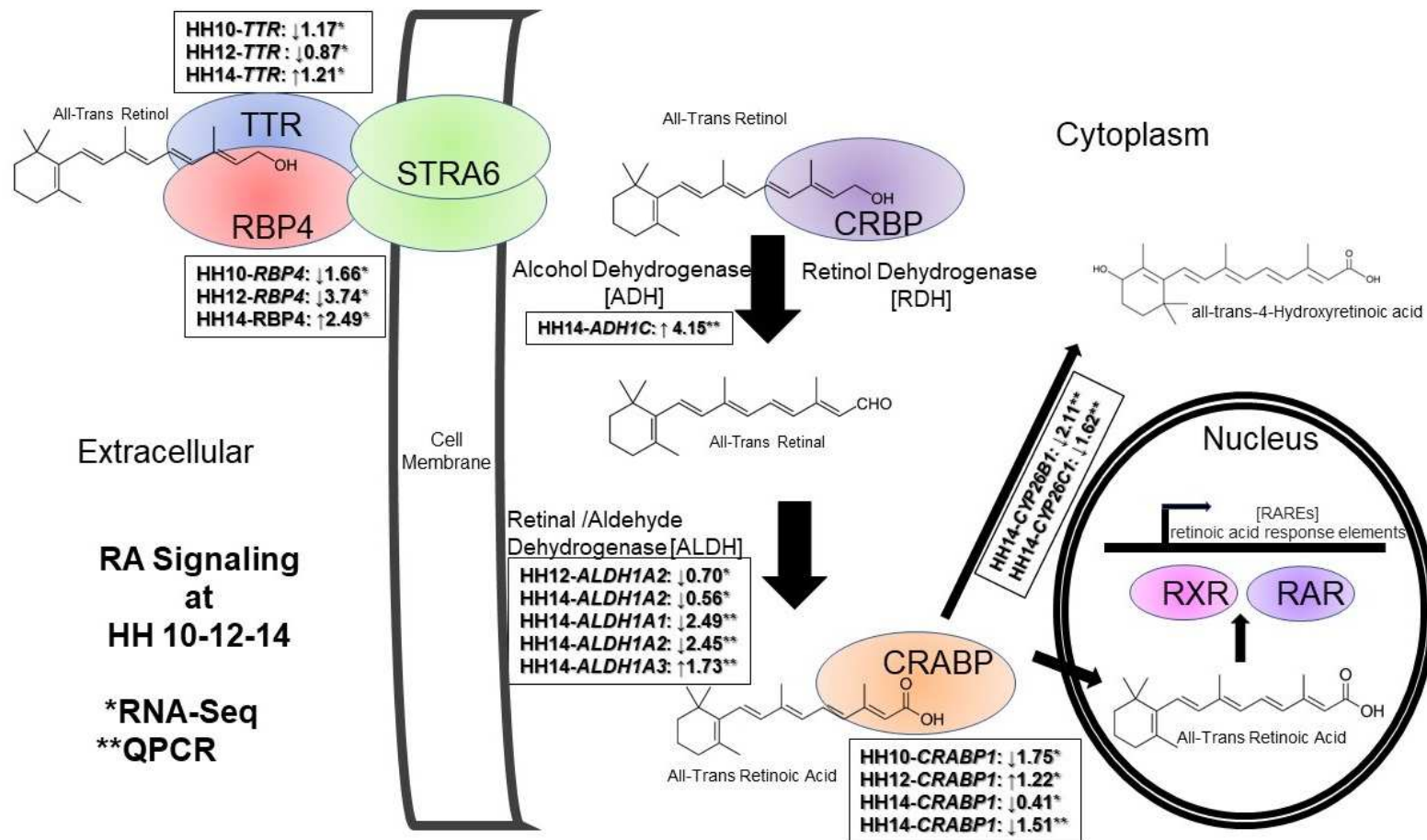


Figure 6. Retinoic Acid Pathway Differential Gene Expression.

Differential genes expression shown from RNA Seq analysis for HH stages 10, 12, and 14, indicated by stage and *. qRTPCR validation of HH14, indicated by **.

KEGG pathway analysis was used to understand the impact of all of the DEGs identified through RNA-Seq analysis. HH10 showed DE genes for heart related pathways including cardiac muscle contraction and adrenergic signaling in cardiomyocytes. Additionally, DEGs input for KEGG analysis show the pentose phosphate pathway (PPP) and fructose and mannose metabolism were significant which may be due to the lack of metabolism of PHE causing other metabolites to build up. Chick embryos lack Phenylalanine Hydroxylase (PAH), thus the ability to metabolize PHE until much later developmental stages than the stages studied. This increased amount of PHE offers an intermediate of the PPP, glycolysis, and mannose metabolism pathways. For HH12 the same cardiac pathways in muscle contraction and adrenergic signaling are significant, but the number of genes in each pathway increases over 2- fold. Embryos exposed to PHE longer display a significant effect on genes relevant to cardiac developmental processes including migration, proliferation, metabolism, and cell survival. Additionally, we begin to see significant effects on genes in patterning of the dorso-ventral axis, including genes known to cause heart and neural tube defects. Proper axis formation is essential for organogenesis, heart development and the prevention of heart defects. For HH14 similar pathways are significantly affected, functioning in metabolism, migration, proliferation, and cell survival.

In addition to KEGG pathway analysis, we investigated significant genes with Gene Ontology (GO) enrichment analysis identifying biological themes. In HH10, the largest numbers of genes are shown in DNA-templated transcription (11), multicellular organism development (7), negative regulation of neuron differential (6), ventricular cardiac muscle tissue morphogenesis (5), protein stabilization (4), and axon guidance (4). Additional significant cardiac biological themes enriched were cardiac muscle contraction (3) and BMP signaling pathway involved in heart development (2). Furthermore, other terms of note that can easily be tied into heart function and development were: stem cell differentiation (3), positive regulation of mesenchymal cell apoptotic processes (2), signal transduction involved in regulation of gene expression (3), protein localization to juxtapanode region of axon (2), Triglyceride catabolic process (2), and ion transport (2).

For HH12, we observed an increase in the number of significant genes attributed to each biological theme and an increase in the overall themes identified. Some of the biological themes identified in HH10 reoccur in HH12 with an increase in gene number such as DNA-templated transcription (36), multicellular organism development (17), axon guidance (13), cardiac muscle contraction (6), negative regulation of transcription regulatory region DNA

binding (3), platelet aggregation (6), protein complex assembly (12), regulation of muscle contraction (3), signal transduction involved in regulation of gene expression (4), and ventricular cardiac muscle tissue morphogenesis (6). Other pathways involved in cardiac function and development including: heart development (12), angiogenesis (9), regulation of heart rate (6), cardiac muscle contraction (6), heart looping (6), positive regulation of angiogenesis (6), cardiac myofibril assembly (4), artery morphogenesis (4), regulation of cardiac muscle contraction by regulation of the release of sequestered calcium ion, regulation of myotube differentiation (3), regulation of ventricular cardiac muscle cell membrane repolarization (3), atrial septum morphogenesis (3), and myoblast fusion (3). In addition to these themes, there are a large number of genes involved in transcription, translation, cell proliferation, migration, differentiation, and cell survival which could all contribute to the development of CVMs.

In analysis of HH14, there is a smaller list of DAVID GO terms, this may be attributed to the reduced power of analysis due to the pooling of vehicle control samples and decreased sample size. Additional sampling should be considered to investigate the effect of PHE at HH14. Nonetheless, there are reoccurring themes in cellular migration, survival, and transcription such as negative regulation of extrinsic apoptotic signaling pathway via death domain receptors (4), cell-matrix

adhesion (2), and transcription from RNA polymerase II promoter. Additionally, significantly affected heart related themes include: response to calcium ion (3), heart looping (3), and heart morphogenesis (2).

Focusing on RA signaling pathways observed in Enriched GO terms, RA signaling themes begin to show up in HH12 and continue to HH14. In HH12 cellular response to retinoic acid (5), and in HH state 14 there is retinoic acid receptor signaling pathway (2), and retinol metabolic process (2, p-value 0.063).

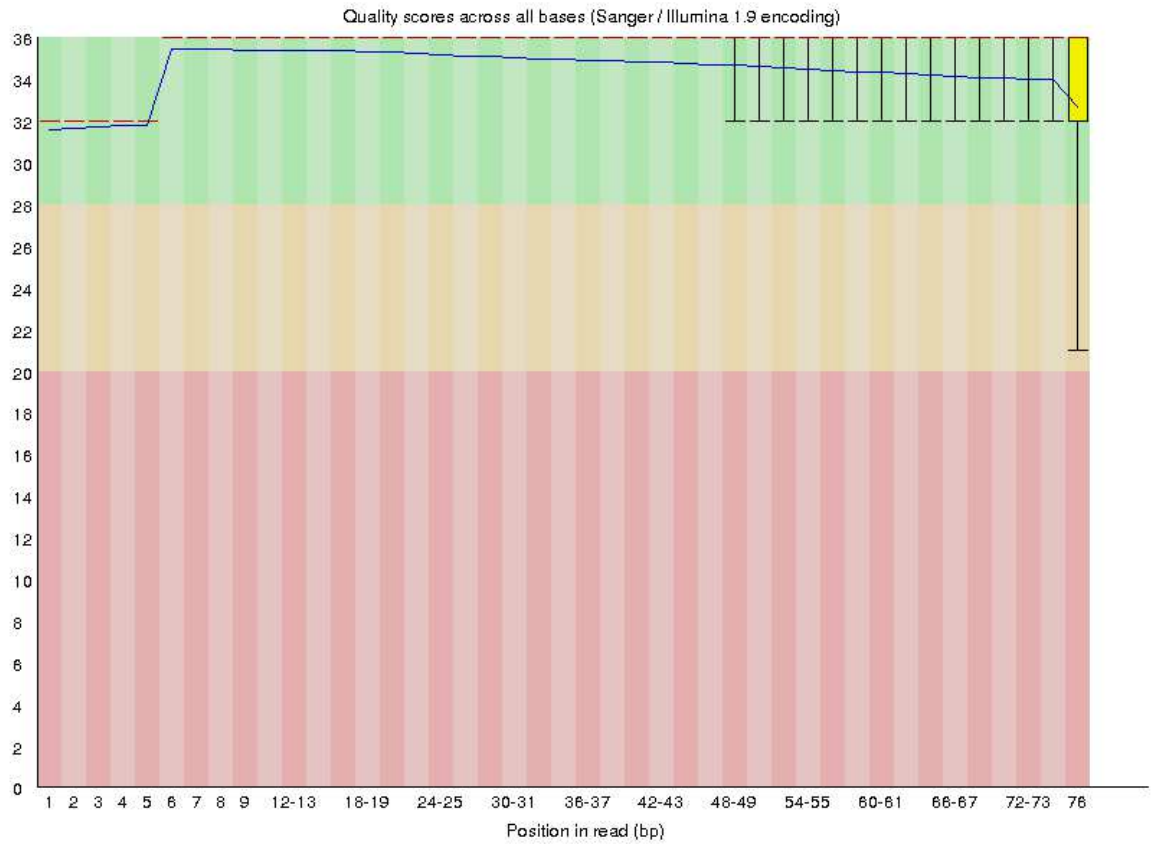
In-vivo analysis by *in situ* hybridization was conducted on several genes from the RA pathway and genes with a known role in heart development. Sequences were cloned into DNA expression vectors to be transcribed into labeled probes for future mRNA analysis. Initial *in-situ* analysis of *CRABP1* and *FGF8* indicates changes of mRNA expression that warrant further investigations of additional stages including HH10, 12, and 14. It is plausible that changes in expression may be too subtle to detect for some of the genes of the RA pathway.

This work has identified potential pathways to determine the mechanism(s) of CVMs in MPKU that were previously unknown and not investigated. In combination, the RNA-Seq and qRTPCR data have pointed to PHE perturbing the RA pathway, a known pathway significant in heart development. This data only begins to elucidate the mechanism by which PHE is perturbing the RA pathway

and to what extent. Therefore, these investigations provide solid foundation for future experiments. Historically, MPKU has shown phenotypic variability and incomplete penetrance, therefore gene expression fluctuation and small differences could cause a spectrum of developmental defects. This observation leads to many additional questions that must be asked and investigated. First, the effect of PHE on the RA pathway can be investigated with *in-vitro* experiments using known RA inhibitors such as DEAB to investigate cellular migration and proliferation. Secondly, using luciferase reporter systems PHE interference can be further explored *in-vitro* by using a RA response element. Third, additional genes can be studied using *in-situ* probes to analyze mRNA expression in the presence of PHE. Finally, biochemical experiments can be performed to investigate if PHE is competitively inhibiting enzymes such as ADH in the retinoic acid pathway. At this point, it is unclear whether perturbing the RA pathway is the only cause of MPKU associated CVMs, but there is sufficient evidence to investigate further.

Supplemental Figures

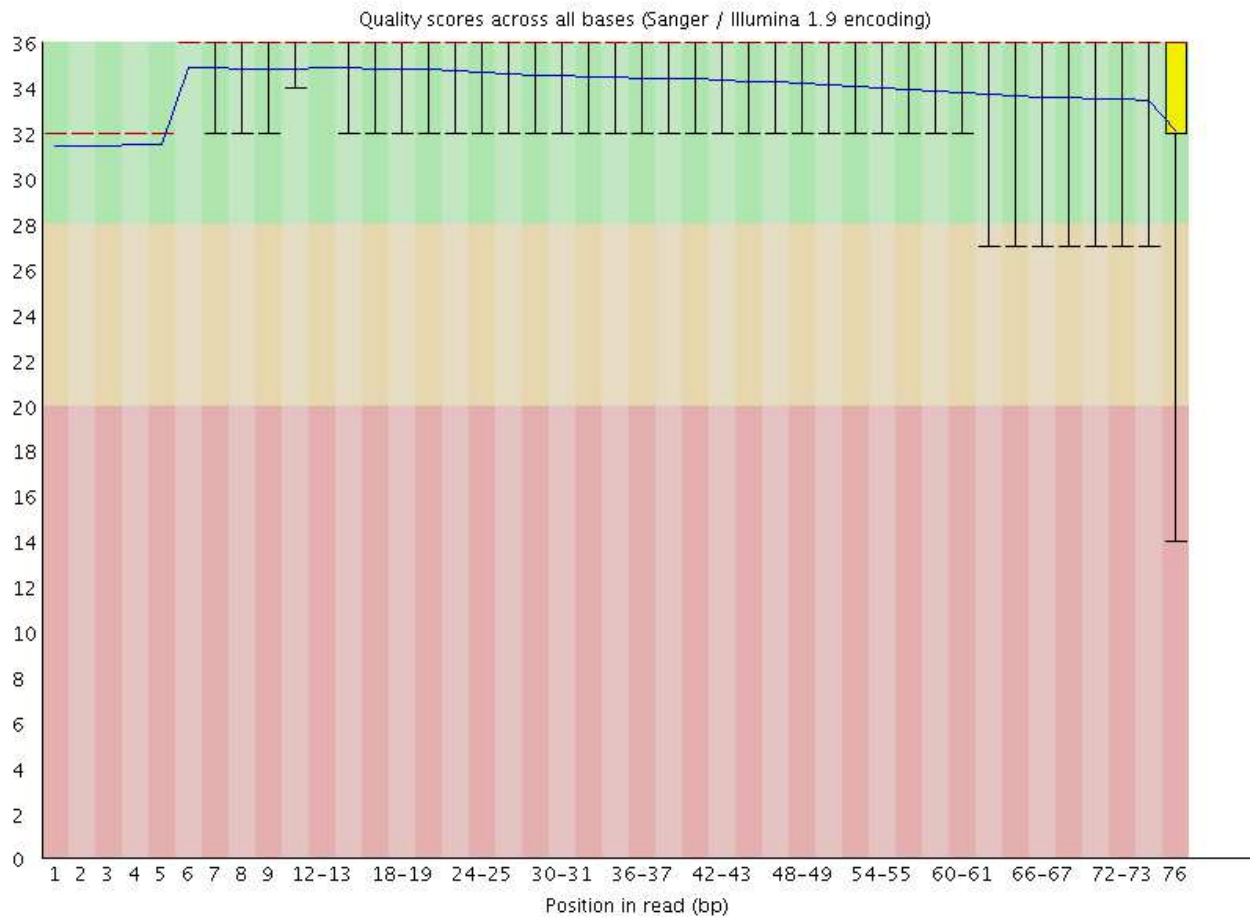
 Per base sequence quality



Supplemental Figure 1. Per Base Sequence Quality of HH Stages 10 and 12.

Representative graph showing per base pair quality of sequencing for HH stages 10 and 12. First 9 bases were trimmed and removed from analysis.

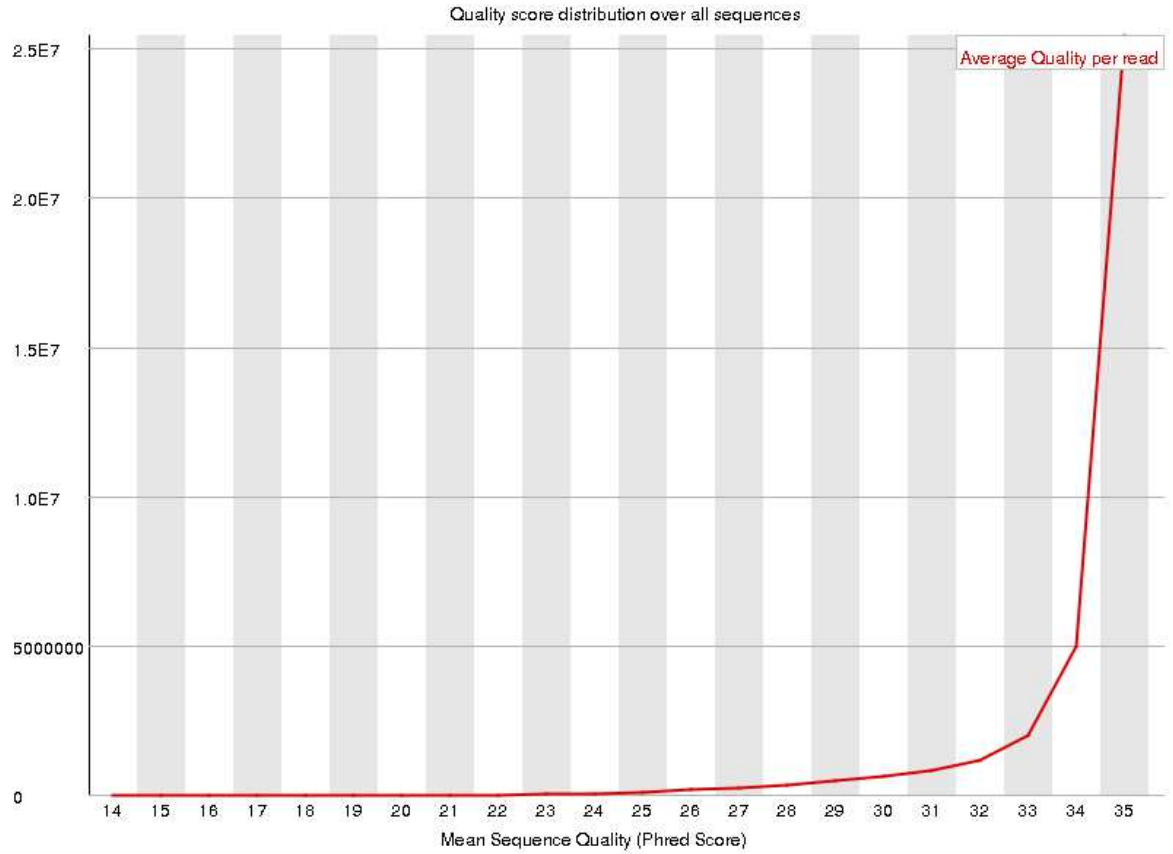
 **Per base sequence quality**



Supplemental Figure 2. Per Base Sequence Quality of HH14.

Representative graph showing per base pair quality of sequencing of HH14. First 6 bases were trimmed and removed from analysis.

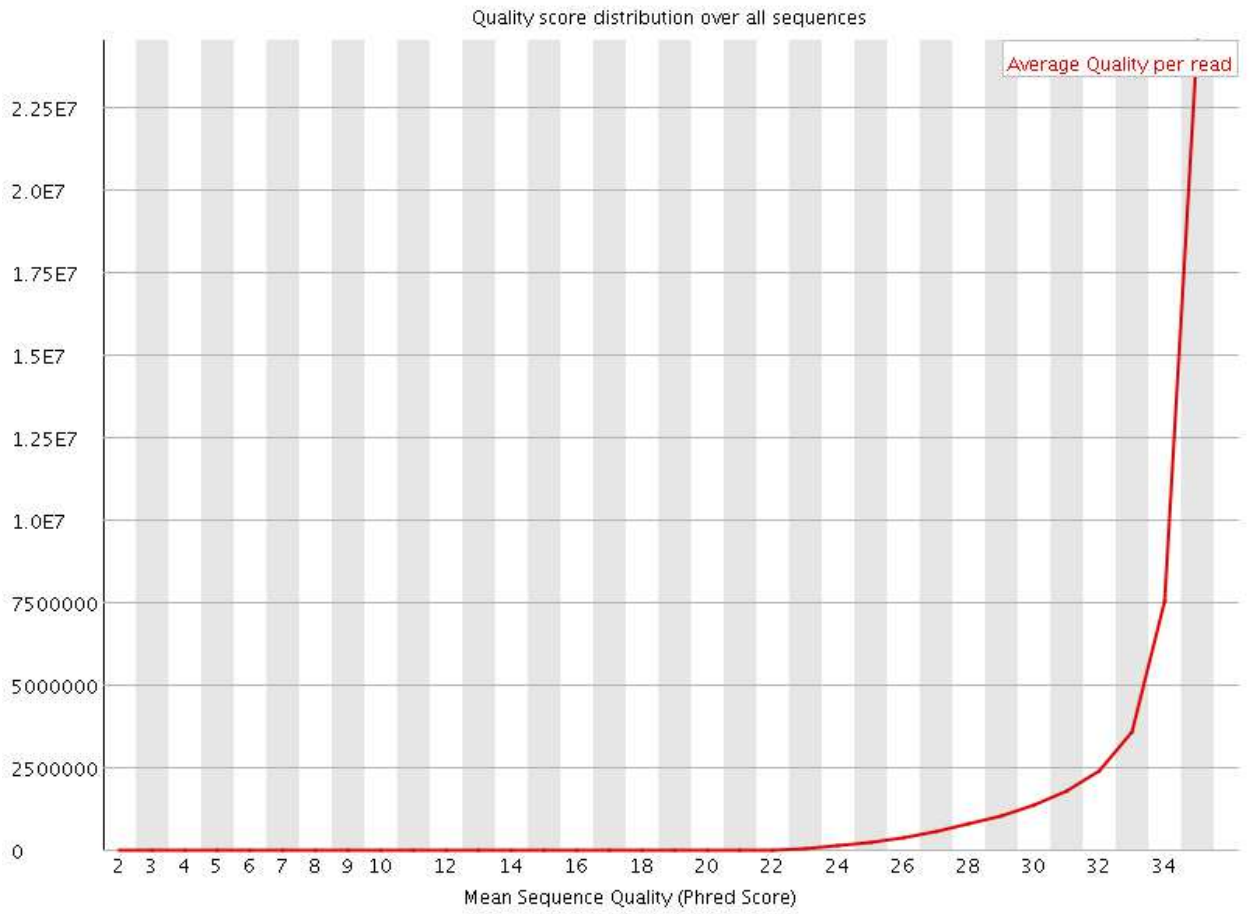
 **Per sequence quality scores**



Supplemental Figure 3. Per Sequence Quality Scores for HH10 and 12.

Representative Phred score of sequencing for HH stages 10 and 12. The average quality per sequence passed quality control testing.

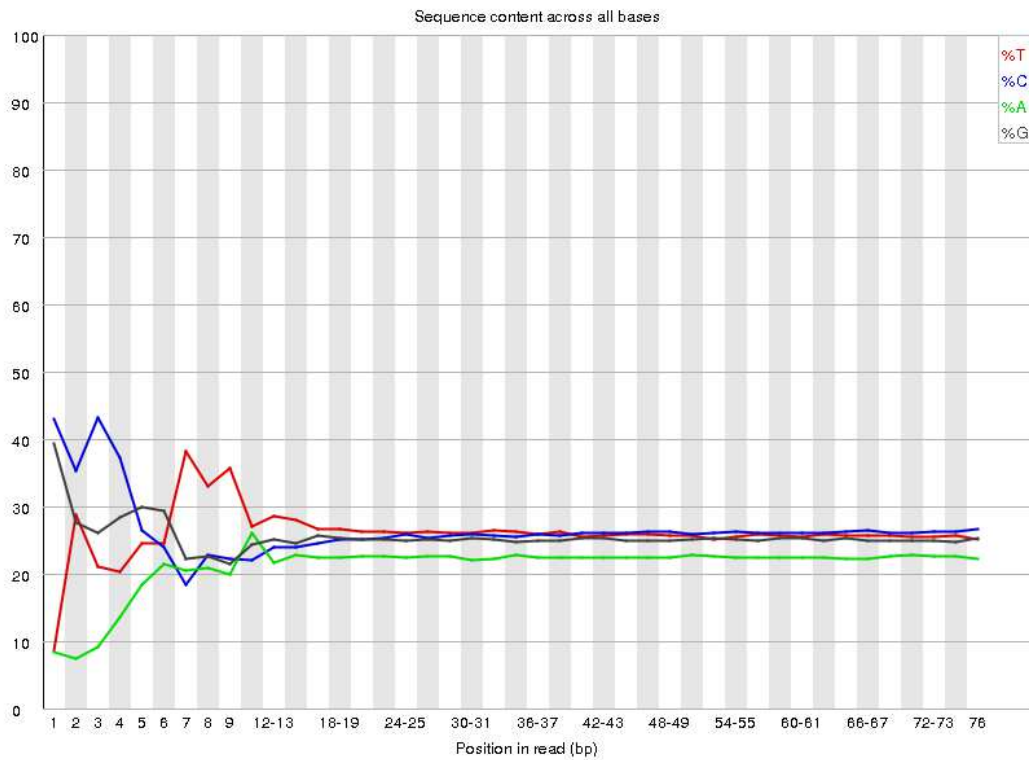
 **Per sequence quality scores**



Supplemental Figure 4. Per Sequence Quality Scores for HH14.

Representative Phred score of sequencing for HH14. The average quality per sequence passed quality control testing.

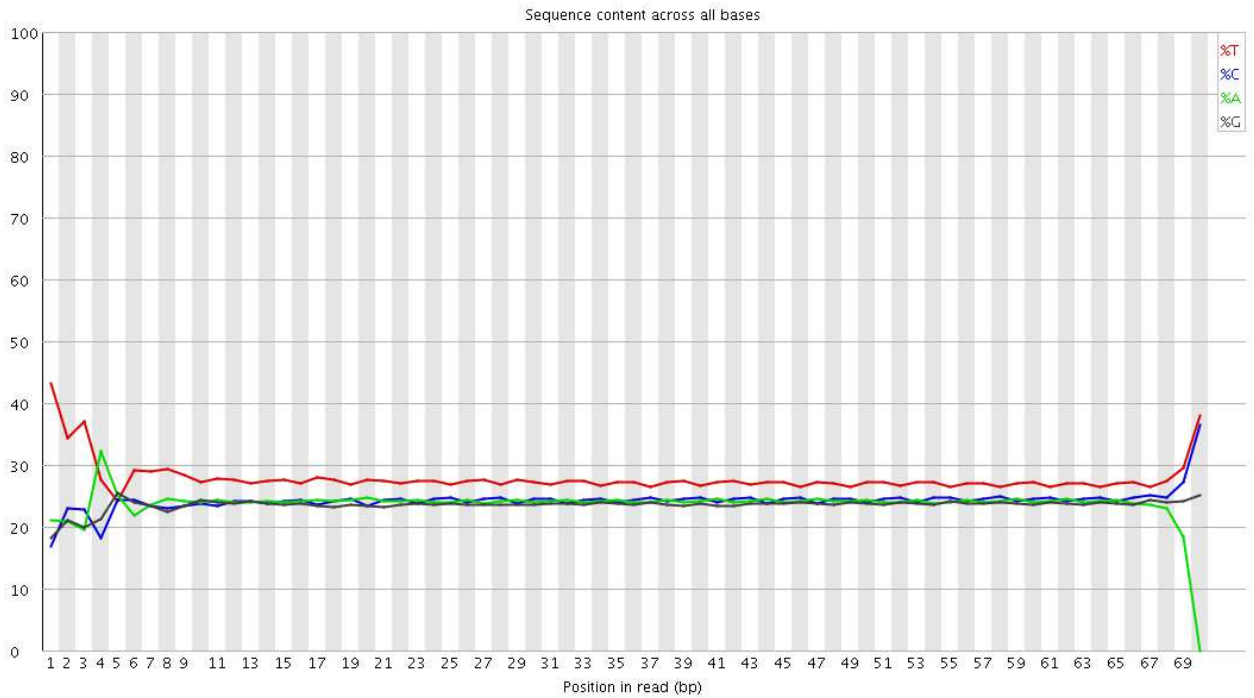
✖ Per base sequence content



Supplemental Figure 5. Per Base Sequence Content HH10 and 12.

Representative chart depicting bases in sequences for HH10 and 12, indicating that first 9 bases needed to be removed from analysis.

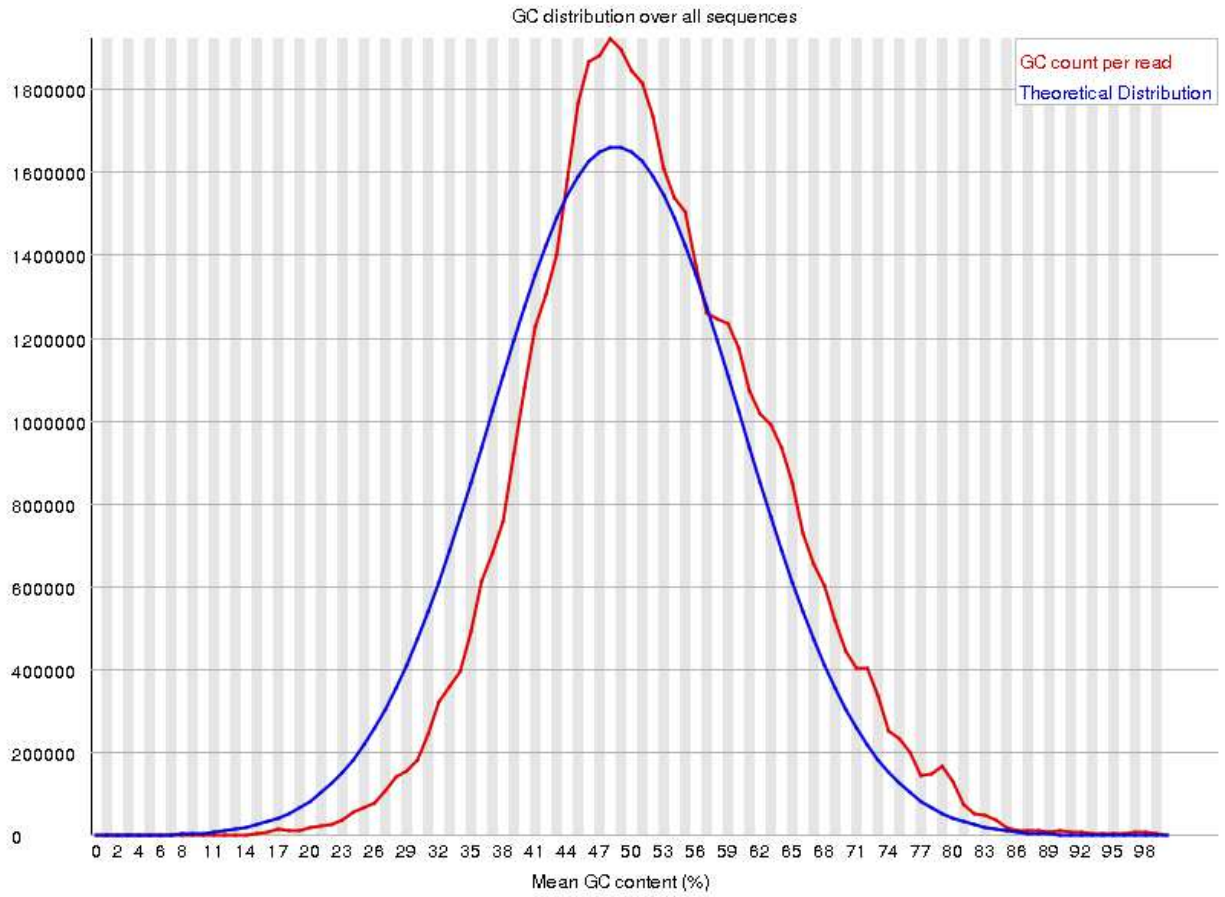
✖ Per base sequence content



Supplemental Figure 6. Per Base Sequence Content for HH14.

Chart depicting bases in sequences for HH14, indicating that first 6 bases needed to be removed from analysis.

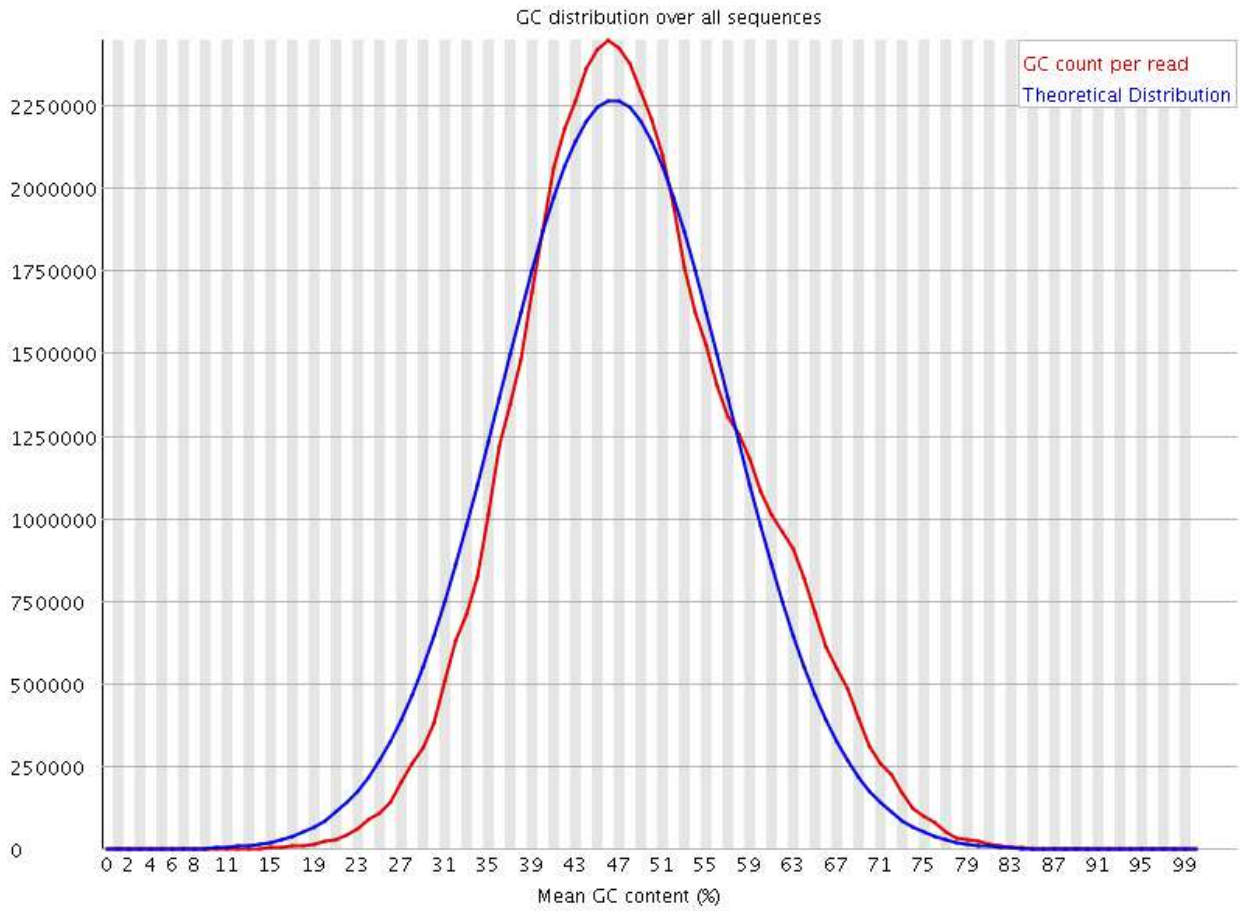
Per sequence GC content



Supplemental Figure 7. Per Sequence GC Content for HH10 and 12.

Representative theoretical distribution of G and C base content in sequencing for HH10 and 12.

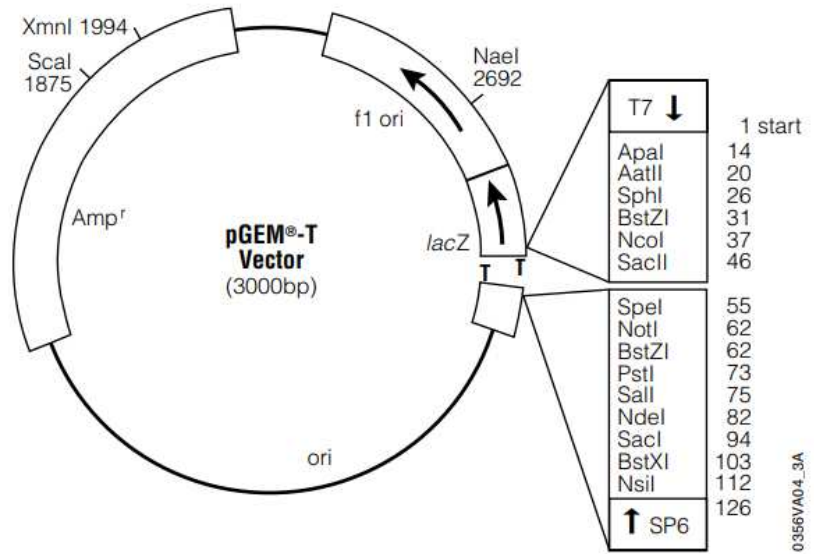
 **Per sequence GC content**



Supplemental Figure 8. Per Sequence GC Content for HH14.

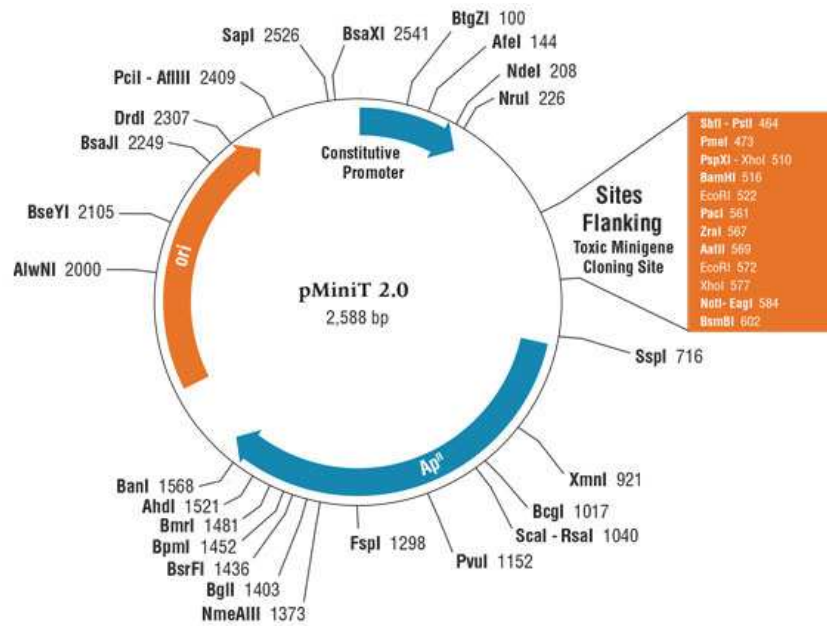
Representative theoretical distribution of G and C base content in sequencing for HH14.

pGEM[®]-T Vector Map and Sequence Reference Points

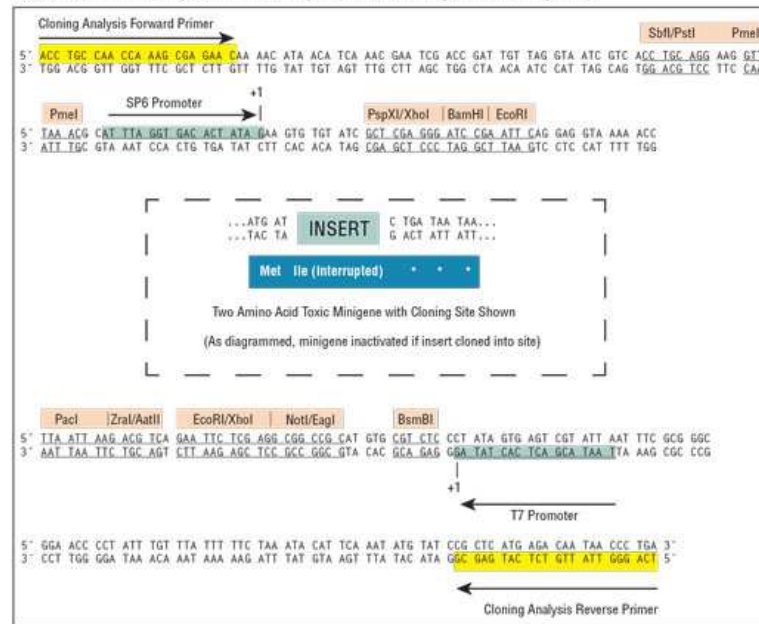


Supplemental Figure 9. Map for p-GEM-T plasmid.

Map showing restriction sites upstream of SP6 and T7 promoters used for transcription.

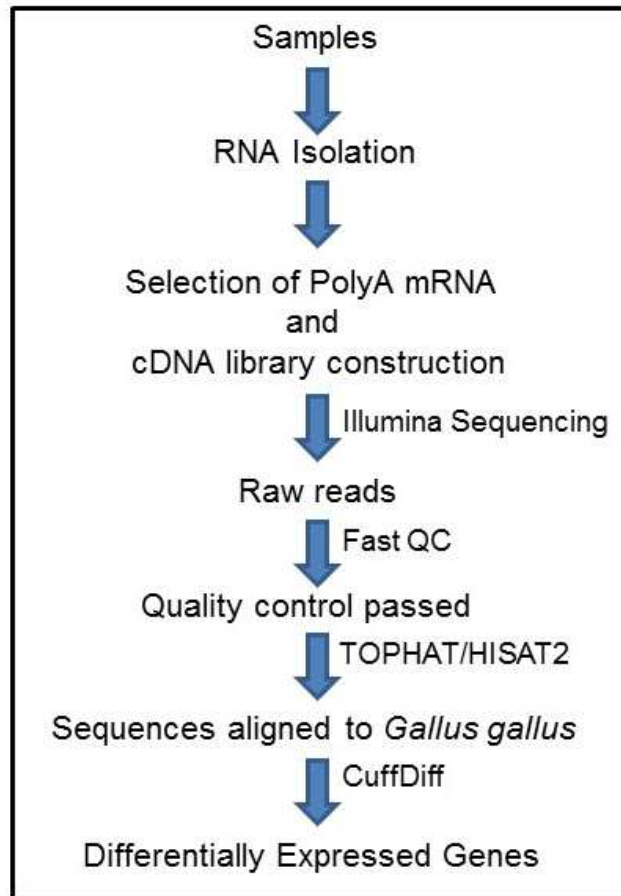


Features within Sequence Flanking the Toxic Minigene/Cloning Site



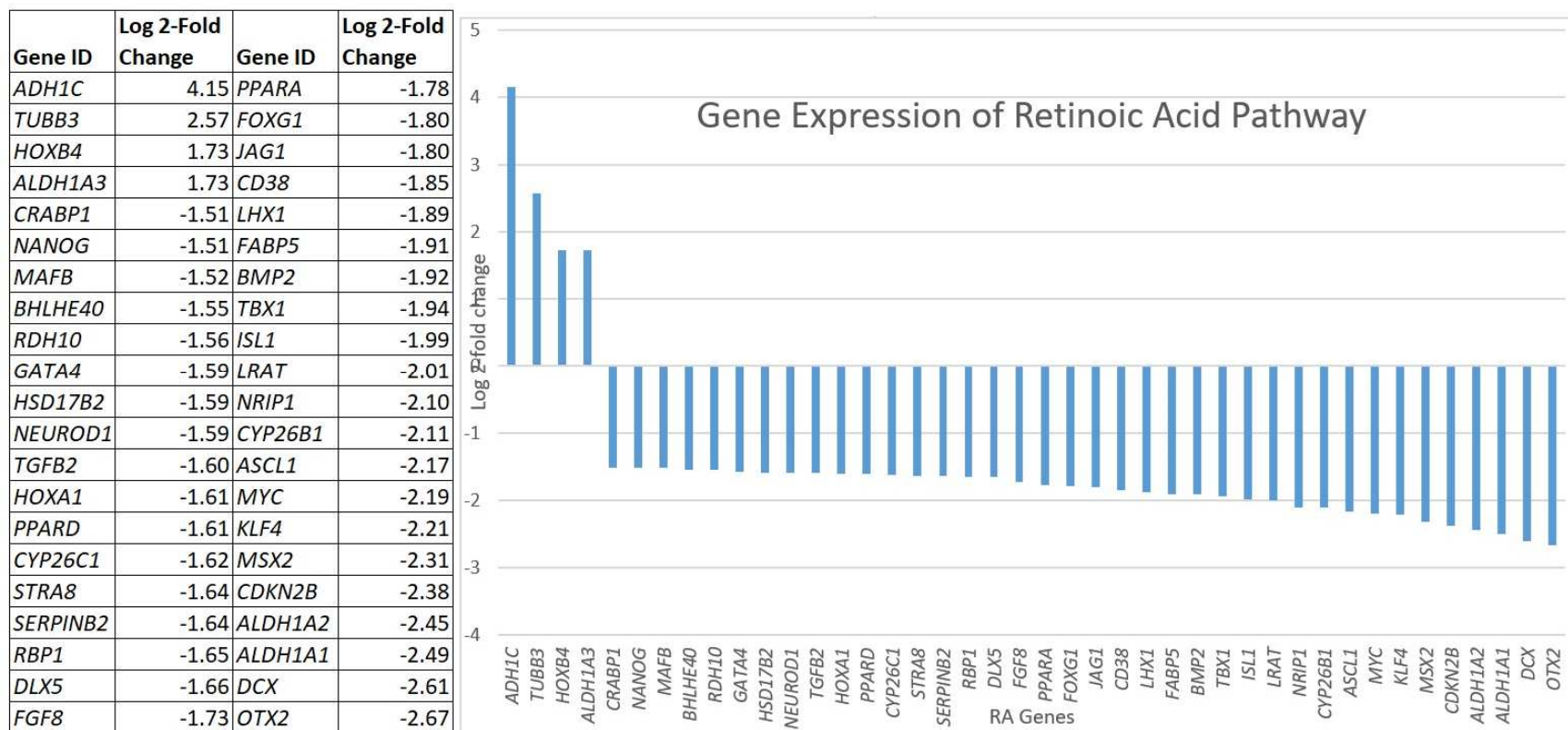
Supplemental Figure 10. Map for p-Mini-T 2.0 plasmid.

Map indicating restriction sites upstream of SP6 and T7 promoters used for transcription.



Supplemental Figure 11. Workflow of sample processing and bioinformatics analysis.

All samples were processed as outlined as outlined in Figure 3. TOPHAT was updated to HISAT2. HH stages 10 and 12 were aligned using HISAT2 whereas, TOPHAT was used for HH14.



Supplemental Figure 12. QRTPCR Figure-Gene List-fold change.

Gene expression of RA pathway genes with a >1.5 fold or < -1.5 fold change. Fold change displayed in log₂ scale.

Significant Differentially Expressed Genes for HH10-12-14

Stage	Gene	Description	log2 fold change	p-value	q-value
HH10	<i>AK1</i>	adenylate kinase 1	-1.22	5.00E-05	5.37E-03
HH10	<i>ALDOB</i>	aldolase B, fructose-bisphosphate	-2.86	5.00E-05	5.37E-03
HH10	<i>APC2</i>	adenomatosis polyposis coli 2	1.60	5.00E-05	5.37E-03
HH10	<i>APOA1</i>	apolipoprotein A-I	-1.75	5.00E-05	5.37E-03
HH10	<i>APOB</i>	apolipoprotein B	-2.97	5.00E-05	5.37E-03
HH10	<i>APOC3</i>	apolipoprotein C3	-1.67	5.00E-05	5.37E-03
HH10	<i>ASTL</i>	astacin-like metallo-endopeptidase (M12 family)	-1.67	5.00E-05	5.37E-03
HH10	<i>C5H11orf31</i>	selenoprotein H	-1.11	5.00E-05	5.37E-03
HH10	<i>CRABP1</i>	cellular retinoic acid binding protein 1	-1.75	5.00E-05	5.37E-03
HH10	<i>DBX1</i>	developing brain homeobox 1	3.22	5.00E-05	5.37E-03
HH10	<i>FABP2</i>	Fatty Acid Binding Protein 2	down	5.00E-05	5.37E-03
HH10	<i>FBP1</i>	fructose-1,6-bisphosphatase 1	-3.59	5.00E-05	5.37E-03
HH10	<i>FGA</i>	fibrinogen alpha chain	-1.88	5.00E-05	5.37E-03
HH10	<i>GPR34</i>	G protein-coupled receptor 34	up	5.00E-05	5.37E-03
HH10	<i>HAND1</i>	heart and neural crest derivatives expressed 1	-1.41	5.00E-05	5.37E-03
HH10	<i>HBE</i>	hemoglobin subunit epsilon	-4.33	5.00E-05	5.37E-03
HH10	<i>HBG1</i>	hemoglobin beta, subunit rho	-4.52	5.00E-05	5.37E-03
HH10	<i>HSPB1</i>	heat shock protein family B (small) member 1	-1.34	5.00E-05	5.37E-03
HH10	<i>ID1</i>	inhibitor of DNA binding 1, dominant negative helix-loop-helix protein	-1.10	5.00E-05	5.37E-03
HH10	<i>PIGB</i>	PIGB opposite strand 1	-1.29	5.00E-05	5.37E-03
HH10	<i>AKR1BL</i>	aldo-keto reductase family 1 member B1-like	3.97	5.00E-05	5.37E-03
HH10	<i>LRRN1</i>	leucine rich repeat neuronal 1	1.30	5.00E-05	5.37E-03
HH10	<i>MRPL41</i>	mitochondrial ribosomal protein L41	-1.17	5.00E-05	5.37E-03

HH10	<i>MT4</i>	metallothionein 4	-1.75	5.00E-05	5.37E-03
HH10	<i>MYL2</i>	myosin, light chain 2, regulatory, cardiac, slow	-2.04	5.00E-05	5.37E-03
HH10	<i>MYL3</i>	myosin, light chain 3, alkali; ventricular, skeletal, slow	-2.27	5.00E-05	5.37E-03
HH10	<i>NDUFA1</i>	NADH:ubiquinone oxidoreductase subunit A1	-1.39	5.00E-05	5.37E-03
HH10	<i>NIP7</i>	NIP7, nucleolar pre-rRNA processing protein	-1.02	5.00E-05	5.37E-03
HH10	<i>NKX2-1</i>	NK2 homeobox 1	3.83	5.00E-05	5.37E-03
HH10	<i>NR2E1</i>	nuclear receptor subfamily 2 group E member 1	4.44	5.00E-05	5.37E-03
HH10	<i>OCX36</i>	BPI fold containing family B member 3	2.54	5.00E-05	5.37E-03
HH10	<i>OLIG3</i>	oligodendrocyte transcription factor 3	3.46	5.00E-05	5.37E-03
HH10	<i>OPN4-1</i>	photopigment melanopsin-like	up	5.00E-05	5.37E-03
HH10	<i>OST4</i>	oligosaccharyltransferase complex subunit 4, non-catalytic	-1.19	5.00E-05	5.37E-03
HH10	<i>OTX2</i>	orthodenticle homeobox 2	2.63	5.00E-05	5.37E-03
HH10	<i>PAX6</i>	paired box 6	1.77	5.00E-05	5.37E-03
HH10	<i>PTGDS</i>	prostaglandin D2 synthase 21kDa	-2.53	5.00E-05	5.37E-03
HH10	<i>RAX</i>	retina and anterior neural fold homeobox	3.90	5.00E-05	5.37E-03
HH10	<i>RBP</i>	riboflavin binding protein	-3.12	5.00E-05	5.37E-03
HH10	<i>RBP4</i>	retinol binding protein 4	-1.66	5.00E-05	5.37E-03
HH10	<i>RGN</i>	regucalcin	-1.31	5.00E-05	5.37E-03
HH10	<i>SEPP1</i>	selenoprotein P1	-2.32	5.00E-05	5.37E-03
HH10	<i>SLC16A3</i>	solute carrier family 16 (monocarboxylate transporter), member 3	1.35	5.00E-05	5.37E-03
HH10	<i>SLCO4A1</i>	solute carrier organic anion transporter family member 4A1	2.99	5.00E-05	5.37E-03
HH10	<i>ST8SIA2</i>	ST8 alpha-N-acetyl-neuraminide alpha-2,8-sialyltransferase 2	1.85	5.00E-05	5.37E-03
HH10	<i>TGM4</i>	transglutaminase 4 (prostate)	-3.62	5.00E-05	5.37E-03

HH10	<i>TIMM10</i>	translocase of inner mitochondrial membrane 10 homolog (yeast)	-1.18	5.00E-05	5.37E-03
HH10	<i>TNNC2</i>	troponin C type 2 (fast)	-1.91	5.00E-05	5.37E-03
HH10	<i>AMN</i>	amnion associated transmembrane protein	-3.12	1.00E-04	9.37E-03
HH10	<i>ASS1</i>	argininosuccinate synthase 1	-1.18	1.00E-04	9.37E-03
HH10	<i>CNTN2</i>	contactin 2 (axonal)	1.25	1.00E-04	9.37E-03
HH10	<i>MAP6</i>	microtubule associated protein 6	1.18	1.00E-04	9.37E-03
HH10	<i>MSX1</i>	msh homeobox 1	-1.04	1.00E-04	9.37E-03
HH10	<i>TESC</i>	tescalcin	-1.09	1.00E-04	9.37E-03
HH10	<i>USPL1</i>	ubiquitin specific peptidase like 1	1.00	1.00E-04	9.37E-03
HH10	<i>KRT19</i>	keratin 19	-1.01	1.50E-04	1.25E-02
HH10	<i>NFASC</i>	neurofascin	1.12	1.50E-04	1.25E-02
HH10	<i>RPS28</i>	ribosomal protein S28	-1.15	1.50E-04	1.25E-02
HH10	<i>SLC2A1</i>	solute carrier family 2 (facilitated glucose transporter), member 1	0.99	1.50E-04	1.25E-02
HH10	<i>SOX1</i>	SRY (sex determining region Y)-box 1	1.21	1.50E-04	1.25E-02
HH10	<i>TNNT2</i>	troponin T type 2 (cardiac)	-1.25	1.50E-04	1.25E-02
HH10	<i>UBAP2</i>	ubiquitin associated protein 2	2.00	1.50E-04	1.25E-02
HH10	<i>KRT17</i>	keratin 17	-1.49	2.00E-04	1.56E-02
HH10	<i>MLN</i>	motilin	up	2.00E-04	1.56E-02
HH10	<i>RTN1</i>	reticulon 1	2.26	2.00E-04	1.56E-02
HH10	<i>TOMM6</i>	translocase of outer mitochondrial membrane 6	-1.01	2.00E-04	1.56E-02
HH10	<i>LINGO1</i>	leucine rich repeat and Ig domain containing 1	1.18	2.50E-04	1.84E-02
HH10	<i>MSX2</i>	msh homeobox 2	-1.69	2.50E-04	1.84E-02
HH10	<i>PPIB</i>	peptidylprolyl isomerase B (cyclophilin B)	-0.96	2.50E-04	1.84E-02
HH10	<i>SIX3</i>	SIX homeobox 3	6.11	2.50E-04	1.84E-02
HH10	<i>AMBP</i>	alpha-1-microglobulin/bikunin precursor	-3.05	3.00E-04	2.01E-02

HH10	<i>CALML4</i>	calmodulin like 4	-1.23	3.00E-04	2.01E-02
HH10	<i>CYP3A7</i>	cytochrome P450 A 37	-3.44	3.00E-04	2.01E-02
HH10	<i>EPAS1</i>	endothelial PAS domain protein 1	-1.25	3.00E-04	2.01E-02
HH10	<i>FAM210B</i>	family with sequence similarity 210 member B	1.16	3.00E-04	2.01E-02
HH10	<i>MRPS21</i>	mitochondrial ribosomal protein S21	-1.06	3.00E-04	2.01E-02
HH10	<i>NRXN1</i>	neurexin 1	1.23	3.00E-04	2.01E-02
HH10	<i>COMMD4</i>	COMM domain containing 4	-1.03	3.50E-04	2.23E-02
HH10	<i>ITIH2</i>	inter-alpha-trypsin inhibitor heavy chain 2	-2.32	3.50E-04	2.23E-02
HH10	<i>MYLK</i>	myosin light chain kinase	1.11	3.50E-04	2.23E-02
HH10	<i>POLR2F</i>	polymerase (RNA) II subunit F(POLR2F)	-0.95	3.50E-04	2.23E-02
HH10	<i>CDH20</i>	cadherin 20, type 2(CDH20)	-1.76	4.00E-04	2.43E-02
HH10	<i>DLX6</i>	distal-less homeobox 6(DLX6)	1.97	4.00E-04	2.43E-02
HH10	<i>GJB1</i>	gap junction protein, beta 1, 32kDa	-1.21	4.00E-04	2.43E-02
HH10	<i>JARID2</i>	jumonji and AT-rich interaction domain containing 2	0.94	4.00E-04	2.43E-02
HH10	<i>ELMO1</i>	engulfment and cell motility 1	1.13	4.50E-04	2.61E-02
HH10	<i>HOXB8</i>	homeobox B8	-1.60	4.50E-04	2.61E-02
HH10	<i>SRA1</i>	steroid receptor RNA activator 1	-1.21	4.50E-04	2.61E-02
HH10	<i>TNNC1</i>	troponin C type 1 (slow)	-1.19	4.50E-04	2.61E-02
HH10	<i>ATP6AP1</i>	ATPase H ⁺ transporting accessory protein 1	1.05	5.00E-04	2.83E-02
HH10	<i>SRL</i>	sarcalumenin	-1.46	5.00E-04	2.83E-02
HH10	<i>MYH7B</i>	myosin, heavy chain 7B, cardiac muscle, beta	-1.15	5.50E-04	3.08E-02
HH10	<i>PPDPF</i>	pancreatic progenitor cell differentiation and proliferation factor	-0.97	6.50E-04	3.60E-02
HH10	<i>CDC26</i>	cell division cycle 26	-1.16	7.50E-04	4.07E-02
HH10	<i>NDFIP2</i>	Nedd4 family interacting protein 2	0.89	7.50E-04	4.07E-02
HH10	<i>ADCK3</i>	aarF domain containing kinase 3	0.87	8.00E-04	4.25E-02

HH10	<i>MIR1774</i>	MIR1774	up	8.00E-04	4.25E-02
HH10	<i>BCAS2</i>	breast carcinoma amplified sequence 2	-0.89	8.50E-04	4.43E-02
HH10	<i>KCNAB1</i>	potassium voltage-gated channel, shaker-related subfamily, beta member 1	1.15	8.50E-04	4.43E-02
HH10	<i>DCTN6</i>	dynactin subunit 6	-0.86	9.00E-04	4.59E-02
HH10	<i>SOX2</i>	SRY (sex determining region Y)-box 2	1.19	9.00E-04	4.59E-02
HH10	<i>ATP5I</i>	ATP synthase, H ⁺ transporting, mitochondrial Fo complex subunit E	-0.90	9.50E-04	4.62E-02
HH10	<i>EXOC5</i>	exocyst complex component 5	0.88	9.50E-04	4.62E-02
HH10	<i>MYL9</i>	myosin, light chain 9, regulatory	-0.90	9.50E-04	4.62E-02
HH10	<i>SNRPF</i>	small nuclear ribonucleoprotein polypeptide F	-0.87	9.50E-04	4.62E-02
HH10	<i>TTR</i>	transthyretin	-1.17	9.50E-04	4.62E-02
HH10	<i>EP400</i>	E1A binding protein p400	0.89	1.00E-03	4.77E-02
HH10	<i>FAM136A</i>	family with sequence similarity 136 member A	-0.86	1.00E-03	4.77E-02
HH10	<i>TF</i>	transferrin (ovotransferrin)	-1.10	1.05E-03	4.92E-02
HH10	<i>UQCR11</i>	ubiquinol-cytochrome c reductase, complex III subunit XI	-0.93	1.05E-03	4.92E-02
HH12	<i>ACTC1</i>	actin, alpha, cardiac muscle 1	1.19	5.00E-05	2.16E-03
HH12	<i>ACTG2</i>	actin, gamma 2, smooth muscle, enteric	1.51	5.00E-05	2.16E-03
HH12	<i>ADCYAP1</i>	adenylate cyclase activating polypeptide 1 (pituitary)	1.60	5.00E-05	2.16E-03
HH12	<i>AMY2A</i>	amylase, alpha 2A	1.41	5.00E-05	2.16E-03
HH12	<i>ANXA2</i>	annexin A2	-1.65	5.00E-05	2.16E-03
HH12	<i>APOB</i>	apolipoprotein B	-5.26	5.00E-05	2.16E-03
HH12	<i>AQP1</i>	aquaporin 1	-2.34	5.00E-05	2.16E-03
HH12	<i>ASB12</i>	ankyrin repeat and SOCS box containing 12	1.34	5.00E-05	2.16E-03
HH12	<i>ATP5I</i>	ATP synthase, H ⁺ transporting, mitochondrial Fo complex subunit E	1.04	5.00E-05	2.16E-03

HH12	<i>BASP1</i>	brain abundant membrane attached signal protein 1	-1.19	5.00E-05	2.16E-03
HH12	<i>BRINP1</i>	bone morphogenetic protein/retinoic acid inducible neural-specific 1	-1.28	5.00E-05	2.16E-03
HH12	<i>BVES</i>	blood vessel epicardial substance	1.34	5.00E-05	2.16E-03
HH12	<i>CAV3</i>	caveolin 3	down	5.00E-05	2.16E-03
HH12	<i>CD93</i>	CD93 molecule	-1.23	5.00E-05	2.16E-03
HH12	<i>CDH20</i>	cadherin 20, type 2	-2.14	5.00E-05	2.16E-03
HH12	<i>CDX1</i>	caudal type homeobox 1	-3.14	5.00E-05	2.16E-03
HH12	<i>CDX4</i>	caudal type homeobox 4	-3.18	5.00E-05	2.16E-03
HH12	<i>CHRD</i>	chordin	-3.38	5.00E-05	2.16E-03
HH12	<i>COL3A1</i>	collagen, type III, alpha 1	-2.23	5.00E-05	2.16E-03
HH12	<i>COLEC12</i>	collectin sub-family member 12	-1.00	5.00E-05	2.16E-03
HH12	<i>COX7A2</i>	cytochrome c oxidase subunit VIIa polypeptide 2 (liver)	0.95	5.00E-05	2.16E-03
HH12	<i>CRABP1</i>	cellular retinoic acid binding protein 1	1.23	5.00E-05	2.16E-03
HH12	<i>CRYAB</i>	crystallin, alpha B	1.30	5.00E-05	2.16E-03
HH12	<i>CSRP3</i>	cysteine and glycine-rich protein 3 (cardiac LIM protein)	1.43	5.00E-05	2.16E-03
HH12	<i>CTNNA3</i>	catenin (cadherin-associated protein), alpha 3	1.39	5.00E-05	2.16E-03
HH12	<i>EEF1A2</i>	eukaryotic translation elongation factor 1 alpha 2	1.09	5.00E-05	2.16E-03
HH12	<i>ENG</i>	endoglin	-1.28	5.00E-05	2.16E-03
HH12	<i>EPAS1</i>	endothelial PAS domain protein 1	-2.17	5.00E-05	2.16E-03
HH12	<i>ETS1</i>	v-ets avian erythroblastosis virus E26 oncogene homolog 1	-1.07	5.00E-05	2.16E-03
HH12	<i>FABP7</i>	fatty acid binding protein 7, brain	-1.03	5.00E-05	2.16E-03
HH12	<i>FKBP1B</i>	FK506 binding protein 1B, 12.6 kDa	1.23	5.00E-05	2.16E-03
HH12	<i>FLNB</i>	filamin B, beta	-0.95	5.00E-05	2.16E-03

HH12	<i>FLT4</i>	fms-related tyrosine kinase 4	-1.00	5.00E-05	2.16E-03
HH12	<i>FMOD</i>	fibromodulin	-1.98	5.00E-05	2.16E-03
HH12	<i>GNG5</i>	guanine nucleotide binding protein (G protein), gamma 5	1.00	5.00E-05	2.16E-03
HH12	<i>GTF2H5</i>	general transcription factor IIH subunit 5	0.92	5.00E-05	2.16E-03
HH12	<i>GUCA2B</i>	guanylate cyclase activator 2B (uroguanylin)	-2.97	5.00E-05	2.16E-03
HH12	<i>HAUS1</i>	HAUS augmin like complex subunit 1	1.01	5.00E-05	2.16E-03
HH12	<i>HBE</i>	hemoglobin subunit epsilon	2.33	5.00E-05	2.16E-03
HH12	<i>HBG1</i>	hemoglobin, beta	2.33	5.00E-05	2.16E-03
HH12	<i>HBG2</i>	hemoglobin, beta	2.48	5.00E-05	2.16E-03
HH12	<i>HIC1</i>	hypermethylated in cancer 1	-1.22	5.00E-05	2.16E-03
HH12	<i>HINT1</i>	histidine triad nucleotide binding protein 12	1.51	5.00E-05	2.16E-03
HH12	<i>HOXB3</i>	homeobox B3	-1.02	5.00E-05	2.16E-03
HH12	<i>HOXB4</i>	homeobox B4	-1.57	5.00E-05	2.16E-03
HH12	<i>HOXB8</i>	homeobox B8	-3.76	5.00E-05	2.16E-03
HH12	<i>HOXC8</i>	homeobox C8	down	5.00E-05	2.16E-03
HH12	<i>HSPB1</i>	heat shock protein family B (small) member 1	1.25	5.00E-05	2.16E-03
HH12	<i>IER3IP1</i>	immediate early response 3 interacting protein 1	1.00	5.00E-05	2.16E-03
HH12	<i>IFI27L2</i>	interferon, alpha-inducible protein 27-like 2	1.81	5.00E-05	2.16E-03
HH12	<i>IRX4</i>	iroquois homeobox 4	1.37	5.00E-05	2.16E-03
HH12	<i>KRT14</i>	keratin 14	-1.48	5.00E-05	2.16E-03
HH12	<i>KRT7</i>	keratin 7	-1.52	5.00E-05	2.16E-03
HH12	<i>LIN28A</i>	lin-28 homolog A (C. elegans)	-0.91	5.00E-05	2.16E-03
HH12	<i>KRT17</i>	keratin, type I cytoskeletal 14-like(LOC100858439)	-1.84	5.00E-05	2.16E-03
HH12	<i>AK6</i>	adenylate kinase 6	0.97	5.00E-05	2.16E-03
HH12	<i>SDHAF2</i>	succinate dehydrogenase complex assembly factor 2	0.85	5.00E-05	2.16E-03

HH12	<i>LOC771947</i>	cytochrome c oxidase subunit 7B, mitochondrial-like(LOC771947)	0.98	5.00E-05	2.16E-03
HH12	<i>C14orf2</i>	chromosome 14 open reading frame 2	0.96	5.00E-05	2.16E-03
HH12	<i>LSM5</i>	LSM5 homolog, U6 small nuclear RNA and mRNA degradation associated	1.28	5.00E-05	2.16E-03
HH12	<i>LSP1</i>	lymphocyte-specific protein 1	-1.09	5.00E-05	2.16E-03
HH12	<i>MAB21L2</i>	mab-21-like 2 (C. elegans)	-1.16	5.00E-05	2.16E-03
HH12	<i>MB</i>	myoglobin	1.78	5.00E-05	2.16E-03
HH12	<i>MEOX1</i>	mesenchyme homeobox 1	-0.97	5.00E-05	2.16E-03
HH12	<i>MESP2</i>	mesoderm posterior bHLH transcription factor 2	down	5.00E-05	2.16E-03
HH12	<i>MFI2</i>	melanotransferrin	-1.28	5.00E-05	2.16E-03
HH12	<i>MINOS1</i>	mitochondrial inner membrane organizing system 1	0.97	5.00E-05	2.16E-03
HH12	<i>MSGN1</i>	mesogenin 1	down	5.00E-05	2.16E-03
HH12	<i>MSX1</i>	msh homeobox 1	-1.23	5.00E-05	2.16E-03
HH12	<i>MT4</i>	metallothionein 4-like	-1.68	5.00E-05	2.16E-03
HH12	<i>MYBPC3</i>	myosin binding protein C, cardiac	1.19	5.00E-05	2.16E-03
HH12	<i>MYL1</i>	myosin, light chain 1, alkali; skeletal, fast	1.18	5.00E-05	2.16E-03
HH12	<i>MYL2</i>	myosin, light chain 2, regulatory, cardiac, slow	1.69	5.00E-05	2.16E-03
HH12	<i>MYL3</i>	myosin, light chain 3, alkali; ventricular, skeletal, slow	1.49	5.00E-05	2.16E-03
HH12	<i>MYLK</i>	myosin light chain kinase	-1.38	5.00E-05	2.16E-03
HH12	<i>NDUFA1</i>	NADH:ubiquinone oxidoreductase subunit A1	1.17	5.00E-05	2.16E-03
HH12	<i>NKX2-5</i>	NK2 homeobox 5	0.99	5.00E-05	2.16E-03
HH12	<i>NKX2-6</i>	NK2 homeobox 6	1.18	5.00E-05	2.16E-03
HH12	<i>NPPB</i>	natriuretic peptide B	1.20	5.00E-05	2.16E-03
HH12	<i>NRP2</i>	neuropilin 2	-1.61	5.00E-05	2.16E-03
HH12	<i>NTN1</i>	netrin 1	-1.73	5.00E-05	2.16E-03

HH12	<i>OLFM1</i>	olfactomedin 1	-1.13	5.00E-05	2.16E-03
HH12	<i>OTX2</i>	orthodenticle homeobox 2	-2.54	5.00E-05	2.16E-03
HH12	<i>OXNAD1</i>	oxidoreductase NAD-binding domain containing 1	1.02	5.00E-05	2.16E-03
HH12	<i>PCDHGC3</i>	protocadherin gamma subfamily C, 3	-1.06	5.00E-05	2.16E-03
HH12	<i>PCP4</i>	Purkinje cell protein 4	-1.53	5.00E-05	2.16E-03
HH12	<i>PDLIM3</i>	PDZ and LIM domain 3	-3.70	5.00E-05	2.16E-03
HH12	<i>PFDN4</i>	prefoldin subunit 4	0.96	5.00E-05	2.16E-03
HH12	<i>PLCXD1</i>	phosphatidylinositol specific phospholipase C X domain containing 1	-1.72	5.00E-05	2.16E-03
HH12	<i>PLN</i>	phospholamban	1.83	5.00E-05	2.16E-03
HH12	<i>POPDC2</i>	popeye domain containing 2	1.06	5.00E-05	2.16E-03
HH12	<i>PRPS2</i>	phosphoribosyl pyrophosphate synthetase 2	-2.09	5.00E-05	2.16E-03
HH12	<i>Pou5f3</i>	POU domain class 5 transcription factor 3	-1.92	5.00E-05	2.16E-03
HH12	<i>RASSF2</i>	Ras association (RalGDS/AF-6) domain family member 2	-1.24	5.00E-05	2.16E-03
HH12	<i>RBM24</i>	RNA binding motif protein 24	0.98	5.00E-05	2.16E-03
HH12	<i>RBP</i>	riboflavin binding protein	-2.79	5.00E-05	2.16E-03
HH12	<i>RBP4</i>	retinol binding protein 4	-3.74	5.00E-05	2.16E-03
HH12	<i>RGL1</i>	ral guanine nucleotide dissociation stimulator-like 1	-0.97	5.00E-05	2.16E-03
HH12	<i>SCIN</i>	scinderin	-1.52	5.00E-05	2.16E-03
HH12	<i>SELK</i>	selenoprotein K	0.92	5.00E-05	2.16E-03
HH12	<i>SEPP1</i>	selenoprotein P1	-1.28	5.00E-05	2.16E-03
HH12	<i>SERPINI1</i>	serpin peptidase inhibitor, clade I (neuroserpin), member 1	1.75	5.00E-05	2.16E-03
HH12	<i>SLC4A1</i>	solute carrier family 4, anion exchanger, member 1	1.70	5.00E-05	2.16E-03
HH12	<i>SMYD1</i>	SET and MYND domain containing 1	0.99	5.00E-05	2.16E-03
HH12	<i>SRL</i>	sarcalumenin	1.19	5.00E-05	2.16E-03

HH12	<i>T</i>	T, brachyury homolog (mouse)	-1.82	5.00E-05	2.16E-03
HH12	<i>TBX22</i>	T-box 22	-1.69	5.00E-05	2.16E-03
HH12	<i>TCF15</i>	transcription factor 15 (basic helix-loop-helix)	-1.01	5.00E-05	2.16E-03
HH12	<i>TF</i>	transferrin (ovotransferrin)	-1.12	5.00E-05	2.16E-03
HH12	<i>TGFR3</i>	transforming growth factor, beta receptor III	-1.54	5.00E-05	2.16E-03
HH12	<i>TMEM167A</i>	transmembrane protein 167A	1.28	5.00E-05	2.16E-03
HH12	<i>TMEM207</i>	transmembrane protein 207	down	5.00E-05	2.16E-03
HH12	<i>TNNC1</i>	troponin C type 1 (slow)	1.42	5.00E-05	2.16E-03
HH12	<i>TNNC2</i>	troponin C type 2 (fast)	1.74	5.00E-05	2.16E-03
HH12	<i>TOMM7</i>	translocase of outer mitochondrial membrane 7	0.98	5.00E-05	2.16E-03
HH12	<i>TRIM55</i>	tripartite motif containing 55	1.08	5.00E-05	2.16E-03
HH12	<i>TUBB1</i>	tubulin, beta 1 class VI	1.39	5.00E-05	2.16E-03
HH12	<i>TYRO3</i>	TYRO3 protein tyrosine kinase	-0.88	5.00E-05	2.16E-03
HH12	<i>UTP15</i>	UTP15, small subunit processome component	1.06	5.00E-05	2.16E-03
HH12	<i>ACTN4</i>	actinin, alpha 4	-0.89	1.00E-04	3.89E-03
HH12	<i>ARPC1B</i>	actin related protein 2/3 complex subunit 1B	-1.19	1.00E-04	3.89E-03
HH12	<i>CACNA2D1</i>	calcium channel, voltage-dependent, alpha 2/delta subunit 1	1.22	1.00E-04	3.89E-03
HH12	<i>CBWD1</i>	COBW domain containing 1	1.10	1.00E-04	3.89E-03
HH12	<i>LSM6</i>	LSM6 homolog, U6 small nuclear RNA associated (<i>S. cerevisiae</i>)	0.94	1.00E-04	3.89E-03
HH12	<i>MRPS10</i>	mitochondrial ribosomal protein S10	0.91	1.00E-04	3.89E-03
HH12	<i>NCOA1</i>	nuclear receptor coactivator 1	-1.06	1.00E-04	3.89E-03
HH12	<i>NDUFB2</i>	NADH:ubiquinone oxidoreductase subunit B2	0.95	1.00E-04	3.89E-03
HH12	<i>PITX1</i>	paired-like homeodomain 1	-2.24	1.00E-04	3.89E-03
HH12	<i>SH3GL1</i>	SH3-domain GRB2-like 1	-0.91	1.00E-04	3.89E-03
HH12	<i>SIN3A</i>	SIN3 transcription regulator family member A	-0.94	1.00E-04	3.89E-03

HH12	<i>SOX9</i>	SRY (sex determining region Y)-box 9	-1.38	1.00E-04	3.89E-03
HH12	<i>TXN</i>	thioredoxin	1.26	1.00E-04	3.89E-03
HH12	<i>AXIN2</i>	axin 2	-1.20	1.50E-04	5.10E-03
HH12	<i>CINP</i>	cyclin dependent kinase 2 interacting protein	0.96	1.50E-04	5.10E-03
HH12	<i>CKS2</i>	CDC28 protein kinase regulatory subunit 2	1.31	1.50E-04	5.10E-03
HH12	<i>DDX55</i>	DEAD (Asp-Glu-Ala-Asp) box polypeptide 55	0.93	1.50E-04	5.10E-03
HH12	<i>FADS2</i>	fatty acid desaturase 2	-0.92	1.50E-04	5.10E-03
HH12	<i>GATA2</i>	GATA binding protein 2	-1.13	1.50E-04	5.10E-03
HH12	<i>GJA5</i>	gap junction protein alpha 5	0.95	1.50E-04	5.10E-03
HH12	<i>IL17RD</i>	interleukin 17 receptor D	-1.23	1.50E-04	5.10E-03
HH12	<i>LMOD2</i>	leiomodoin 2	1.15	1.50E-04	5.10E-03
HH12	<i>LOC420411</i>	uncharacterized LOC420411	1.05	1.50E-04	5.10E-03
HH12	<i>MNX1</i>	motor neuron and pancreas homeobox 1	-2.26	1.50E-04	5.10E-03
HH12	<i>MSX2</i>	msh homeobox 2	-1.04	1.50E-04	5.10E-03
HH12	<i>MYH15</i>	myosin, heavy chain 15	1.22	1.50E-04	5.10E-03
HH12	<i>PIWIL1</i>	piwi-like 1 (Drosophila)	-1.22	1.50E-04	5.10E-03
HH12	<i>SAMD11</i>	sterile alpha motif domain containing 11	-1.06	1.50E-04	5.10E-03
HH12	<i>SEC61G</i>	Sec61 translocon gamma subunit	0.95	1.50E-04	5.10E-03
HH12	<i>SP1</i>	Sp1 transcription factor	-0.88	1.50E-04	5.10E-03
HH12	<i>TESC</i>	tescalcin	0.88	1.50E-04	5.10E-03
HH12	<i>UQCR11</i>	ubiquinol-cytochrome c reductase, complex III subunit XI	0.97	1.50E-04	5.10E-03
HH12	<i>ADAM33</i>	ADAM metallopeptidase domain 33	-1.20	2.00E-04	6.22E-03
HH12	<i>CLDN5</i>	claudin 5	-1.31	2.00E-04	6.22E-03
HH12	<i>COX17</i>	COX17 cytochrome c oxidase copper chaperone	0.82	2.00E-04	6.22E-03
HH12	<i>DNASE2B</i>	deoxyribonuclease II beta	-1.44	2.00E-04	6.22E-03
HH12	<i>DRAXIN</i>	dorsal inhibitory axon guidance protein	-0.97	2.00E-04	6.22E-03

HH12	<i>FUS</i>	FUS RNA binding protein	-0.81	2.00E-04	6.22E-03
HH12	<i>NAA35</i>	N(alpha)-acetyltransferase 35, NatC auxiliary subunit	0.86	2.00E-04	6.22E-03
HH12	<i>NREP</i>	neuronal regeneration related protein	0.83	2.00E-04	6.22E-03
HH12	<i>SLC9A8</i>	solute carrier family 9 member A8	0.99	2.00E-04	6.22E-03
HH12	<i>TARS</i>	threonyl-tRNA synthetase	0.93	2.00E-04	6.22E-03
HH12	<i>TFAP2B</i>	transcription factor AP-2 beta	-1.19	2.00E-04	6.22E-03
HH12	<i>TFCP2</i>	transcription factor CP2	-0.84	2.00E-04	6.22E-03
HH12	<i>TTR</i>	transthyretin	-0.87	2.00E-04	6.22E-03
HH12	<i>XPA</i>	xeroderma pigmentosum, complementation group A	0.90	2.00E-04	6.22E-03
HH12	<i>ANGPTL3</i>	angiopoietin like 3	-1.64	2.50E-04	7.46E-03
HH12	<i>C15ORF15</i>	ribosomal L24 domain containing 1	0.91	2.50E-04	7.46E-03
HH12	<i>CYGB</i>	cytoglobin	-1.48	2.50E-04	7.46E-03
HH12	<i>GCSH</i>	glycine cleavage system protein H (aminomethyl carrier)	0.81	2.50E-04	7.46E-03
HH12	<i>LMNB2</i>	lamin B2	-0.87	2.50E-04	7.46E-03
HH12	<i>TMOD1</i>	tropomodulin 1	0.84	2.50E-04	7.46E-03
HH12	<i>VCL</i>	vinculin	-0.87	2.50E-04	7.46E-03
HH12	<i>ALG6</i>	ALG6, alpha-1,3-glucosyltransferase	0.93	3.00E-04	8.42E-03
HH12	<i>BRX1</i>	BRX1, biogenesis of ribosomes	1.01	3.00E-04	8.42E-03
HH12	<i>CXCL12</i>	chemokine (C-X-C motif) ligand 12	-1.30	3.00E-04	8.42E-03
HH12	<i>ETV5</i>	ets variant 5	-0.91	3.00E-04	8.42E-03
HH12	<i>FLT1</i>	fms-related tyrosine kinase 1	-0.98	3.00E-04	8.42E-03
HH12	<i>MYH7B</i>	myosin, heavy chain 7B, cardiac muscle, beta	1.07	3.00E-04	8.42E-03
HH12	<i>POPDC3</i>	popeye domain containing 3	1.06	3.00E-04	8.42E-03
HH12	<i>SALL3</i>	spalt-like transcription factor 3	-0.96	3.00E-04	8.42E-03

HH12	<i>SEPT19</i>		-0.87	3.00E-04	8.42E-03
HH12	<i>SOHO-1</i>	sensory organ homeobox protein SOHo	1.31	3.00E-04	8.42E-03
HH12	<i>TNNT2</i>	troponin T type 2 (cardiac)	1.13	3.00E-04	8.42E-03
HH12	<i>ANGPT1</i>	angiopoietin 1	1.04	3.50E-04	9.41E-03
HH12	<i>ARID3B</i>	actin related protein 2/3 complex, subunit 1B, 41kDa	-0.86	3.50E-04	9.41E-03
HH12	<i>DAG1</i>	dystroglycan 1 (dystrophin-associated glycoprotein 1)	-0.79	3.50E-04	9.41E-03
HH12	<i>DPYSL2</i>	dihydropyrimidinase-like 2	-0.78	3.50E-04	9.41E-03
HH12	<i>MYH9</i>	myosin, heavy chain 9, non-muscle	-0.89	3.50E-04	9.41E-03
HH12	<i>PTK2</i>	protein tyrosine kinase 2	-0.78	3.50E-04	9.41E-03
HH12	<i>ST3GAL1</i>	ST3 beta-galactoside alpha-2,3-sialyltransferase 1	-0.93	3.50E-04	9.41E-03
HH12	<i>SULT1C3</i>	sulfotransferase family, cytosolic, 1C, member 3	-1.96	3.50E-04	9.41E-03
HH12	<i>CNP</i>	2',3'-cyclic nucleotide 3' phosphodiesterase	-1.02	4.00E-04	1.04E-02
HH12	<i>DLL1</i>	delta-like 1 (Drosophila)	-1.14	4.00E-04	1.04E-02
HH12	<i>EFNB2</i>	ephrin-B2	-1.43	4.00E-04	1.04E-02
HH12	<i>GLI1</i>	GLI family zinc finger 1	-0.92	4.00E-04	1.04E-02
HH12	<i>LSM3</i>	LSM3 homolog, U6 small nuclear RNA and mRNA degradation associated	0.83	4.00E-04	1.04E-02
HH12	<i>SREBF1</i>	sterol regulatory element binding transcription factor 1	-0.84	4.00E-04	1.04E-02
HH12	<i>COX20</i>	COX20 cytochrome c oxidase assembly factor	0.88	4.50E-04	1.12E-02
HH12	<i>EFNA2</i>	ephrin-A2	-1.33	4.50E-04	1.12E-02
HH12	<i>ETS2</i>	v-ets avian erythroblastosis virus E26 oncogene homolog 2	-0.94	4.50E-04	1.12E-02
HH12	<i>FOSL2</i>	FOS like antigen 2	-2.73	4.50E-04	1.12E-02
HH12	<i>IRF8</i>	interferon regulatory factor 8	-1.08	4.50E-04	1.12E-02

HH12	<i>LSS</i>	lanosterol synthase (2,3-oxidosqualene-lanosterol cyclase)	-0.87	4.50E-04	1.12E-02
HH12	<i>PAX7</i>	paired box 7	-1.58	4.50E-04	1.12E-02
HH12	<i>PCDH15</i>	protocadherin-related 15	1.28	4.50E-04	1.12E-02
HH12	<i>SNRPF</i>	small nuclear ribonucleoprotein polypeptide F	0.86	4.50E-04	1.12E-02
HH12	<i>FSCN1</i>	fascin actin-bundling protein 1	-0.78	5.00E-04	1.22E-02
HH12	<i>GSTK1</i>	glutathione S-transferase kappa 1	0.82	5.00E-04	1.22E-02
HH12	<i>LAMB2</i>	laminin, beta 2 (laminin S)	1.02	5.00E-04	1.22E-02
HH12	<i>SEPT15</i>		0.77	5.00E-04	1.22E-02
HH12	<i>TRAPPC13</i>	trafficking protein particle complex 13	1.00	5.00E-04	1.22E-02
HH12	<i>EFNB1</i>	ephrin-B1	-0.77	5.50E-04	1.29E-02
HH12	<i>AKR1B1L</i>	aldo-keto reductase family 1 member B1-like	1.01	5.50E-04	1.29E-02
HH12	<i>DYL1</i>	dynein light chain 1 cytoplasmic	0.82	5.50E-04	1.29E-02
HH12	<i>NR5A2</i>	nuclear receptor subfamily 5, group A, member 2	-1.59	5.50E-04	1.29E-02
HH12	<i>PDZK1IP1</i>	PDZK1 interacting protein 1	-1.52	5.50E-04	1.29E-02
HH12	<i>RALBP1</i>	ralA binding protein 1	-0.80	5.50E-04	1.29E-02
HH12	<i>TBX5</i>	T-box 5	0.80	5.50E-04	1.29E-02
HH12	<i>TCF3</i>	transcription factor 3	-0.75	5.50E-04	1.29E-02
HH12	<i>FZR1</i>	fizzy/cell division cycle 20 related 1	-0.85	6.00E-04	1.38E-02
HH12	<i>FDFT1</i>	farnesyl-diphosphate farnesyltransferase 1	-0.77	6.00E-04	1.38E-02
HH12	<i>NDUFA5</i>	NADH:ubiquinone oxidoreductase subunit A5	0.80	6.00E-04	1.38E-02
HH12	<i>SPP1</i>	secreted phosphoprotein 1	-0.90	6.00E-04	1.38E-02
HH12	<i>VAV2</i>	vav 2 guanine nucleotide exchange factor	-0.87	6.00E-04	1.38E-02
HH12	<i>CDH11</i>	cadherin 11, type 2, OB-cadherin (osteoblast)	-0.73	6.50E-04	1.43E-02
HH12	<i>CNOT4</i>	CCR4-NOT transcription complex subunit 4	-0.91	6.50E-04	1.43E-02
HH12	<i>DPF2</i>	D4, zinc and double PHD fingers family 2	-0.88	6.50E-04	1.43E-02
HH12	<i>GLG1</i>	golgi glycoprotein 1	-0.74	6.50E-04	1.43E-02

HH12	<i>MYEOV2</i>	COP9 signalosome subunit 9	0.81	6.50E-04	1.43E-02
HH12	<i>NFASC</i>	neurofascin	-0.93	6.50E-04	1.43E-02
HH12	<i>ODF2</i>	outer dense fiber of sperm tails 2	-0.72	6.50E-04	1.43E-02
HH12	<i>RPL17</i>	ribosomal protein L17	1.07	6.50E-04	1.43E-02
HH12	<i>RRAD</i>	Ras-related associated with diabetes	1.19	6.50E-04	1.43E-02
HH12	<i>ELL</i>	elongation factor RNA polymerase II	-0.80	7.00E-04	1.50E-02
HH12	<i>GEM</i>	GTP binding protein overexpressed in skeletal muscle	-2.66	7.00E-04	1.50E-02
HH12	<i>NRK</i>	Nik related kinase	-1.07	7.00E-04	1.50E-02
HH12	<i>RPL34</i>	ribosomal protein L34	0.82	7.00E-04	1.50E-02
HH12	<i>STAT3</i>	signal transducer and activator of transcription 3 (acute-phase response factor)	-0.80	7.00E-04	1.50E-02
HH12	<i>YRK</i>	proto-oncogene tyrosine-protein kinase Yrk	-1.14	7.00E-04	1.50E-02
HH12	<i>NAB1</i>	NGFI-A binding protein 1 (EGR1 binding protein 1)	-1.06	7.50E-04	1.60E-02
HH12	<i>NDUFB5</i>	NADH:ubiquinone oxidoreductase subunit B5	0.78	7.50E-04	1.60E-02
HH12	<i>CECR2</i>	cat eye syndrome chromosome region, candidate 2	-0.84	8.00E-04	1.67E-02
HH12	<i>GAP43</i>	growth associated protein 43	-0.95	8.00E-04	1.67E-02
HH12	<i>RBMS1</i>	RNA binding motif single stranded interacting protein 1	-0.77	8.00E-04	1.67E-02
HH12	<i>RGMA</i>	RGM domain family, member A	-1.03	8.00E-04	1.67E-02
HH12	<i>TMLHE</i>	trimethyllysine hydroxylase, epsilon	-0.72	8.00E-04	1.67E-02
HH12	<i>ASNS</i>	asparagine synthetase (glutamine-hydrolyzing)	0.75	8.50E-04	1.74E-02
HH12	<i>CALD1</i>	caldesmon 1	-0.76	8.50E-04	1.74E-02
HH12	<i>GNOT1</i>	Gnot1 homeodomain protein	-1.74	8.50E-04	1.74E-02
HH12	<i>PCDH1</i>	protocadherin 1	-0.90	8.50E-04	1.74E-02
HH12	<i>SUB1</i>	SUB1 homolog (<i>S. cerevisiae</i>)	0.80	8.50E-04	1.74E-02
HH12	<i>ADCK3</i>	aarF domain containing kinase 3	-0.74	9.00E-04	1.81E-02

HH12	<i>BMPER</i>	BMP binding endothelial regulator	-1.51	9.00E-04	1.81E-02
HH12	<i>C26H6ORF125</i>	chromosome 26 open reading frame, human C6orf125	0.77	9.00E-04	1.81E-02
HH12	<i>REEP5</i>	receptor accessory protein 5	0.83	9.00E-04	1.81E-02
HH12	<i>RPRD2</i>	regulation of nuclear pre-mRNA domain containing 2	-0.76	9.00E-04	1.81E-02
HH12	<i>APBB1IP</i>	amyloid beta (A4) precursor protein-binding, family B, member 1 interacting protein	-1.20	9.50E-04	1.88E-02
HH12	<i>LSM8</i>	LSM8 homolog, U6 small nuclear RNA associated (<i>S. cerevisiae</i>)	0.83	9.50E-04	1.88E-02
HH12	<i>MRPS25</i>	mitochondrial ribosomal protein S25	0.72	9.50E-04	1.88E-02
HH12	<i>DIO3</i>	deiodinase, iodothyronine, type III	0.97	1.00E-03	1.96E-02
HH12	<i>TCF7</i>	transcription factor 7 (T-cell specific, HMG-box)	-1.86	1.00E-03	1.96E-02
HH12	<i>ZNF609</i>	zinc finger protein 609	-0.77	1.00E-03	1.96E-02
HH12	<i>CST3</i>	cystatin C	0.70	1.05E-03	2.02E-02
HH12	<i>HAND1</i>	heart and neural crest derivatives expressed 1	-0.80	1.05E-03	2.02E-02
HH12	<i>LDB3</i>	LIM domain binding 3	1.17	1.05E-03	2.02E-02
HH12	<i>LSAMP</i>	limbic system-associated membrane protein	-1.25	1.05E-03	2.02E-02
HH12	<i>STK40</i>	serine/threonine kinase 40	-0.73	1.05E-03	2.02E-02
HH12	<i>ACTA1</i>	actin, alpha 1, skeletal muscle	0.87	1.10E-03	2.08E-02
HH12	<i>COL4A2</i>	collagen, type IV, alpha 2	-0.76	1.10E-03	2.08E-02
HH12	<i>SMPX</i>	small muscle protein, X-linked	1.13	1.10E-03	2.08E-02
HH12	<i>TMEM121</i>	transmembrane protein 121	0.74	1.10E-03	2.08E-02
HH12	<i>ACACA</i>	acetyl-CoA carboxylase alpha	-0.74	1.15E-03	2.14E-02
HH12	<i>COL4A1</i>	collagen, type IV, alpha 1	-0.74	1.15E-03	2.14E-02
HH12	<i>ELF1</i>	E74-like factor 1 (ets domain transcription factor)	-1.02	1.15E-03	2.14E-02
HH12	<i>MRPL48</i>	mitochondrial ribosomal protein L48	0.73	1.15E-03	2.14E-02
HH12	<i>NBL1</i>	neuroblastoma, suppression of tumorigenicity 1	-0.83	1.15E-03	2.14E-02

HH12	<i>ACTN2</i>	actinin, alpha 2	0.85	1.20E-03	2.19E-02
HH12	<i>CCDC50</i>	coiled-coil domain containing 50	-0.79	1.20E-03	2.19E-02
HH12	<i>HDLBP</i>	high density lipoprotein binding protein	-0.85	1.20E-03	2.19E-02
HH12	<i>MYH10</i>	myosin, heavy chain 10, non-muscle	-0.80	1.20E-03	2.19E-02
HH12	<i>TGM4</i>	transglutaminase 4 (prostate)	-2.26	1.20E-03	2.19E-02
HH12	<i>TMEM60</i>	transmembrane protein 60	0.92	1.20E-03	2.19E-02
HH12	<i>SLC30A5</i>	solute carrier family 30 (zinc transporter), member 5	0.73	1.25E-03	2.26E-02
HH12	<i>TMEM258</i>	transmembrane protein 258	0.74	1.25E-03	2.26E-02
HH12	<i>FMO6P</i>	Flavin Containing Monooxygenase 6 Pseudogene	-1.70	1.35E-03	2.40E-02
HH12	<i>HAT1</i>	histone acetyltransferase 1	0.72	1.35E-03	2.40E-02
HH12	<i>LMO2</i>	LIM domain only 2 (rhombotin-like 1)	-0.73	1.35E-03	2.40E-02
HH12	<i>SRGAP3</i>	SLIT-ROBO Rho GTPase activating protein 3	-0.90	1.35E-03	2.40E-02
HH12	<i>TSPAN18</i>	tetraspanin 18	-1.39	1.35E-03	2.40E-02
HH12	<i>C1H7orf73</i>	chromosome 7 open reading frame 73	0.75	1.40E-03	2.47E-02
HH12	<i>EMC2</i>	ER membrane protein complex subunit 2	0.72	1.40E-03	2.47E-02
HH12	<i>APOD</i>	apolipoprotein D	-2.08	1.45E-03	2.52E-02
HH12	<i>LDB1</i>	LIM domain binding 1	-0.84	1.45E-03	2.52E-02
HH12	<i>MEIS1</i>	Meis homeobox 1	-0.72	1.45E-03	2.52E-02
HH12	<i>N6AMT1</i>	N-6 adenine-specific DNA methyltransferase 1 (putative)	0.73	1.45E-03	2.52E-02
HH12	<i>C10H15orf61</i>	chromosome 26 open reading frame, human C6orf125(C26H6ORF125)	0.85	1.50E-03	2.56E-02
HH12	<i>FOXL2</i>	forkhead box L2	-2.38	1.50E-03	2.56E-02
HH12	<i>ITIH2</i>	inter-alpha-trypsin inhibitor heavy chain 2	-1.84	1.50E-03	2.56E-02
HH12	<i>PCDH19</i>	protocadherin 19	-1.01	1.50E-03	2.56E-02
HH12	<i>POLR3H</i>	polymerase (RNA) III subunit H	0.72	1.50E-03	2.56E-02

HH12	<i>SDC3</i>	syndecan 3	-1.20	1.50E-03	2.56E-02
HH12	<i>MYO1A</i>	myosin IA	-0.95	1.55E-03	2.64E-02
HH12	<i>COL22A1</i>	collagen, type XXII, alpha 1	-0.97	1.60E-03	2.71E-02
HH12	<i>LHX1</i>	LIM homeobox 1	-3.01	1.65E-03	2.76E-02
HH12	<i>MSRB3</i>	methionine sulfoxide reductase B3	0.96	1.65E-03	2.76E-02
HH12	<i>NKX3-2</i>	NK3 homeobox 2	-0.82	1.65E-03	2.76E-02
HH12	<i>XIRP1</i>	xin actin-binding repeat containing 1	0.79	1.65E-03	2.76E-02
HH12	<i>AP3S2</i>	adaptor related protein complex 3 sigma 2 subunit	0.74	1.70E-03	2.79E-02
HH12	<i>APCDD1</i>	adenomatosis polyposis coli down-regulated 1	-0.72	1.70E-03	2.79E-02
HH12	<i>GATAD2A</i>	GATA zinc finger domain containing 2A	-0.68	1.70E-03	2.79E-02
HH12	<i>PITX2</i>	paired-like homeodomain 2	-0.69	1.70E-03	2.79E-02
HH12	<i>PTCHD2</i>	dispatched RND transporter family member 3	-1.15	1.70E-03	2.79E-02
HH12	<i>UQCRCF1</i>	ubiquinol-cytochrome c reductase, Rieske iron-sulfur polypeptide 1	0.69	1.70E-03	2.79E-02
HH12	<i>ATP6V1G1</i>	ATPase, H+ transporting, lysosomal 13kDa, V1 subunit G1	0.69	1.75E-03	2.81E-02
HH12	<i>C12ORF57</i>	chromosome 1 open reading frame, human C12orf57	0.74	1.75E-03	2.81E-02
HH12	<i>CFC1B</i>	cripto, FRL-1, cryptic family 1B	0.76	1.75E-03	2.81E-02
HH12	<i>DNAJC12</i>	DnaJ heat shock protein family (Hsp40) member C12	0.95	1.75E-03	2.81E-02
HH12	<i>NDUFA4</i>	NADH dehydrogenase (ubiquinone) 1 alpha subcomplex, 4, 9kDa	0.73	1.75E-03	2.81E-02
HH12	<i>RGS6</i>	regulator of G-protein signaling 6	0.99	1.75E-03	2.81E-02
HH12	<i>WDR44</i>	WD repeat domain 44	-0.72	1.75E-03	2.81E-02
HH12	<i>ISL1</i>	ISL LIM homeobox 1	0.99	1.80E-03	2.86E-02
HH12	<i>KANK1</i>	KN motif and ankyrin repeat domains 1	-0.72	1.80E-03	2.86E-02
HH12	<i>ZNF692</i>	zinc finger protein 692	-0.78	1.80E-03	2.86E-02

HH12	<i>ABRACL</i>	ABRA C-terminal like	0.79	1.90E-03	2.99E-02
HH12	<i>GTF2A2</i>	general transcription factor IIA 2	0.71	1.90E-03	2.99E-02
HH12	<i>MAT1A</i>	methionine adenosyltransferase I, alpha	1.41	1.90E-03	2.99E-02
HH12	<i>RBPM52</i>	RNA binding protein with multiple splicing 2	0.69	1.95E-03	3.06E-02
HH12	<i>CSNK1E</i>	casein kinase 1, epsilon	-0.71	2.00E-03	3.10E-02
HH12	<i>PIGBOS1</i>	PIGB opposite strand 1	0.85	2.00E-03	3.10E-02
HH12	<i>PPIH</i>	peptidylprolyl isomerase H	0.69	2.00E-03	3.10E-02
HH12	<i>WDR61</i>	WD repeat domain 61	0.70	2.00E-03	3.10E-02
HH12	<i>RPL27A</i>	ribosomal protein L27a	0.83	2.05E-03	3.17E-02
HH12	<i>CCDC58</i>	coiled-coil domain containing 58	0.73	2.10E-03	3.22E-02
HH12	<i>DTYMK</i>	deoxythymidylate kinase	0.69	2.10E-03	3.22E-02
HH12	<i>SHFM1</i>	split hand/foot malformation (ectrodactyly) type 1	0.86	2.10E-03	3.22E-02
HH12	<i>ARHGEF6</i>	Rac/Cdc42 guanine nucleotide exchange factor (GEF) 6	-0.95	2.15E-03	3.26E-02
HH12	<i>COMMD4</i>	COMM domain containing 4	0.74	2.15E-03	3.26E-02
HH12	<i>MRPL21</i>	mitochondrial ribosomal protein L21	0.70	2.15E-03	3.26E-02
HH12	<i>TUBB</i>	tubulin, beta class I	-0.90	2.15E-03	3.26E-02
HH12	<i>HPGDS</i>	hematopoietic prostaglandin D synthase	2.06	2.20E-03	3.30E-02
HH12	<i>RBM38</i>	RNA binding motif protein 38	0.68	2.20E-03	3.30E-02
HH12	<i>VGLL2</i>	vestigial like family member 2	1.47	2.20E-03	3.30E-02
HH12	<i>VMA21</i>	VMA21 vacuolar H ⁺ -ATPase homolog (<i>S. cerevisiae</i>)	0.74	2.25E-03	3.37E-02
HH12	<i>CXCR7</i>	chemokine (C-X-C motif) receptor 7	0.71	2.30E-03	3.42E-02
HH12	<i>MRPS35</i>	mitochondrial ribosomal protein S35	0.67	2.30E-03	3.42E-02
HH12	<i>AP3S1</i>	adaptor-related protein complex 3, sigma 1 subunit	0.72	2.35E-03	3.48E-02
HH12	<i>CHRM4</i>	cholinergic receptor, muscarinic 4	-1.10	2.35E-03	3.48E-02
HH12	<i>LYRM2</i>	LYR motif containing 2	0.92	2.40E-03	3.53E-02
HH12	<i>RPL37</i>	ribosomal protein L37	0.74	2.40E-03	3.53E-02

HH12	<i>EDEM1</i>	ER degradation enhancer, mannosidase alpha-like 1	-0.86	2.45E-03	3.58E-02
HH12	<i>NDUFA8</i>	NADH:ubiquinone oxidoreductase subunit A8	0.68	2.45E-03	3.58E-02
HH12	<i>LGI2</i>	leucine-rich repeat LGI family, member 2	0.97	2.50E-03	3.65E-02
HH12	<i>PAX6</i>	paired box 6	-0.81	2.55E-03	3.70E-02
HH12	<i>RIOK2</i>	RIO kinase 2	0.68	2.55E-03	3.70E-02
HH12	<i>GSTO1</i>	glutathione S-transferase omega 1	0.68	2.60E-03	3.75E-02
HH12	<i>ITPKA</i>	inositol-trisphosphate 3-kinase A	-0.94	2.60E-03	3.75E-02
HH12	<i>CRTAP</i>	cartilage associated protein	0.75	2.65E-03	3.79E-02
HH12	<i>DPYSL3</i>	dihydropyrimidinase-like 3	-0.66	2.65E-03	3.79E-02
HH12	<i>SPECC1L</i>	sperm antigen with calponin homology and coiled-coil domains 1-like	-0.72	2.65E-03	3.79E-02
HH12	<i>PTTG1</i>	pituitary tumor-transforming 1	0.70	2.70E-03	3.84E-02
HH12	<i>SEMA3D</i>	sema domain, immunoglobulin domain (Ig), short basic domain, secreted, (semaphorin) 3D	-0.74	2.70E-03	3.84E-02
HH12	<i>ALDH1A2</i>	aldehyde dehydrogenase 1 family, member A2	-0.70	2.75E-03	3.86E-02
HH12	<i>DENR</i>	density-regulated protein	0.68	2.75E-03	3.86E-02
HH12	<i>NTPCR</i>	nucleoside-triphosphatase, cancer-related	0.77	2.75E-03	3.86E-02
HH12	<i>PNRC1</i>	proline rich nuclear receptor coactivator 1	-0.67	2.75E-03	3.86E-02
HH12	<i>STXBP1</i>	syntaxin binding protein 1	-0.86	2.75E-03	3.86E-02
HH12	<i>IMMP1L</i>	inner mitochondrial membrane peptidase subunit 1	0.95	2.80E-03	3.92E-02
HH12	<i>TLN1</i>	talin 1	-0.67	2.85E-03	3.98E-02
HH12	<i>ENY2</i>	enhancer of yellow 2 homolog (Drosophila)	0.69	2.90E-03	4.01E-02
HH12	<i>GRB2</i>	growth factor receptor bound protein 2	-0.74	2.90E-03	4.01E-02
HH12	<i>MYOM1</i>	myomesin 1	0.72	2.90E-03	4.01E-02
HH12	<i>CHST6</i>	carbohydrate (N-acetylglucosamine 6-O) sulfotransferase 6	0.68	2.95E-03	4.06E-02

HH12	<i>IL17D</i>	interleukin 17D	down	2.95E-03	4.06E-02
HH12	<i>PXN</i>	paxillin	-0.75	3.15E-03	4.32E-02
HH12	<i>FURIN</i>	furin (paired basic amino acid cleaving enzyme)	-0.79	3.20E-03	4.35E-02
HH12	<i>PBRM1</i>	polybromo 1	-0.65	3.20E-03	4.35E-02
HH12	<i>TCEB1</i>	transcription elongation factor B subunit 1	0.67	3.20E-03	4.35E-02
HH12	<i>WNT3A</i>	wingless-type MMTV integration site family, member 3A	-1.49	3.20E-03	4.35E-02
HH12	<i>NELL2</i>	NEL-like 2	-0.72	3.25E-03	4.40E-02
HH12	<i>CASQ2</i>	calsequestrin 2 (cardiac muscle)	0.98	3.30E-03	4.42E-02
HH12	<i>PSMA2</i>	Uncharacterized protein	0.66	3.30E-03	4.42E-02
HH12	<i>RPS6</i>	ribosomal protein S6	1.13	3.30E-03	4.42E-02
HH12	<i>SIK1</i>	salt-inducible kinase 1	0.69	3.30E-03	4.42E-02
HH12	<i>UQCR10</i>	ubiquinol-cytochrome c reductase, complex III subunit X	0.71	3.35E-03	4.47E-02
HH12	<i>VEZF1</i>	vascular endothelial zinc finger 1	-0.72	3.35E-03	4.47E-02
HH12	<i>DPY30</i>	dpy-30, histone methyltransferase complex regulatory subunit	0.68	3.40E-03	4.48E-02
HH12	<i>EDNRB</i>	endothelin receptor type B	-0.95	3.40E-03	4.48E-02
HH12	<i>PGC</i>	progastricsin	1.01	3.40E-03	4.48E-02
HH12	<i>POLR2F</i>	polymerase (RNA) II subunit F	0.67	3.40E-03	4.48E-02
HH12	<i>RPL37A</i>	ribosomal protein L37a	0.71	3.40E-03	4.48E-02
HH12	<i>YAP1</i>	Yes-associated protein 1	-0.70	3.45E-03	4.53E-02
HH12	<i>NF2</i>	neurofibromin 2 (bilateral acoustic neuroma)	-0.66	3.50E-03	4.56E-02
HH12	<i>PODXL</i>	podocalyxin-like	-0.68	3.50E-03	4.56E-02
HH12	<i>WDR36</i>	WD repeat domain 36	0.65	3.50E-03	4.56E-02
HH12	<i>AGTPBP1</i>	ATP/GTP binding protein 1	1.23	3.55E-03	4.59E-02
HH12	<i>FGF19</i>	fibroblast growth factor 19	0.89	3.55E-03	4.59E-02

HH12	<i>TOP2A</i>	topoisomerase (DNA) II alpha 170kDa	-0.68	3.55E-03	4.59E-02
HH12	<i>RBP5</i>	retinol binding protein 5, cellular	0.65	3.60E-03	4.64E-02
HH12	<i>HDAC7</i>	histone deacetylase 7	-0.67	3.65E-03	4.70E-02
HH12	<i>LRP1</i>	low density lipoprotein receptor-related protein 1	-0.69	3.70E-03	4.74E-02
HH12	<i>TNNI3K</i>	TNNI3 interacting kinase	1.94	3.70E-03	4.74E-02
HH12	<i>COLEC10</i>	collectin sub-family member 10 (C-type lectin)	-1.61	3.75E-03	4.78E-02
HH12	<i>GHRL</i>	ghrelin/obestatin prepropeptide	2.00	3.75E-03	4.78E-02
HH12	<i>GNAI2</i>	guanine nucleotide binding protein (G protein), alpha inhibiting activity polypeptide 2	-0.66	3.80E-03	4.82E-02
HH12	<i>VIT</i>	vitrin	-1.07	3.80E-03	4.82E-02
HH12	<i>RAD54L2</i>	RAD54-like 2	-0.65	3.85E-03	4.87E-02
HH12	<i>DYRK1A</i>	dual-specificity tyrosine-(Y)-phosphorylation regulated kinase 1A	-0.83	3.90E-03	4.91E-02
HH12	<i>PMEL</i>	premelanosome protein	-0.81	3.90E-03	4.91E-02
HH12	<i>MELK</i>	maternal embryonic leucine zipper kinase	0.66	3.95E-03	4.96E-02
HH12	<i>HMHA1</i>	histocompatibility (minor) HA-1	-0.96	4.00E-03	4.99E-02
HH12	<i>TP53I11</i>	tumor protein p53 inducible protein 11	-0.73	4.00E-03	4.99E-02
HH12	<i>YES1</i>	v-yes-1 Yamaguchi sarcoma viral oncogene homolog 1	-0.72	4.00E-03	4.99E-02
HH14	<i>MARC2</i>	Mitochondrial Amidoxime Reducing Component 2	-0.53	8.20E-03	9.67E-02
HH14	<i>ACTN4</i>	actinin, alpha 4	0.39	4.53E-02	3.25E-01
HH14	<i>AKR1B10</i>	aldo-keto reductase family 1, member B10 (aldose reductase)	-1.59	4.15E-03	5.72E-02
HH14	<i>AKR1B1L</i>	aldo-keto reductase family 1, member B1-like (aldose reductase)	-0.58	1.71E-02	1.67E-01
HH14	<i>ALDH1A2</i>	aldehyde dehydrogenase 1 family, member A2	-0.56	7.10E-03	8.75E-02
HH14	<i>ANGPTL2</i>	angiopoietin-like 2	-0.51	2.87E-02	2.41E-01
HH14	<i>AQP1</i>	aquaporin 1	1.23	2.00E-04	4.37E-03

HH14	<i>BFSP2</i>	beaded filament structural protein 2	-0.74	5.00E-02	3.46E-01
HH14	<i>C9H21ORF2</i>	chromosome 9 open reading frame, human C21orf2(C9H21ORF2)	-0.47	2.80E-02	2.37E-01
HH14	<i>CACNG3</i>	calcium channel, voltage-dependent, gamma subunit 3	-0.68	4.14E-02	3.09E-01
HH14	<i>CAPN2</i>	calpain 2, (m/II) large subunit	-0.54	3.25E-02	2.62E-01
HH14	<i>CD44</i>	CD44 molecule (Indian blood group)	-1.27	2.80E-02	2.37E-01
HH14	<i>CDX1</i>	caudal type homeobox 1	1.42	2.01E-02	1.88E-01
HH14	<i>CENPF</i>	centromere protein F	-0.42	3.11E-02	2.55E-01
HH14	<i>CETN2</i>	centrin, EF-hand protein, 2	-0.47	1.81E-02	1.74E-01
HH14	<i>COL2A1</i>	collagen, type II, alpha 1	0.63	1.60E-03	2.61E-02
HH14	<i>CPPED1</i>	calcineurin-like phosphoesterase domain containing 1	-0.49	3.18E-02	2.58E-01
HH14	<i>CRABP1</i>	cellular retinoic acid binding protein 1	-0.41	3.55E-02	2.78E-01
HH14	<i>CRYGS</i>	crystallin, gamma S	up	1.50E-04	3.38E-03
HH14	<i>CXCL14</i>	C-X-C motif chemokine ligand 14	-0.41	3.92E-02	2.98E-01
HH14	<i>DENR</i>	density-regulated protein	-0.39	4.65E-02	3.30E-01
HH14	<i>ENPP4</i>	ectonucleotide pyrophosphatase/phosphodiesterase 4 (putative)	-0.55	4.42E-02	3.20E-01
HH14	<i>ERN1</i>	early response to neural induction ERN1	-1.22	1.75E-02	1.70E-01
HH14	<i>FABP3</i>	fatty acid binding protein 3, muscle and heart (mammary-derived growth inhibitor)	-0.61	2.01E-02	1.87E-01
HH14	<i>FAM133B</i>	family with sequence similarity 133, member B	-0.46	1.89E-02	1.79E-01
HH14	<i>FGA</i>	fibrinogen alpha chain	-1.07	1.40E-03	2.32E-02
HH14	<i>FGB</i>	fibrinogen beta chain	-0.60	1.39E-02	1.43E-01
HH14	<i>FGG</i>	fibrinogen gamma chain	-0.61	1.90E-02	1.80E-01
HH14	<i>FST</i>	follicle-stimulating hormone receptor 1	0.51	2.28E-02	2.06E-01
HH14	<i>G0S2</i>	G0/G1 switch 2	-1.33	3.08E-02	2.53E-01

HH14	<i>GBP</i>	guanylate binding protein	-1.57	4.55E-02	3.26E-01
HH14	<i>GLI1</i>	GLI family zinc finger 1	0.48	2.75E-02	2.34E-01
HH14	<i>GUCA2B</i>	guanylate cyclase activator 2B (uroguanylin)	5.27	5.00E-05	1.23E-03
HH14	<i>HAND1</i>	heart and neural crest derivatives expressed 1	0.53	2.46E-02	2.17E-01
HH14	<i>HGF</i>	hepatocyte growth factor	-0.93	2.05E-02	1.90E-01
HH14	<i>HK2</i>	hexokinase 2	0.44	2.67E-02	2.29E-01
HH14	<i>HMGN3</i>	high mobility group nucleosomal binding domain 3	-0.40	4.23E-02	3.13E-01
HH14	<i>HNRPK</i>	heterogeneous nuclear ribonucleoprotein K	-0.62	1.40E-02	1.44E-01
HH14	<i>IFT52</i>	intraflagellar transport 52	-0.48	2.45E-02	2.16E-01
HH14	<i>JUN</i>	jun proto-oncogene	-0.56	5.35E-03	7.01E-02
HH14	<i>KHDRBS1</i>	KH domain containing, RNA binding, signal transduction associated 1	-0.45	2.16E-02	1.98E-01
HH14	<i>LAMB2</i>	laminin, beta 2 (laminin S)	0.60	3.90E-02	2.97E-01
HH14	<i>LOC425137</i>	aldo-keto reductase family 1, member B1-like(LOC425137)	-0.75	1.46E-02	1.49E-01
HH14	<i>LOC427025</i>	Nipped-B homolog-like(LOC427025)	-0.57	2.83E-02	2.39E-01
HH14	<i>LSP1</i>	lymphocyte-specific protein 1	-0.41	3.98E-02	3.01E-01
HH14	<i>MAP6</i>	microtubule associated protein 6	-0.46	4.37E-02	3.19E-01
HH14	<i>MEOX1</i>	mesenchyme homeobox 1	-0.45	2.36E-02	2.10E-01
HH14	<i>MFI2</i>	melanotransferrin	0.68	3.96E-02	3.00E-01
HH14	<i>MIR1306</i>	microRNA 1306	down	7.40E-03	8.90E-02
HH14	<i>MIR130B</i>	microRNA 130b	up	2.32E-02	2.08E-01
HH14	<i>MIR135A1</i>	microRNA 135a-1	up	1.80E-02	1.73E-01
HH14	<i>MIR1454</i>	microRNA 1454	up	4.67E-02	3.31E-01
HH14	<i>MIR1562</i>	microRNA 1562	down	7.40E-03	8.90E-02
HH14	<i>MIR1564</i>	microRNA 1564	up	2.32E-02	2.08E-01
HH14	<i>MIR1612</i>	microRNA 1612	down	7.40E-03	8.90E-02

HH14	<i>MIR1615</i>	microRNA 1615	up	2.32E-02	2.08E-01
HH14	<i>MIR1653</i>	microRNA 1653	up	1.06E-02	1.17E-01
HH14	<i>MIR1683</i>	microRNA 1683	up	1.06E-02	1.17E-01
HH14	<i>MIR1689</i>	microRNA 1689	up	4.40E-02	3.20E-01
HH14	<i>MIR1747</i>	microRNA 1747	down	7.40E-03	8.90E-02
HH14	<i>MIR1773</i>	microRNA 1773	down	7.40E-03	8.90E-02
HH14	<i>MIR1774</i>	microRNA 1774	up	4.40E-02	3.20E-01
HH14	<i>MIR1778</i>	microRNA 1778	down	7.40E-03	8.90E-02
HH14	<i>MIR1787</i>	microRNA 1787	up	2.32E-02	2.08E-01
HH14	<i>MIR216B</i>	microRNA 216b	up	3.12E-02	2.56E-01
HH14	<i>MIR3607</i>	microRNA 3607	up	4.40E-02	3.20E-01
HH14	<i>MIR454</i>	microRNA 454	up	2.32E-02	2.08E-01
HH14	<i>MIR6569</i>	microRNA 6569	down	7.40E-03	8.90E-02
HH14	<i>MIR6580</i>	microRNA 6580	down	7.40E-03	8.90E-02
HH14	<i>MIR6592</i>	microRNA 6592	up	4.40E-02	3.20E-01
HH14	<i>MIR6602</i>	microRNA 6602	up	1.80E-02	1.73E-01
HH14	<i>MIR6618</i>	microRNA 6618	up	4.40E-02	3.20E-01
HH14	<i>MIR6640</i>	microRNA 6640	down	7.40E-03	8.90E-02
HH14	<i>MIR6700</i>	microRNA 6700	up	4.40E-02	3.20E-01
HH14	<i>MIR7-1</i>	microRNA 7-1	up	2.32E-02	2.08E-01
HH14	<i>MIR762</i>	microRNA 762	down	7.40E-03	8.90E-02
HH14	<i>MTERFD1</i>	mitochondrial transcription termination factor 3	-0.45	2.33E-02	2.09E-01
HH14	<i>MXD4</i>	MAX dimerization protein 4	-0.61	4.03E-02	3.03E-01
HH14	<i>MYOM2</i>	myomesin 2	0.60	6.15E-03	7.82E-02
HH14	<i>OVAL</i>	ovalbumin (SERPINB14)	-1.95	4.80E-03	6.40E-02
HH14	<i>PDLIM3</i>	PDZ and LIM domain 3	0.97	3.42E-02	2.71E-01
HH14	<i>PEX2</i>	peroxisomal biogenesis factor 2	-0.51	1.61E-02	1.60E-01

HH14	<i>PKIB</i>	protein kinase (cAMP-dependent, catalytic) inhibitor beta	-0.97	4.29E-02	3.15E-01
HH14	<i>PLCXD1</i>	phosphatidylinositol-specific phospholipase C, X domain containing 1	1.39	1.70E-03	2.73E-02
HH14	<i>PMEL</i>	premelanosome protein	0.84	1.52E-02	1.53E-01
HH14	<i>PRKDC</i>	protein kinase, DNA-activated, catalytic polypeptide	-0.51	2.57E-02	2.23E-01
HH14	<i>PSMB1</i>	proteasome subunit beta 1	-0.40	4.62E-02	3.29E-01
HH14	<i>PSMB5</i>	proteasome subunit beta 5	0.84	1.19E-02	1.27E-01
HH14	<i>PTCH1</i>	patched 1	0.47	2.32E-02	2.08E-01
HH14	<i>PTGR2</i>	prostaglandin reductase 2	-0.54	1.23E-02	1.30E-01
HH14	<i>RAD9A</i>	RAD9 checkpoint clamp component A	0.48	4.87E-02	3.40E-01
HH14	<i>RBP</i>	riboflavin binding protein	1.23	4.09E-02	3.05E-01
HH14	<i>RBP4</i>	retinol binding protein 4	2.49	5.00E-05	1.23E-03
HH14	<i>RDM1</i>	RAD52 motif containing 1	-0.55	1.97E-02	1.85E-01
HH14	<i>RPAP3</i>	RNA polymerase II associated protein 3	-0.40	4.65E-02	3.30E-01
HH14	<i>RPL32</i>	ribosomal protein L32	-0.41	3.98E-02	3.01E-01
HH14	<i>SELM</i>	selenoprotein M	-0.44	3.57E-02	2.80E-01
HH14	<i>SEPP1</i>	selenoprotein P, plasma, 1	-0.45	4.08E-02	3.05E-01
HH14	<i>SLC4A1</i>	solute carrier family 4, anion exchanger, member 1	0.58	3.60E-02	2.82E-01
HH14	<i>SLC7A9</i>	solute carrier family 7 (amino acid transporter light chain, bo,+ system), member 9	2.39	4.50E-04	8.97E-03
HH14	<i>SNRPA1</i>	small nuclear ribonucleoprotein polypeptide A'	-0.44	2.76E-02	2.34E-01
HH14	<i>SULT1C3</i>	sulfotransferase family, cytosolic, 1C, member 3	1.62	7.00E-03	8.66E-02
HH14	<i>THG1L</i>	tRNA-histidine guanylyltransferase 1 like	-0.45	2.65E-02	2.28E-01
HH14	<i>THYN1</i>	thymocyte nuclear protein 1	-0.42	4.05E-02	3.04E-01
HH14	<i>TIMM10</i>	translocase of inner mitochondrial membrane 10 homolog (yeast)	-0.48	3.78E-02	2.91E-01

HH14	<i>TTR</i>	transthyretin	1.21	5.00E-05	1.23E-03
HH14	<i>UBAP2</i>	ubiquitin associated protein 2	-0.68	1.03E-02	1.14E-01
HH14	<i>UCHL5</i>	ubiquitin C-terminal hydrolase L5	-0.38	4.89E-02	3.41E-01
HH14	<i>UFSP2</i>	UFM1-specific peptidase 2	-0.62	3.70E-03	5.20E-02
HH14	<i>VIPR2</i>	vasoactive intestinal peptide receptor 2	1.99	1.35E-03	2.26E-02
HH14	<i>WT1</i>	Wilms tumor protein homolog	-0.93	1.02E-02	1.13E-01

Supplemental Table 1. DEG HH10, 12, and 14.

Complete list of all significant genes from RNA-Seq for all three stages, HH10, 12, and 14.

Enriched Gene Ontology Terms for HH 10-12-14			
Stage	DAVID Enriched Go Terms	Genes	P-Value
HH10	DNA-templated transcription	11	2.55E-03
HH10	Multicellular organism development	7	4.65E-03
HH10	Negative regulation of neuron differentiation	6	1.22E-05
HH10	Ventricular cardiac muscle tissue morphogenesis	5	1.74E-06
HH10	Protein stabilization	4	2.01E-02
HH10	Axon guidance	4	2.17E-02
HH10	Regulation of muscle contraction	3	7.49E-04
HH10	Positive regulation of ATPase activity	3	3.98E-03
HH10	Signal transduction involved in regulation of gene expression	3	4.75E-03
HH10	Cardiac muscle contraction	3	7.43E-03
HH10	Stem cell differentiation	3	8.44E-03
HH10	Platelet aggregation	3	1.71E-02
HH10	Protein complex assembly	3	1.86E-02
HH10	Response to virus	3	2.83E-02
HH10	Activation of meiosis	2	1.75E-02
HH10	Positive regulation of mesenchymal cell apoptotic process	2	1.75E-02
HH10	BMP signaling pathway involved in heart development	2	1.75E-02
HH10	Protein localization to juxtaparanode region of axon	2	2.61E-02
HH10	Lipoprotein biosynthetic process	2	2.61E-02
HH10	Thyroid hormone transport	2	2.61E-02
HH10	Embryonic nail plate morphogenesis	2	2.61E-02
HH10	Cartilage morphogenesis	2	3.47E-02
HH10	Positive regulation of protein processing	2	4.32E-02
HH10	Forebrain dorsal/ventral pattern formation	2	4.32E-02
HH10	Negative regulation of transcription regulatory region DNA binding	2	4.32E-02
HH10	Triglyceride catabolic process	2*	8.45E-02
HH10	Ion transport	2*	9.25E-02
HH10	Iron ion homeostasis	2*	9.25E-02
HH12	DNA-templated transcription	36	4.15E-07
HH12	DNA-templated regulation of transcription	31	1.29E-05
HH12	Positive regulation of transcription from RNA polymerase II promoter	29	2.62E-04
HH12	Cell differentiation	20	5.89E-07

HH12	Multicellular organism development	17	4.64E-04
HH12	Negative regulation of transcription from RNA polymerase II promoter	16	4.98E-02
HH12	Regulation of transcription from RNA polymerase II promoter	14	1.24E-02
HH12	Axon guidance	13	3.23E-06
HH12	Heart development	12	5.72E-04
HH12	Negative regulation of cell proliferation	12	1.55E-02
HH12	Transcription from RNA polymerase II promoter	11	1.66E-03
HH12	Cell adhesion	11	1.44E-02
HH12	Negative regulation of apoptotic process	11	5.43E-02
HH12	Positive regulation of cell proliferation	10	9.13E-02
HH12	Angiogenesis	9	1.46E-02
HH12	Positive regulation of cell migration	8	5.43E-02
HH12	Positive regulation of defense response to virus by host	7	1.07E-02
HH12	Ventricular cardiac muscle tissue morphogenesis	6	1.92E-05
HH12	Regulation of heart rate	6	3.20E-05
HH12	Cardiac muscle contraction	6	1.11E-04
HH12	Muscle contraction	6	7.99E-04
HH12	Platelet aggregation	6	9.92E-04
HH12	Heart looping	6	6.00E-03
HH12	Regulation of cell migration	6	8.64E-03
HH12	Neural crest cell migration	6	1.61E-02
HH12	Positive regulation of angiogenesis	6	2.49E-02
HH12	Negative regulation of cell migration	6	2.70E-02
HH12	Anterior/posterior pattern specification	6	4.45E-02
HH12	Brain development	6	6.04E-02
HH12	Wnt signaling pathway	6	6.39E-02
HH12	Negative regulation of neuron apoptotic process	6	7.13E-02
HH12	Pituitary gland development	5	2.99E-03
HH12	Positive regulation of cell adhesion	5	3.69E-03
HH12	Cellular response to retinoic acid	5	7.55E-03
HH12	Ephrin receptor signaling pathway	5	8.81E-03
HH12	Vasculogenesis	5	2.40E-02
HH12	Positive regulation of neuron differentiation	5	3.23E-02
HH12	Lung development	5	4.20E-02
HH12	Xenophagy	5	9.52E-02
HH12	Cardiac myofibril assembly	4	1.32E-03
HH12	Negative regulation of cell-cell adhesion	4	3.00E-03

HH12	Hydrogen ion transmembrane transport	4	4.18E-03
HH12	Morphogenesis of an epithelium	4	5.59E-03
HH12	Artery morphogenesis	4	5.59E-03
HH12	Signal transduction involved in regulation of gene expression	4	7.27E-03
HH12	Anterior/posterior axis specification	4	9.21E-03
HH12	Heart morphogenesis	4	1.39E-02
HH12	Bone morphogenesis	4	1.39E-02
HH12	Cellular protein localization	4	3.07E-02
HH12	Embryonic forelimb morphogenesis	4	3.49E-02
HH12	Embryonic hindlimb morphogenesis	4	3.94E-02
HH12	Skeletal muscle tissue development	4	4.42E-02
HH12	Patterning of blood vessels	4	4.42E-02
HH12	Protein complex assembly	4	4.92E-02
HH12	Forebrain development	4	5.46E-02
HH12	Retina development in camera-type eye	4	6.60E-02
HH12	Organ morphogenesis	4	8.50E-02
HH12	Actin filament organization	4	9.88E-02
HH12	Regulation of cardiac muscle contraction by regulation of the release of sequestered calcium ion	3	3.54E-03
HH12	Regulation of myotube differentiation	3	3.54E-03
HH12	Skeletal muscle thin filament assembly	3	6.91E-03
HH12	Regulation of muscle contraction	3	1.13E-02
HH12	Negative regulation of transcription regulatory region DNA binding	3	1.13E-02
HH12	Positive regulation of megakaryocyte differentiation	3	1.65E-02
HH12	Spinal cord association neuron differentiation	3	1.65E-02
HH12	Regulation of axon extension	3	1.65E-02
HH12	Cerebellar Purkinje cell differentiation	3	2.26E-02
HH12	Regulation of ventricular cardiac muscle cell membrane repolarization	3	2.26E-02
HH12	Positive regulation of myotube differentiation	3	2.26E-02
HH12	Endothelial cell activation	3	2.26E-02
HH12	Intracellular receptor signaling pathway	3	2.94E-02
HH12	Atrial septum morphogenesis	3	2.94E-02
HH12	mRNA transcription from RNA polymerase II promoter	3	2.94E-02
HH12	Hindlimb morphogenesis	3	3.70E-02
HH12	Positive regulation of transcription elongation from RNA polymerase II promoter	3	3.70E-02
HH12	Actin filament-based movement	3	4.52E-02

HH12	Myoblast fusion	3	4.52E-02
HH12	Respiratory system process	3	4.52E-02
HH12	Positive regulation of protein tyrosine kinase activity	3*	5.40E-02
HH12	Embryo development ending in birth or egg hatching	3*	5.40E-02
HH12	Anatomical structure formation involved in morphogenesis	3*	5.40E-02
HH12	Embryonic digestive tract morphogenesis	3*	5.40E-02
HH12	Regulation of protein binding	3*	6.33E-02
HH12	Embryonic digestive tract development	3*	6.33E-02
HH12	Cellular response to gamma radiation	3*	6.33E-02
HH12	Smooth muscle contraction	3*	8.34E-02
HH12	Gastrulation with mouth forming second	3*	8.34E-02
HH12	Post-anal tail morphogenesis	3*	8.34E-02
HH12	Positive regulation of myoblast differentiation	3*	8.34E-02
HH12	Positive regulation of DNA binding	3*	9.41E-02
HH12	Activation of meiosis	2*	6.84E-02
HH12	Cardiac left ventricle formation	2*	6.84E-02
HH12	Negative regulation of CREB transcription factor activity	2*	6.84E-02
HH12	Positive regulation of epithelial cell differentiation	2*	6.84E-02
HH12	Eye photoreceptor cell differentiation	2*	6.84E-02
HH12	Negative regulation of low-density lipoprotein particle receptor catabolic process	2*	6.84E-02
HH12	Positive regulation of interleukin-1 beta production	2*	6.84E-02
HH12	Positive regulation of mesenchymal cell apoptotic process	2*	6.84E-02
HH12	Extraocular skeletal muscle development	2*	6.84E-02
HH12	BMP signaling pathway involved in heart development	2*	6.84E-02
HH12	Detection of muscle stretch	2*	6.84E-02
HH14	Negative regulation of extrinsic apoptotic signaling pathway via death domain receptors	4	1.10E-04
HH14	Positive regulation of heterotypic cell-cell adhesion	3	1.20E-04
HH14	Protein polymerization	3	4.00E-04
HH14	Plasminogen activation	3	6.00E-04
HH14	Positive regulation of peptide hormone secretion	3	1.10E-03
HH14	Fibrinolysis	3	1.80E-03
HH14	Positive regulation of exocytosis	3	1.80E-03
HH14	Smoothed signaling pathway	4	2.80E-03
HH14	Positive regulation of vasoconstriction	3	4.60E-03
HH14	Negative regulation of endothelial cell apoptotic process	3	5.20E-03

HH14	Positive regulation of protein secretion	3	5.90E-03
HH14	Platelet aggregation	3	9.50E-03
HH14	Response to calcium ion	3	1.00E-02
HH14	Proteolysis involved in cellular protein catabolic process	3	1.10E-02
HH14	Negative regulation of epithelial cell proliferation	3	1.50E-02
HH14	Positive regulation of ERK1 and ERK2 cascade	4	1.70E-02
HH14	RNA Splicing	3	1.70E-02
HH14	Induction of bacterial agglutination	2	1.90E-02
HH14	Blood coagulation, fibrin clot formation	2	1.90E-02
HH14	Heart looping	3	2.00E-02
HH14	Transcription from RNA polymerase II promoter	4	2.50E-02
HH14	Cell-matrix adhesion	3	2.70E-02
HH14	Retinoic acid receptor signaling pathway	2	3.80E-02
HH14	Retinol metabolic process	2*	6.30E-02
HH14	Spinal cord motor neuron differentiation	2*	7.50E-02
HH14	Heart morphogenesis	2*	9.30E-02
HH14	Negative regulation of transcription from RNA polymerase II promoter	5*	9.60E-02

*denotes GO term not significant by p-value

Supplemental Table 2. Full Gene Ontology HH10, 12, and 14.

Complete list of all Gene Ontology terms for all three stages, HH10, 12, and 14.

References

1. *Phenylketonuria (PKU): screening and management*. NIH Consens Statement, 2000. **17**(3): p. 1-33.
2. Levy, H.L., et al., *Congenital heart disease in maternal phenylketonuria: report from the Maternal PKU Collaborative Study*. *Pediatr Res*, 2001. **49**(5): p. 636-42.
3. Hanley, W.B., *Finding the fertile woman with phenylketonuria*. *Eur J Obstet Gynecol Reprod Biol*, 2008. **137**(2): p. 131-5.
4. Groselj, U., M.Z. Tansek, and T. Battelino, *Fifty years of phenylketonuria newborn screening - A great success for many, but what about the rest?* *Mol Genet Metab*, 2014. **113**(1-2): p. 8-10.
5. Levy, H.L., *Congenital heart disease in maternal PKU*. *Mol Genet Metab*, 2012. **107**(4): p. 648-9.
6. Lowitzer, A.C., *Maternal phenylketonuria: cause for concern among women with PKU*. *Res Dev Disabil*, 1987. **8**(1): p. 1-14.
7. Ferencz, C., et al., *Congenital cardiovascular malformations: questions on inheritance. Baltimore-Washington Infant Study Group*. *J Am Coll Cardiol*, 1989. **14**(3): p. 756-63.
8. Hoffman, J.I. and S. Kaplan, *The incidence of congenital heart disease*. *J Am Coll Cardiol*, 2002. **39**(12): p. 1890-900.
9. Jenkins, K.J., et al., *Noninherited risk factors and congenital cardiovascular defects: current knowledge: a scientific statement from the American Heart Association Council on Cardiovascular Disease in the Young: endorsed by the American Academy of Pediatrics*. *Circulation*, 2007. **115**(23): p. 2995-3014.
10. Pierpont, M.E., et al., *Genetic basis for congenital heart defects: current knowledge: a scientific statement from the American Heart Association Congenital Cardiac Defects Committee, Council on Cardiovascular Disease in the Young: endorsed by the American Academy of Pediatrics*. *Circulation*, 2007. **115**(23): p. 3015-38.
11. Koch, R., F. Trefz, and S. Waisbren, *Psychosocial issues and outcomes in maternal PKU*. *Mol Genet Metab*, 2010. **99 Suppl 1**: p. S68-74.
12. Platt, L.D., et al., *The international study of pregnancy outcome in women with maternal phenylketonuria: report of a 12-year study*. *Am J Obstet Gynecol*, 2000. **182**(2): p. 326-33.
13. Wittig, J.G. and A. Munsterberg, *The Early Stages of Heart Development: Insights from Chicken Embryos*. *J Cardiovasc Dev Dis*, 2016. **3**(2).
14. Stern, C.D., *The chick; a great model system becomes even greater*. *Dev Cell*, 2005. **8**(1): p. 9-17.
15. Kain, K.H., et al., *The chick embryo as an expanding experimental model for cancer and cardiovascular research*. *Dev Dyn*, 2014. **243**(2): p. 216-28.
16. Stern, C.D., *The chick embryo--past, present and future as a model system in developmental biology*. *Mech Dev*, 2004. **121**(9): p. 1011-3.
17. Plein, A., A. Fantin, and C. Ruhrberg, *Neural crest cells in cardiovascular development*. *Curr Top Dev Biol*, 2015. **111**: p. 183-200.
18. Hamburger, V. and H.L. Hamilton, *A series of normal stages in the development of the chick embryo. 1951*. *Dev Dyn*, 1992. **195**(4): p. 231-72.
19. Martinsen, B.J., *Reference guide to the stages of chick heart embryology*. *Dev Dyn*, 2005. **233**(4): p. 1217-37.

20. Rana, M.S., et al., *Trabeculated right ventricular free wall in the chicken heart forms by ventricularization of the myocardium initially forming the outflow tract*. *Circ Res*, 2007. **100**(7): p. 1000-7.
21. Zhang, Y. and L.B. Ruest, *Analysis of neural crest cell fate during cardiovascular development using Cre-activated lacZ/beta-galactosidase staining*. *Methods Mol Biol*, 2012. **843**: p. 125-38.
22. Bressan, M., et al., *Reciprocal myocardial-endocardial interactions pattern the delay in atrioventricular junction conduction*. *Development*, 2014. **141**(21): p. 4149-57.
23. Metzler, M.A. and L.L. Sandell, *Enzymatic Metabolism of Vitamin A in Developing Vertebrate Embryos*. *Nutrients*, 2016. **8**(12).
24. Kanai, M., A. Raz, and D.S. Goodman, *Retinol-binding protein: the transport protein for vitamin A in human plasma*. *J Clin Invest*, 1968. **47**(9): p. 2025-44.
25. Stefanovic, S. and S. Zaffran, *Mechanisms of retinoic acid signaling during cardiogenesis*. *Mech Dev*, 2017. **143**: p. 9-19.
26. Kawaguchi, R., et al., *Receptor-mediated cellular uptake mechanism that couples to intracellular storage*. *ACS Chem Biol*, 2011. **6**(10): p. 1041-51.
27. Kawaguchi, R., et al., *A membrane receptor for retinol binding protein mediates cellular uptake of vitamin A*. *Science*, 2007. **315**(5813): p. 820-5.
28. Dong, D., et al., *Distinct roles for cellular retinoic acid-binding proteins I and II in regulating signaling by retinoic acid*. *J Biol Chem*, 1999. **274**(34): p. 23695-8.
29. Sakai, Y., et al., *The retinoic acid-inactivating enzyme CYP26 is essential for establishing an uneven distribution of retinoic acid along the antero-posterior axis within the mouse embryo*. *Genes Dev*, 2001. **15**(2): p. 213-25.
30. Niederreither, K., et al., *Embryonic retinoic acid synthesis is essential for early mouse post-implantation development*. *Nat Genet*, 1999. **21**(4): p. 444-8.
31. Duester, G., *Retinoic acid synthesis and signaling during early organogenesis*. *Cell*, 2008. **134**(6): p. 921-31.
32. Wilson, J.G. and J. Warkany, *Aortic-arch and cardiac anomalies in the offspring of vitamin A deficient rats*. *Am J Anat*, 1949. **85**(1): p. 113-55.
33. Wilson, J.G. and J. Warkany, *Cardiac and aortic arch anomalies in the offspring of vitamin A deficient rats correlated with similar human anomalies*. *Pediatrics*, 1950. **5**(4): p. 708-25.
34. Kostetskii, I., et al., *Retinoid signaling required for normal heart development regulates GATA-4 in a pathway distinct from cardiomyocyte differentiation*. *Dev Biol*, 1999. **206**(2): p. 206-18.
35. Lammer, E.J., et al., *Retinoic acid embryopathy*. *N Engl J Med*, 1985. **313**(14): p. 837-41.
36. Blau, N., *Genetics of Phenylketonuria: Then and Now*. *Hum Mutat*, 2016. **37**(6): p. 508-15.
37. Ho, G. and J. Christodoulou, *Phenylketonuria: translating research into novel therapies*. *Transl Pediatr*, 2014. **3**(2): p. 49-62.
38. Guthrie, R. and A. Susi, *A Simple Phenylalanine Method for Detecting Phenylketonuria in Large Populations of Newborn Infants*. *Pediatrics*, 1963. **32**: p. 338-43.
39. Berry, S.A., et al., *Newborn screening 50 years later: access issues faced by adults with PKU*. *Genet Med*, 2013. **15**(8): p. 591-9.
40. Belanger-Quintana, A., et al., *Diet in phenylketonuria: a snapshot of special dietary costs and reimbursement systems in 10 international centers*. *Mol Genet Metab*, 2012. **105**(3): p. 390-4.

41. MacDonald, A., et al., *The reality of dietary compliance in the management of phenylketonuria*. J Inherit Metab Dis, 2010. **33**(6): p. 665-70.
42. Lenke, R.R. and H.L. Levy, *Maternal phenylketonuria and hyperphenylalaninemia. An international survey of the outcome of untreated and treated pregnancies*. N Engl J Med, 1980. **303**(21): p. 1202-8.
43. Zeile, W.L., et al., *Maternal phenylketonuria syndrome: studies in mice suggest a potential approach to a continuing problem*. Pediatr Res, 2018.
44. Matalon, R., et al., *Abnormal expression of genes associated with development and inflammation in the heart of mouse maternal phenylketonuria offspring*. Int J Immunopathol Pharmacol, 2005. **18**(3): p. 557-65.
45. Seagraves, N.J. and K.L. McBride, *Cardiac teratogenicity in mouse maternal phenylketonuria: defining phenotype parameters and genetic background influences*. Mol Genet Metab, 2012. **107**(4): p. 650-8.
46. Levy, H.L. and M. Ghavami, *Maternal phenylketonuria: a metabolic teratogen*. Teratology, 1996. **53**(3): p. 176-84.
47. Komrower, G.M., et al., *Management of maternal phenylketonuria: an emerging clinical problem*. Br Med J, 1979. **1**(6175): p. 1383-7.
48. Scott, T.M., W.M. Fyfe, and D.M. Hart, *Maternal phenylketonuria: abnormal baby despite low phenylalanine diet during pregnancy*. Arch Dis Child, 1980. **55**(8): p. 634-7.
49. Koch, R., et al., *The Maternal Phenylketonuria International Study: 1984-2002*. Pediatrics, 2003. **112**(6 Pt 2): p. 1523-9.
50. Drake, V.J., et al., *Gastrulating chick embryo as a model for evaluating teratogenicity: a comparison of three approaches*. Birth Defects Res A Clin Mol Teratol, 2006. **76**(1): p. 66-71.
51. Schroeder, A., et al., *The RIN: an RNA integrity number for assigning integrity values to RNA measurements*. BMC Mol Biol, 2006. **7**: p. 3.
52. Andrews, S., *FastQC A Quality Control Tool for High Throughput Sequence Data*.
53. Kim, D., et al., *TopHat2: accurate alignment of transcriptomes in the presence of insertions, deletions and gene fusions*. Genome Biol, 2013. **14**(4): p. R36.
54. Kim, D., B. Langmead, and S.L. Salzberg, *HISAT: a fast spliced aligner with low memory requirements*. Nat Methods, 2015. **12**(4): p. 357-60.
55. Trapnell, C., et al., *Transcript assembly and quantification by RNA-Seq reveals unannotated transcripts and isoform switching during cell differentiation*. Nat Biotechnol, 2010. **28**(5): p. 511-5.
56. Huang, D.W., et al., *DAVID Bioinformatics Resources: expanded annotation database and novel algorithms to better extract biology from large gene lists*. Nucleic Acids Res, 2007. **35**(Web Server issue): p. W169-75.
57. Becker, K.G., et al., *The genetic association database*. Nat Genet, 2004. **36**(5): p. 431-2.
58. Yue, H., et al., *Reference gene selection for normalization of PCR analysis in chicken embryo fibroblast infected with H5N1 AIV*. Virol Sin, 2010. **25**(6): p. 425-31.
59. Xavier-Neto, J., et al., *Signaling through retinoic acid receptors in cardiac development: Doing the right things at the right times*. Biochim Biophys Acta, 2015. **1849**(2): p. 94-111.
60. Rhinn, M. and P. Dolle, *Retinoic acid signalling during development*. Development, 2012. **139**(5): p. 843-58.
61. Pan, J. and K.M. Baker, *Retinoic acid and the heart*. Vitam Horm, 2007. **75**: p. 257-83.
62. Marrs, J.A., et al., *Zebrafish fetal alcohol syndrome model: effects of ethanol are rescued by retinoic acid supplement*. Alcohol, 2010. **44**(7-8): p. 707-15.

63. Kot-Leibovich, H. and A. Fainsod, *Ethanol induces embryonic malformations by competing for retinaldehyde dehydrogenase activity during vertebrate gastrulation*. *Dis Model Mech*, 2009. **2**(5-6): p. 295-305.
64. Muralidharan, P., et al., *Fetal Alcohol Spectrum Disorder (FASD) Associated Neural Defects: Complex Mechanisms and Potential Therapeutic Targets*. *Brain Sci*, 2013. **3**(2): p. 964-91.
65. Deltour, L., H.L. Ang, and G. Duester, *Ethanol inhibition of retinoic acid synthesis as a potential mechanism for fetal alcohol syndrome*. *FASEB J*, 1996. **10**(9): p. 1050-7.
66. Clagett-Dame, M. and H.F. DeLuca, *The role of vitamin A in mammalian reproduction and embryonic development*. *Annu Rev Nutr*, 2002. **22**: p. 347-81.
67. Dersch, H. and M.H. Zile, *Induction of normal cardiovascular development in the vitamin A-deprived quail embryo by natural retinoids*. *Dev Biol*, 1993. **160**(2): p. 424-33.
68. Dickman, E.D., C. Thaller, and S.M. Smith, *Temporally-regulated retinoic acid depletion produces specific neural crest, ocular and nervous system defects*. *Development*, 1997. **124**(16): p. 3111-21.
69. Bell, G.W., T.A. Yatskievych, and P.B. Antin, *GEISHA, a whole-mount in situ hybridization gene expression screen in chicken embryos*. *Dev Dyn*, 2004. **229**(3): p. 677-87.
70. Acloque, H., D.G. Wilkinson, and M.A. Nieto, *In situ hybridization analysis of chick embryos in whole-mount and tissue sections*. *Methods Cell Biol*, 2008. **87**: p. 169-85.
71. Nieto, M.A., K. Patel, and D.G. Wilkinson, *In situ hybridization analysis of chick embryos in whole mount and tissue sections*. *Methods Cell Biol*, 1996. **51**: p. 219-35.
72. Napoli, J.L., *Functions of Intracellular Retinoid Binding-Proteins*. *Subcell Biochem*, 2016. **81**: p. 21-76.
73. Park, E.J., et al., *Required, tissue-specific roles for Fgf8 in outflow tract formation and remodeling*. *Development*, 2006. **133**(12): p. 2419-33.
74. Jiang, X., et al., *Fate of the mammalian cardiac neural crest*. *Development*, 2000. **127**(8): p. 1607-16.
75. Macatee, T.L., et al., *Ablation of specific expression domains reveals discrete functions of ectoderm- and endoderm-derived FGF8 during cardiovascular and pharyngeal development*. *Development*, 2003. **130**(25): p. 6361-74.
76. Henrique, D., et al., *Expression of a Delta homologue in prospective neurons in the chick*. *Nature*, 1995. **375**(6534): p. 787-90.
77. Mikawa, T., et al., *Induction and patterning of the primitive streak, an organizing center of gastrulation in the amniote*. *Dev Dyn*, 2004. **229**(3): p. 422-32.